The Thousand Asteroid Light Curve Survey[1]

Joseph Masiero[2], Robert Jedicke[2], Josef Ďurech[3], Stephen Gwyn[4],
Larry Denneau[2], Jeff Larsen[5]

ABSTRACT

We present the results of our Thousand Asteroid Light Curve Survey (TALCS) conducted with the Canada-France-Hawaii Telescope in September 2006. Our untargeted survey detected 828 Main Belt asteroids to a limiting magnitude of $g' \sim 22.5$ corresponding to a diameter range of 0.4 km $\leq D \leq 10$ km. Of these, 278 objects had photometry of sufficient quality to perform rotation period fits. We debiased the observations and light curve fitting process to determine the true distribution of rotation periods and light curve amplitudes of Main Belt asteroids. We confirm a previously reported excess in the fraction of fast rotators but find a much larger excess of slow rotating asteroids ($\sim 15\%$ of our sample). A few percent of objects in the TALCS size range have large light curve amplitudes of ~ 1 mag. Fits to the debiased distribution of light curve amplitudes indicate that the distribution of triaxial ellipsoid asteroid shapes is proportional to the square of the axis-ratio, $(b/a)^2$, and may be bi-modal. Finally, we find six objects with rotation periods that may be less than 2 hours with diameters between 400 m and 1.5 km, well above the break-up limit for a gravitationally-bound aggregate. Our debiased data indicate that this population represents $< 4\%$ of the Main Belt in the $1 - 10$ km size range.

---

[1]Based on observations obtained with MegaPrime/MegaCam, a joint project of CFHT and CEA/DAPNIA, at the Canada-France-Hawaii Telescope (CFHT) which is operated by the National Research Council (NRC) of Canada, the Institute National des Sciences de l'Univers of the Centre National de la Recherche Scientifique of France, and the University of Hawaii.

[2]Institute for Astronomy, University of Hawaii, 2680 Woodlawn Dr, Honolulu, HI 96822, *masiero, jedicke, denneau@ifa.hawaii.edu*

[3]Astronomical Institute, Faculty of Mathematics and Physics, Charles University in Prague, V Holesovickach 2, 18000 Prague, Czech Republic, *durech@sirrah.troja.mff.cuni.cz*

[4]Canadian Astronomical Data Centre, Herzberg Institute of Astrophysics, Victoria, BC, V9E 2E7, Canada *Stephen.Gwyn@nrc-cnrc.gc.ca*

[5]Physics Department, United States Naval Academy, Annapolis, MD 21402, *larsen@usna.edu*

1. Introduction

Following the call by Pravec et al. (2002) for an asteroid rotation survey free from biases against low amplitude and long period objects, we have conducted a large, untargeted survey of small Main Belt asteroids. Our Thousand Asteroid Light Curve Survey (TALCS) was designed to use the flexibility of the Canada-France-Hawaii Telescope (CFHT) queue schedule observing to discover and obtain light curves for a large and random sampling of Main Belt asteroids with controlled and understood biases.

Rotation measurements of asteroids are one of the primary ways of deriving physical properties of these bodies from Earth-based instruments. If assumed to have shapes described by triaxial ellipsoids and constant albedos across their surface, the intensity of the reflected light can be well described by a simple sinusoidal relationship (Lacerda & Luu 2003). More complicated models are needed to describe the light curves generated by asteroids with realistic shapes (see Fig. 1 from Sullivan et al. (2002) for a composite of asteroid photos from *in situ* studies). Harris et al. (1989) presented a method for describing complex light curves with multi-order sinusoids which has become the standard for fitting light curves with a high-density of data (*e.g.* Pravec & Harris 2000; Pravec et al. 2002). For asteroids with sparse data sampling, light curve inversion has become a powerful tool for finding rotation rates while its application to high density data has provided excellent models of asteroid shapes (Kaasalainen 2004; Kaasalainen & Ďurech 2007; Ďurech et al. 2007, 2009).

Pravec et al. (2002) discuss the relationship between asteroid spin rate and diameter using all published periods for Main Belt and Near Earth asteroids. They point out a strong barrier in rotation period at $P \approx 2$ hours for objects larger than $D > 150$ m. Gravitationally bound aggregates of smaller boulders will have a spin rate limit of $2 - 3$ hours depending on the density of the composite rocks and their characteristic size (Pravec & Harris 2000). Objects with diameters smaller than 150 m have been observed rotating considerably faster than this limit and can be explained as monolithic rocks with internal tensile strength. The two hour spin limit implies that bodies larger than 150 m are unable to survive as monoliths in the collisionally processed inner Main Belt (Harris 1996) which also feeds the Near Earth Object (NEO) population (Bottke et al. 2002).

The spin rates of a collisionally evolved system should fit a Maxwellian distribution as the spin vectors parallel to the plane of motion should be normally distributed around zero while the orthogonal vector will have a slight asymmetry due to the bulk motion of the system (Salo 1987). This produces a distribution of the form:

$$N \propto \frac{\omega^2}{a^3}\, e^{(-0.5\ \omega^2\ a^{-2})}$$

where ω is the spin rate and a is a constant, which does an excellent job of describing the spin rates observed for large ($D > 40$ km) Main Belt asteroids (Pravec et al. 2002). This relation breaks down at smaller sizes (Pravec et al. 2002; Polishook & Brosch 2008) when non-collisional forces, in particular the Yarkovsky-O'Keefe-Radzievskii-Paddack (YORP) effect (Rubincam 2000), create excesses of objects with very slow and very fast rotation rates (Vokrouhlický & Čapek 2002).

Holsapple (2007) proposed a size-dependent strength for asteroids that can explain both the cutoff in rotation rates of the largest objects at $P \sim 2$ hours as well as the existence of rapidly rotating small NEOs without requiring a sharp transition in composition or evolution. It would also imply that there should exist some objects rotating faster than the 2 hour "spin limit" in the $0.15 - 5$ km size regime. Pravec et al. (2002) discuss a single object found to be above the rotation limit (2001 OE_{84}, a Mars Crossing asteroid with period of ~ 29.19min and size of ~ 0.9 km) however the authors indicate that this object is likely an exceptional one. Recently, Pravec et al. (2008) performed a similar study to ours of small inner-Main Belt asteroids. They find an excess of slow rotators in their $3-15$ km diameter range sample but a flat rotation rate distribution from spin rates of $1 - 9.5$ rev day^{-1}. They explain this distinctly non-Maxwellian distribution by modeling the YORP effect on small bodies and showing that when the YORP timescale is dominant any previous distribution is erased.

2. Observations

The TALCS program was designed to obtain orbits, colors, and basic light curves for approximately 1000 Main Belt asteroids. Using the Canada-France-Hawaii Telescope's (CFHT) MegaCam instrument (Boulade et al. 2000) we surveyed approximately 12 deg^2 of the ecliptic (*i.e.* 12 MegaCam pointings of ~ 1 deg^2 each) for six nights across a two-week period in September 2006. Using the flexibility that is only possible under Queue-scheduled observing, we spread our allocated time over the instrument's run, observing only 3-4 hours per night. The asymmetric spacing increased our sensitivity to slower rotating objects while giving us a longer orbital arc for better orbit determination than would be possible for the same amount of observing performed in a classical mode.

The survey was centered 1 hr away from opposition to minimize the opposition effect, a non-linear increase in the reflected light at low phase angles ($\alpha \leq 5°$). Though this would have increased our sensitivity to fainter targets it would have complicated the light curve analysis. The phase angles of our targets ranged from $4° - 13°$ depending on their distance from the Sun and the times of observation. To reduce loss of objects between nights the center of our survey pattern drifted each night to follow a hypothetical mid-Main Belt

asteroid on a circular orbit. Table 1 provides the dates, central position and setup for each night of observing. One night (20 Sep 2006) was devoted to a subset of the whole field to decrease the time between exposures and thus improve light curve resolution. Additionally, all images on the night of 17 Sep 2006 were taken with the r' filter (as opposed to g' for all other nights) to allow for color determination of the asteroids.

Over the two-week observing run we obtained 1079 images totaling 20.4 hours of queue time. Initial data reduction was accomplished on location by the standard Elixir pipeline (Magnier & Cuillandre 2004). Post-processing was performed using the MegaPipe service provided by the CADC (Gywn 2008). Astrometric calibrations were initially based on the USNO catalog with a deeper internal catalog generated from all stationary objects in the survey. Photometric calibrations were based on the initial Elixir calibrations and then finalized based on a set of secondary standards from the photometric nights. Images taken on non-photometric nights were calibrated with these secondary standards. The systematic astrometric error was $\sim 0.05''$ and systematic error on relative and absolute photometry was ~ 0.015 and ~ 0.03 mag respectively.

Source identification used SExtractor (Bertin & Arnouts 1996) with the requirement of a detection $\geq 1.5\ \sigma_{sky}$ on four contiguous pixels. Pre-filtering of the images yielded an effective signal-to-noise limit of 4 σ above background. Source lists were then cleaned based on the half-light radius of the detection, selecting point-like PSFs and rejecting sources with measured radii that were too small (*e.g.* bad pixel, cosmic rays) or too large (*e.g.* galaxies, flat-field variations). Stationary objects, defined as those appearing at the same location in three or more images, were also removed from the detection list.

3. Object Identification

Moving objects were identified and linked by the Pan-STARRS telescope's Moving Object Processing System (MOPS). The heart of the MOPS detection linking code is a variable kd-tree algorithm that allows the depth of the kd-tree branches to be dynamically modified to increase search efficiency (Kubica et al. 2005). This reduces the time requirements for linking large numbers of detections in moderate-to-high noise data sets. Orbits were computed using the techniques of Milani et al. (2007) as implemented for MOPS. Our search was restricted to only those objects moving with Main Belt-like rates of motion.

We identified 828 Main Belt objects with magnitudes brighter than $g' \sim 22.5$. All detections for these objects were submitted to the Minor Planet Center and 333 had no previous reported observations. MPC designations for all objects, as well as orbital elements,

lengths of orbital arc, number of observations, estimated albedos and derived diameters, are listed in Table 2.

Figure 1 shows number distributions of the semimajor axes, eccentricities, inclinations and absolute magnitudes of the TALCS asteroids compared to the known distribution from the Minor Planet Center (MPC)[1]. For comparison to the currently known population of asteroids, the dotted lines show the arbitrarily normalized distributions of semimajor axes, eccentricities and inclinations for all asteroids with $H_v < 15$ (*i.e.* a "complete" distribution) while the dashed line shows the normalized absolute magnitude distribution for all asteroids known. The TALCS semimajor axis distribution shows that the survey has nearly equal sampling from the inner-, mid-, and outer-Main Belts, in contrast to the actual distribution of objects with semimajor axis. This is the result of inner Main Belt asteroids being brighter and thus easier to identify in a magnitude-limited survey. Figure 1 also shows that the TALCS objects' eccentricity distribution is very similar to the MPC data, while the inclination distribution shows a strong preference for low inclination objects, as is expected for a survey restricted to the ecliptic over a short time span. The TALCS absolute magnitude distribution peaks about two magnitudes fainter than the MPC data reflecting our focus on small asteroids. The scatter plots in Fig 2 show no serious gaps in the orbital element coverage of TALCS, with the semimajor axis vs absolute magnitude figure showing the effects of the apparent magnitude limit of our survey with the lack of faint, distant objects.

Albedos for all objects were estimated based on their heliocentric distance following the known decrease in albedo with distance from the Sun (Tedesco et al. 2005). The semimajor axis (a) ranges for assumed albedos (p_v) were: $a \leq 2.5$ AU, $p_v = 0.20$; $2.5 < a \leq 2.8$ AU, $p_v = 0.08$; $a > 2.8$ AU, $p_v = 0.04$, as shown in Fig 3. Diameters were then calculated using:

$$D = \frac{1329}{\sqrt{p_v}} 10^{-H/5}$$

(see Harris & Lagerros 2002, and references therein). Figure 3a shows that TALCS is sensitive to objects as small as 1 km diameter through the entire Main Belt with much better sensitivity to smaller objects at smaller semimajor axes as expected in a magnitude limited survey. We compare our diameter distribution for all TALCS asteroids and for only the light curve fit objects to the diameter distribution of the smallest objects with known periods[2] in Fig 3b. The known objects show a flatter diameter distribution than the TALCS data indicating that TALCS is preferentially sensitive to smaller Main Belt asteroids. Asteroid

---

[1] *http://www.cfa.harvard.edu/iau/lists/MPDistribution.html*

[2] compiled by A.W. Harris, et al. in November 2008; available online: *http://www.minorplanetobserver.com/astlc/LightcurveParameters.htm*

(755) Quintilla was the only TALCS object observed in the IRAS survey and has a derived diameter of 36.0 ± 2.1 km (Tedesco et al. 2002). This is significantly lower than our estimate of ~ 62 km, however it was found to have an unusually high albedo of $p_v = 0.1621$ for an object with $a > 3$ AU.

4. Light Curve Analysis

The TALCS observing program was designed to have sensitivity to light curve periods ranging from as short as 1 hour to over 50 hours. This was accomplished by varying the transient time interval (TTI; the time between repeated exposures on the same field) from 2 to 17 minutes as listed in Table 1. The observations were spread out over nights with different spacings to reduce the effect of aliasing and extend the period sensitivity window. Because of this survey design the number of points in the light curve of different objects varied from 20 to 140 with a maximum of four hours of consecutive observations on any single night. This placed our light curves in a difficult regime between the typical dense data sets generated by single-object light curve surveys and the sparse light curve data that will be generated by the next generation surveys like Pan-STARRS (Kaasalainen 2004; Ďurech et al. 2007).

Light curve periods were fit to each data set that was of sufficient photometric quality. The statistical and systematic errors of the photometry established a limiting magnitude for the fits of $g' \sim 21$ mag corresponding to S/N$\sim$ 15. We fit periods and amplitudes to 278 TALCS asteroids using the Fourier series method that was developed by Harris et al. (1989) and has since become the standard for light curve fitting (*e.g.* Pravec et al. 2005). Figure 4 shows that no objects larger than $D = 2$ km were found to have periods less than 2 hours. (The cluster of objects with $P = 0$ hr are those that show no significant photometric variation with rotation.) Other than this there is no strong relationship observed between diameter and either period or amplitude. The bulk of the TALCS objects have periods between two and ten hours and amplitudes less than 0.4 mag, though a number of objects were found with periods up to and above 50 hours. Few objects were found with amplitudes at or above 0.75 mag which would indicate extreme shapes not typical for relaxed bodies. The error in the amplitude determination for many objects was of order 0.1 mag, causing a cluster of objects at *e.g.* 0.4 mag, 0.5 mag and 0.7 mag values. These peaks in the amplitude distribution should be considered observational artifacts though the overall trend in the distribution is real. Comparisons to the previously known light curve data are shown for both distributions and confirm that prior to debiasing TALCS shows the same general trends as seen in earlier surveys. The major exceptions to this are objects with very short ($P < 2$ hr) and very long ($P > 30$ hr) rotation periods. This result is discussed in § 6.

A full list of period and amplitude fits as well as $g' - r'$ color and reliability parameter (U) is given in Table 3. The reliability parameter follows the definition by Harris & Young (1983) with a modification to the “0” value:

0 : no observed variation beyond photometric error

1 : fragmentary or inconclusive coverage, possibly wrong

2 : fairly conclusive result, may be incorrect at the $10-20\%$ level or a multiple (*e.g.* 0.5, 2, etc) of the true period

3 : secure result with essentially all of the rotation phase covered

4 : multiple opposition coverage with pole estimation

Due to the nature of the TALCS data set and the absence of overlap with any previous light curve survey, all results presented here are single-opposition light curves and thus none will have a reliability parameter of U= 4.

The raw spin rate distribution for TALCS asteroids in Fig 5 reveals a decrease in the number of objects with increasing spin rates in contrast with recent results presented by Pravec et al. (2008) who found a nearly flat spin rate distribution. We discuss the implications of these contrasting results in § 6.

5. Debiasing

TALCS was designed to minimize the influence of biases found in targeted surveys such as favoring brighter and closer asteroids but was still susceptible to three serious and unavoidable biases: 1) a decreasing sensitivity to low amplitude rotators for fainter objects in our magnitude limited survey, 2) fits becoming unconstrained as the rotation period becomes a significant fraction of the total survey time window, and 3) data-loss due to objects falling on chip gaps or moving out of the survey area.

For any set of light curve observations that do not have complete continuous coverage of an object’s full rotation, underlying periodicities in the data can be mistaken for the rotation period, especially for weakly varying objects. This aliasing of survey periods into apparent rotation periods is a major source of error in light curve surveys. Examples of aliased periods include: an apparent 24 hour period arising from observing a target the same time every night; periods on the order of a few minutes as dictated by the time between subsequent exposures; integer multiples of the actual period due to incomplete coverage. Although the

TALCS survey cadence was designed to avoid aliasing problems, they can arise if one or more nights of data were lost due to objects falling off of chips or out of the field of view. Additionally, objects with light curve amplitudes comparable to the photometric noise are difficult or impossible to fit correctly.

To measure these biases we generated a population of synthetic asteroids and used automated light curve fitting software to determine our fitting efficiency over a range of light curve periods and amplitudes. To validate the rotation periods from the TALCS survey we obtained followup observations of a subset of objects.

5.1. Synthetic Light Curves

We generated $100,000$ synthetic light curves including realistic photometric noise over a range of periods, amplitudes, and magnitudes spanning the values found in TALCS. The rotation periods and amplitudes were generated with a flat distribution over the ranges: 1 hr $< P <$ 30 hr, 0.05 mag $< A <$ 1.2 mag.[3] To ensure that the synthetic objects' apparent magnitude distribution matched the TALCS objects' apparent magnitude distribution we randomly generated the synthetic objects' magnitudes from a fit to the observed magnitude (M) distribution of the form:

$$N = \frac{2.5^{M-18.6}}{1 + e^{(M-20.6)/0.25}}$$

This function simultaneously accounts for the increase in the number of objects with apparent magnitude as well as the falloff in detection efficiency inherent to a magnitude-limited survey (Jedicke & Herron 1997).

Assuming the synthetic objects are relaxed triaxial ellipsoids, the b and c axes are equal, and the asteroids are in a principal-axis rotation state, their light curves are described by:

$$m = 2.5 \log_{10} \sqrt{1 + \left[\left(\frac{b}{a} \right)^2 - 1 \right] \cos^2(2\pi\phi) \sin^2 \theta}$$

and the amplitude of the light curve (Δm) is:

$$\Delta m = 2.5 \log \left[\cos^2 \theta + \left(\frac{b}{a} \right)^2 \sin^2 \theta \right]^{-1/2} \qquad (1)$$

[3]Although correlations in rotation states have been observed for asteroids of the Koronis family (Slivan et al. 2003) no such relationship has been found for the Main Belt as a whole and we found no evidence of any correlation in our raw TALCS data.

where m is the relative magnitude, b/a the ellipsoidal axis ratio, θ is the angle of the spin vector with respect to the line of sight and ϕ the rotation phase (Lacerda & Luu 2003; Lacerda & Jewitt 2007). The orientation of the poles of the synthetic asteroids as well as the initial phases were isotropically distributed across the full range of values.

Synthetic photometric measures were drawn from the light curves using the TALCS observing cadence. Data loss for single observations and whole nights was simulated based on the actual data loss rate for the real objects. The most common reason for loss of a single observation was passage through a star or diffraction spike while loss of a whole night occurred when objects moved into chip gaps.

The Fourier series method of light curve fitting requires significant user interaction and is not a feasible method for fitting the light curves generated from the $100,000$ synthetic objects. Instead we used an adapted, simplified version of the light curve inversion method presented in Kaasalainen & Ďurech (2007). This technique uses the full data set to constrain all possible periods for a range of triaxial ellipsoid shapes that could be responsible for the observed light curve to determine the best-fitting period and shape solution. Due to our survey covering only a single opposition the shape/pole solution is unconstrained but the period solution is usually good. Ďurech et al. (2007) used this same technique to efficiently determine light curve periods from synthetic data of a simulated 10-year Pan-STARRS survey. Amplitudes for our synthetic light curves were then determined using the best-fit periods to fit sinusoids to the data.

It must be noted that the use of triaxial ellipsoids to generate the synthetic data followed by restricting the solution to be a triaxial ellipsoids will contaminate the final efficiency measurement as the real TALCS asteroids are almost certainly not perfect triaxial ellipsoids. Due to the artificial restrictions this puts on the fit parameters it is likely that the efficiency measurement if incorrect will be too large, especially for low-amplitude objects however an underestimation of the efficiency is not ruled out. To quantify the systematic impact of our technique we would need to generate and fit a series of different synthetic shapes based on a variety of physical models. Alternate methods for generating synthetic asteroid shapes and light curves include "genetic" combination of currently known shapes (Kaasalainen & Ďurech 2007) and randomized Gaussian-sphere models (*e.g.* Muinonen 1996, 1998; Vokrouhlický & Čapek 2002). While both methods would remove some uncertainty created when restricting the fit to the type of shape generated practical considerations prohibit their use for the current investigation. Both require finite element modeling to describe shapes and applications of scattering theory at each time step to generate light curves for each of the $100,000$ synthetic object, a task beyond the scope of this current work. Future investigations using these models will be conducted however for the present paper we will

restrict ourselves to the simplified model.

We restricted the range for period fitting to $1-30$ hours to reduce the number of wrong solutions and computation time. The lower limit was set to prevent false solutions that arise from the aliasing of the $\sim$ 15 min observing cadence. The upper bound was required to reduce the processing time for the synthetic survey to a reasonable level while maintaining good coverage of the real objects' rotation periods. Most real objects with $P > 30$ hours had large error bars on the period and increasing the range to *e.g.* $1-40$ hours would only increase the number of real objects contained in the range by five: less than 2% of the total sample.

Starting with all TALCS objects that had Fourier-fit rotation periods between $1-30$ hr we re-fit the observations using the light curve inversion method. A comparison between the two methods is shown in Fig 6. The top panel shows the percentage difference in the period between the two methods where the shaded bar indicates all errors greater than 30%. The median difference was 0.2% while a difference of 4.2% encompasses $\sim$ 66% ($\sim$ 1-σ) of the sample. We used the latter value as the error on the inversion period as shown in the lower panel. The automated fitting of the real objects recovered the Fourier period to within a 4.2% margin of error for over 85% of the sample as shown in Fig 6a. For the cases where there was a larger disagreement between the two methods, we found that the Fourier periods were randomly distributed while the inversion method periods showed a preference for $\sim$ 24 hour. This is likely the result of incomplete filtering of aliasing due to the nightly cycle of observations. In the remainder of this work we use the Fourier-fitted periods for interpretation of the data and restrict the use of inversion fitting to the determination of the observational biases.

To debias the survey as a function of rotation period and amplitude we divided the period-space into nine 3.25 hour wide bins and the amplitude space into eleven 0.05 mag wide bins. The number of objects, n_{ij}, observed in bin (i,j) in the period-amplitude space is given by:

$$n_{ij} = \epsilon_{ij} N_{ij} + \sum_m \sum_n c_{ijmn} N_{mn}$$

where N_{ij} is the number of objects generated in bin (i,j), ϵ_{ij} is the efficiency of recovery in that bin, and c_{ijmn} is the crosstalk between bins: the fraction of objects generated in bin (m,n) that are recovered in bin (i,j). In our simulation we found that only 14 of the $100,000$ objects were generated in one bin and recovered in another, thus $c_{ijmn} \sim 0$ in all cases. Nearly all the objects that were not correctly identified failed the fitting process and were placed in the $P = 0$, $\Delta m = 0$ bin (which was not covered in our debiasing). Thus, we

calculate the efficiency in each bin as:

$$\epsilon_{ij} = n_{ij}/N_{ij}$$

Figure 7 is a map of our light curve fitting efficiency in period-amplitude space. Objects with periods less than 20 hours and amplitudes larger than 0.3 mags are recovered with $90-100\%$ efficiency, with the efficiency decreasing for longer periods and smaller light curve amplitudes. Using these efficiencies we calculate the actual number of objects in each bin from the number of detected objects and set upper limits on the population for bins that do not contain real objects. This results in a grid of debiased populations for each period-amplitude bin. We then collapse these bins into distributions in period and amplitude space as discussed in § 6.

While the determination of the efficiency from the synthetic models is straight-forward, measuring the errors on that efficiency is considerably more difficult. Standard counting statistics (*e.g.* Poisson statistics) cannot be applied, as measurement of efficiency is not an inherently random process. Instead, we turn to the Jackknife method of error analysis used frequently in cosmology where a plethora of synthetic models exist and must be compared to a single sample, the Universe. Jackknife measurements have been used *e.g.* for determining covariance matrices in the large-scale structure power spectrum (Pope & Szapudi 2008; Henry et al. 2008), and a detailed mathematical description of this methodology can be found in both Gottleib (2001) and Lupton (1993). In short, the jackknife method involves removing a subset of the modeled population and recomputing the quantity of interest. This is done for all subsets and the variance in the computed quantity is then calculated, modulo a normalization factor accounting for the population size and subset size. Typically, each unit in the model is considered a subset and removed individually. For our synthetic simulation we computed errors by solving for the efficiency in each bin with each unit removed. Without exception we found that the errors in each bin due to the synthetic population were significantly smaller than the errors due to the small number statistics of the population of each bin. For example, the largest jackknife efficiency error on a single bin was 0.54 ± 0.02, while the bin with the largest fractional error was 0.11 ± 0.01 or a 9% error. This is well below the fractional errors due to the small numbers of objects in each bin ($\sigma \geq 15\%$), meaning that our synthetic model does not dominate the error on the final debiased value. Both jackknife and small-number errors are included in the final error for each debiased bin population.

5.2. Followup Observations

To further validate our light curve determination we obtained followup observations of a subsample of our TALCS targets. Using the Tektronix $2k \times 2k$ CCD on the University of Hawaii's 2.2 meter telescope located on Mauna Kea we reobserved 10 asteroids over two runs in January and March of 2008. Followup observations occurred when all targets were fainter than when initially observed and this, coupled with using a smaller telescope, meant that photometric errors were sometimes larger than in the TALCS data yielding less precise periods. The change in cadence between surveys, however, meant that aliasing problems in TALCS could be identified.

For seven of the followup objects we obtained enough data to make light curve determinations. Starting from the period initially found from the TALCS data we explored the surrounding period-space for the best-fitting period. All 5 objects for which we obtained sufficient followup coverage to re-measure their periods confirmed the original TALCS periods to within 2σ as shown in Table 4. The followup observations indicate that the U parameters for short period rotators from the initial CFHT data are correct, while objects initially determined to have very long periods ($P > 30$ hr) do indeed show rotation over long timescales. Amplitudes from the followup cannot be compared to those measured in the CFHT data as changes in pole orientation will alter light curve amplitude and shape.

6. Results

Given the agreement between our two period fitting technique as shown in Fig 6 and the agreement between the TALCS data and the followup observations in Table 4 we believe that the TALCS data is suitable for studying the distribution of Main Belt asteroid rotation rates and amplitudes. Figure 8 shows the Fourier-fit periods and amplitudes for the TALCS objects compared to previously published data.[4] Those data show a strong cutoff in period at 2.1 hours for objects larger than ~ 200 m. This rotation rate corresponds to the limit for a gravitationally bound aggregate, or "rubble pile" (Pravec & Harris 2000). Above this spin rate rubble pile asteroids should fission into binary systems with both components having periods below this limit (Scheeres 2007b; Walsh et al. 2008). The single exception in the known data was 2001 OE_{84} which was thought to be a unique circumstance of a very large monolithic body (Pravec et al. 2002).

---

[4]compiled by A.W. Harris, et al. in November 2008; available online: *http://www.minorplanetobserver.com/astlc/LightcurveParameters.htm*

The TALCS results are distinct from the previously known data in two ways: First, our survey detected six objects between 400 m and 2 km in diameter with periods less than two hours — faster than the critical spin rate for objects in this size range. Unfortunately, the accuracy of these spin rates are questionable because the light curve amplitude for these objects is close to the level of the photometric noise in the TALCS data sample. At this level the photometric noise may show random fluctuations at similar timescales which could lead to a false period identification. If these objects are not rotating above the spin barrier, it would appear that the gravitationally bound strength regime dominates Main Belt asteroids with $D \gtrsim 1$ km.

However, if any of these six fast rotators are confirmed by followup observations they will support a size-dependent strength for Solar system bodies as described by Holsapple (2007). That work examined the effect of a power-law distribution of cracks throughout a rocky object that induces a falloff in tensile strength with increasing diameter. Gravity stresses dominate the strength of the largest asteroids ($D > 10$ km) and a ~ 2 hr rotation limit exists even for bodies that are not rubble piles. For smaller objects the limiting critical spin rate (ω_{crit}) increases as their size decreases with $\omega_{crit} \propto D^{-1.2}$. Holsapple (2007)'s spin rate envelope encompasses both the largest objects rotating just beneath the two hour 'spin limit' as well as the smallest observed NEAs with rotation periods of $P \sim 1$ min. All six of our objects with $P < 2$ hr fall within the envelope created by an assumed static strength coefficient of $\kappa = 2.25 \times 10^7$ dynes cm$^{-3/2}$ as shown in Fig 8. (The static strength, k, would then be $k = \kappa \bar{r}^{-1/2}$ where $\bar{r}$ is the object's radius.) From our debiased distribution we expect that no more than $\sim 4\%$ of Main Belt objects are in the superfast rotation regime.

The second distinction between TALCS and previous surveys is the fraction of objects found to have very long rotation periods. We find in the TALCS data 41 asteroids with very long rotation periods ($P > 30$ hr) out of 278 objects with $D = 1 - 10$ km. The previously published data only contain 209 objects with periods greater than 30 hours out of 2669 for all sizes (87 of these have diameters between $1 - 10$ km out of a total known population of 871 in that same size range). This indicates that the biases against long period objects in previous surveys are severe and that long period objects are a significant fraction of the population of asteroids in the Main Belt, especially at smaller sizes. Pravec et al. (2008) find a similar fraction of $P > 30$ hr objects in their survey ($\sim 18\%$). Although the Yarkovsky-O'Keefe-Radzievskii-Paddack effect (YORP) can be used to explain an excess of slow rotators beyond that expected by collisional evolution (*e.g.* Rubincam 2000; Vokrouhlický & Čapek 2002; Bottke et al. 2006; Rossi, Marzari & Scheeres 2009, etc) it is unclear whether such a large excess of very slow rotators can be accounted for from this effect alone.

Vokrouhlický et al. (2007) show that as YORP slows the rotation of asteroids they

fall into a tumbling rotation state (non-principal axis rotation, or NPA). TALCS is not sensitive to NPA rotation, which can only be seen for data sets with complete coverage of at least two rotation periods. Additionally the two-dimensional Fourier series fit used to characterize NPA rotation requires an order of magnitude more data points than standard light curve determination, up to 1000 measurements for a high quality fit (Pravec et al. 2005) — well beyond the TALCS data set. The identification of a large population of tumbling, slow-rotating asteroids would support a YORP-driven model explaining the excess of slow-rotating objects. A competing possibility is that these objects have very high porosities which would be very efficient at absorbing impacts, preventing energy transfer from collisions to rotation. This theory has been used to explain the extremely large craters on (253) Mathilde as well as its slow rotation (Chapman 2002, and references therein) and could also explain the slow rotating population in our data. Additionally, as the TALCS data are not able to distinguish binary asteroids from single objects the large excess of slow-rotators could be close- or contact-binary objects with the observed light curve variations indicating the orbital period (Harris 2002).

Using our calculated efficiency in period-amplitude space (Fig 7) we debiased our distribution of light curves to find the actual Main Belt period-amplitude distribution. Collapsing that distribution in amplitude yields the period distribution shown in Fig 9a while Fig 9b shows the debiased spin rate distribution as well as the best-fitting Maxwellian with a mean spin rate of 4.19 rev day^{-1}. The Maxwellian was fit to a continuous distribution of debiased spin rates but is shown in a binned differential distribution as is common in the literature (*e.g.* Pravec et al. 2002, 2008, etc.). There are clear deviations from the fit at both high and low rotation rates and these excesses cannot be explained with collisional evolution alone but are likely due to the effects of other processes such as YORP (Rubincam 2000) or binary breakup (Harris 2002).

There were 180 out of 278 ($\sim 65\%$) of our period-fitted objects with rotation periods in the debiased range of 1 hr $< P <$ 30 hr. Outside this range, three objects ($\sim 1\%$) have $P <$ 1 hr and 41 objects ($\sim 15\%$) had $P >$ 30 hr. While the long period objects have uncertain periods, all show clear light curve variation that is significantly longer than 30 hr and can be treated with confidence as a long-period group. Finally, 54 of our targets ($\sim 19\%$) showed no variation in their light curves above the photometric noise. A lack of observable light curve will result from one of three scenarios: 1) the asteroid has a shape that is nearly a perfect sphere with no variation in albedo across the surface; 2) the object is rotating with a period much longer than the survey window, in the case of TALCS a multiple-month long period; or 3) the asteroid's rotation pole is aligned very closely with the line of sight. The YORP effect, used to explain the slow-rotator population, breaks down when the rotation period is a significant fraction of the orbital period (Vokrouhlický & Čapek 2002), making it

difficult to create objects with multi-month periods. It is also impossible to explain this large population of flat light curves with pole orientation alone without invoking an arbitrary and unphysical distribution of asteroid rotation axes which should be isotropic due to collisional processing (Salo 1987). Asteroid poles have been shown to be correlated for some families (Slivan et al. 2003) but this result cannot be applied to the Main Belt as a whole. Thus, a combination of shape and pole orientation are required to explain this population of objects with flat light curves.

In their recent work with a similar size data set, Pravec et al. (2008) found a flat spin rate distribution between 1 and 9 rev day^{-1} for asteroids with 3 km $\leq D \leq$ 15 km and an excess of objects with spin rates less than 1 rev day^{-1}. They cite the YORP effect as the cause of both the excess of slow-rotating objects and the flattening of the spin rate distribution. The characteristic time to double or halve the rotation rate of a 1 km object is $\sim 12 - 14$ Myr (Čapek & Vokrouhlický 2004) with approximately equal numbers of objects accelerating and decelerating, though both the amplitude and sign of YORP depend strongly on the shape of the asteroid (Scheeres 2007a). The short timescales imply that the rotation rate evolution of small Main Belt asteroids is dominated by YORP. Its effect is predicted to be independent of rotation rate until the object slows to periods of hundreds of hours. At very long rotation periods the current models break down (Vokrouhlický & Čapek 2002; Scheeres 2007a) and the object either remains at a slow rotation rate or enters a tumbling state and evolves as a non-principal axis rotator (Pravec et al. 2005). In this way, YORP can be used to explain some of the excess of slow rotators seen in both our data and that of Pravec et al. (2008).

Pravec et al. (2008) explain their flat distribution rate using the same YORP models, arguing that the independence of YORP from the current rotation rate leads to the erasure of any initial distribution function and results in a flat rotation rate distribution. They arrive at this conclusion using simulations of YORP evolution. In order to deal with the slow and fast boundary conditions imposed by tumbling and breakup, respectively, they reassign values of rotation rate changes when a boundary is reached. Objects slowed to 0 rev day^{-1} were reassigned a new value for change in spin rate, while objects reaching the upper limit were wrapped to the same spin rate in the opposite direction and allowed to slow from there. If instead we consider that objects with increasing rotation rates would eventually reach the disruption limit, at which point they might disrupt into a binary or shed mass (Scheeres 2007b; Walsh et al. 2008), the resultant shape change would lead to changes in the amplitude and/or sign of the YORP effect on the body, restarting its YORP evolution. After many YORP-timescales have passed we would find a population with a range of objects at different stages of YORP-braking that started at various times. This would lead to an increase in the number of objects with decreasing rotation rate as observed in the TALCS

data.

We believe the difference in the measured spin rate distribution between Pravec et al. (2008) and this work is due primarily to the differences in survey methods. TALCS was an untargeted survey while the Photometric Survey for Asynchronous Binary Asteroids (BinAstPhotSurvey) from Pravec et al. (2008) targeted individual objects. A Kolmogorov-Smirnov test was used to compare the two raw data sets and yielded a probability of $P = 0.005$ that they were drawn from the same population. An important point is that TALCS samples through the entire Main Belt while the BinAstPhotSurvey focused on the inner-Main Belt where the YORP effect is more pronounced due to the relative proximity to the Sun.

The binned differential distribution of debiased light curve amplitudes is shown in Fig 10. Most asteroid light curves have low amplitude but there exists a long tail in the distribution such that a few percent of asteroids have light curve amplitudes of $\gtrsim 1$ mag, suggesting that a similar fraction of asteroids are very elongated.

The unbinned cumulative distribution of the debiased light curve amplitudes shown in Fig 11 was created by giving each real object a weight based on the fitting efficiency of the bin in which it was located. We assumed that the fraction of debiased objects with "zero" amplitude (*i.e.* < 0.1 mag) was the same as the observed fraction of TALCS targets with no amplitude variation (19%). This assumption has only a small affect on the following analysis.

Assuming an isotropic distribution of rotation poles it is possible to convert an asteroid shape distribution ($f(b/a)$) into a light curve amplitude distribution or vice versa. Following Eq 1 and assuming random pole orientations we generated theoretical cumulative amplitude distributions from different polynomial functional forms for the shape distribution (testing orders 2, 3 and 4). We required that $f(b/a) = 0$ when $b/a = 0$ and allowed the other polynomial coefficients to vary to obtain the best fit to the debiased cumulative light curve amplitude distribution. Our fitting metric was the 'minimum greatest distance' between the generated and debiased amplitude distributions, similar to a K-S test. The second, third and fourth order polynomials in b/a yielded nearly identical fits so we discuss only the second order result as shown in Fig 11a.

The parameter with the strongest effect on the resultant shape distribution was the smallest "trusted" amplitude. As amplitudes decrease to within a few sigma of the photometric noise even the most robust automated or manual method of period fitting will begin to fit variations in the noise, especially in data sets with non-continuous coverage like TALCS. This results in a large number of low-amplitude fits for fainter targets, similar to the data from the Dermawan (2004) study. To study and mitigate this effect we reanalyzed the

TALCS data cropping all amplitudes less than 0.2 mag (a level confirmed by our successful followup observations, see § 5.2). The best fitting polynomial for the shape distribution in each case is

$$\begin{array}{lcl} \Delta m > 0.10 & : & f(\frac{b}{a}) = \left(\frac{b}{a}\right)^2 + 1.76\frac{b}{a} \\ \Delta m > 0.15 & : & f(\frac{b}{a}) = \left(\frac{b}{a}\right)^2 + 0.07\frac{b}{a} \\ \Delta m > 0.20 & : & f(\frac{b}{a}) = \left(\frac{b}{a}\right)^2 \end{array}$$

as shown in Fig 11a. (We have suppressed a normalizing constant that would guarantee that $\int_0^1 f(\frac{b}{a}) = 1$). The best fit is for $\Delta m > 0.2$ mag, where the greatest distance of $dist = 0.06$ can be compared to $dist = 0.07$ for $\Delta m > 0.15$ and $dist = 0.13$ for $\Delta m > 0.10$. The fact that the fit metric improves as we increase the cutoff amplitude could be indicative of an overestimate in the efficiency for fitting the lowest amplitude objects.[5] This could also indicate that a simple polynomial function is not a good representation of $f(b/a)$.

To test this possibility we performed an 'unparameterized' fit of the cumulative light curve amplitudes to a normalized 'step' distribution where $f(b/a) = f_i$, $0.1(i) < b/a \leq 0.1(1+i)$, for $i = 0, 9$. We assumed that the b/a values were distributed evenly within each 0.1 wide bin and integrated over all pole orientations. The set of labeled smooth curves in Fig 11b shows the cumulative fractional distribution in light curve amplitudes resulting from this test. As expected, as b/a increases the power moves to higher amplitudes in the cumulative distribution. We then determined the combination of contributions from each single step distribution that gave the best match to the observed distribution. That fit, the solid line labeled 'step fit' in Fig 11b, is better ($dist = 0.05$) than any of the polynomial fits *and* included all light curves with amplitude$>$ 0.1 mag.

Figure 12 shows the b/a probability distribution for the polynomial and step fits. Both types of fit are in general agreement in that they suggest most main belt objects are closer to being spherical ($b/a \lesssim 1$) than not. Furthermore, the three polynomial fits with different minimum amplitude cutoffs are roughly the same shape, two of which are essentially indistinguishable. The most interesting feature is the shape of the step fit — the fact that the quadratic polynomial is unable to fit the cumulative light curve amplitude distribution and the relatively large fraction of objects in the $0.3 < \frac{b}{a} \leq 0.4$ range of the step fit suggests a bi-modality in the shape of these asteroids.

Since only small b/a objects can produce large amplitude light curves, and since we expect large objects to be more spherical due to gravitational forces, we examined the di-

---

[5]As a further test, we performed the same analysis after removing all U=1 objects — those for which the periods and amplitudes are most uncertain. There was no significant change in the fit parameters and the result distribution in the b/a axis ratios were essentially identical.

ameter distribution for large and small amplitude objects. However, a K-S test between the diameter distributions of large (> 0.8 mag) and small (≤ 0.8 mag) light curve amplitude objects suggests that they are drawn from the same intrinsic distribution — at least within the TALCS sample there is no reason to suggest that small objects are more elongated than large objects in the size range sampled here.

7. Conclusions

We present results from the Thousand Asteroid Light Curve Survey (TALCS), a program designed to survey 12 deg^2 of sky on the ecliptic and find approximately 1000 Main Belt objects in an untargeted manner using the wide field MegaCam imager on CFHT and measure their light curves. Using the power of new software tools such as MegaPipe from the CADC and the Moving Object Processing System from the Pan-STARRS telescope we have determined orbits and photometry for all 828 moving objects identified in the survey to a 4 σ detection limit corresponding to a magnitude limit of $g' \sim 22.5$. Of these, 278 asteroids had photometry of sufficient quality to fit multi-order sinusoids to the light curve and derive their rotation period and amplitude. Through a combination of survey design, cadence, and synthetic light curve simulation we have debiased our sensitivity to both period and amplitude in order to derive the actual light curve period and amplitude distributions for the Main Belt.

We find that our debiased distribution of asteroids with rotation periods between $1\text{ hr} \leq P \leq 30\text{ hr}$ can be roughly fit by a Maxwellian distribution of rotation rates as expected for a collisionally evolved system (Salo 1987) and as found for the largest ($D > 40$ km) Main Belt objects (Pravec et al. 2002). However, there are strong deviations from a Maxwellian at high and low rotation rates as reported by Pravec et al. (2002) for a mostly Near Earth Object sample in the $0.15\text{ km} < D < 10\text{ km}$ size range. The over-density of very slow rotators in the TALCS data exceeds that of the NEO population.

The excess of slow-rotators becomes more pronounced including objects with periods $P > 30$ hr that fell outside our debiasing range. We found that nearly 15% of our survey sample had periods greater than 30 hours - a much larger fraction than found in previous surveys (*e.g.* Pravec et al. 2002, 2008). The discrepancy between TALCS and previous work is probably due to the untargeted design of our survey with wide observation spacing to allow sufficient coverage of long and short period objects.

We find 6 objects in our survey with diameters $D \geq 400$ m that are candidates for having rotation periods shorter than 2 hours. However, we note that the periods for these objects

are not well determined because of their low amplitude light curves. At small amplitudes and short periods it becomes difficult to disentangle noise fluctuations from the signal. Previous works (Pravec et al. 2002, and references therein) have shown that an empirical limit to rotation period exists at ~ 2 hours that can be explained as the rotation rate at which a gravitationally bound rubble-pile aggregate will break up or begin shedding mass. Objects with faster rotation rates must have a non-zero internal strength holding the object together in addition to gravity. Prior to TALCS, only a single object in this regime was confirmed (Pravec et al. 2002) and was believed to be an unusual and unique object. Our six asteroids may represent a small population of Main Belt bodies larger than 150 m (the previously observed size limit for objects with $P < 2$ hours) that have some internal strength while our debiasing results indicate this population to represent no more than 4% of the Main Belt in the $1 - 10$ km size range. If these objects are confirmed during followup observations they will lend support to the size-dependent strength model for rocky bodies (*e.g.* Holsapple 2007).

Finally, our fits to the debiased amplitude distribution ($\Delta m > 0.2$ mags) for objects with periods in the range 1 hr $\leq P \leq$ 30 hr indicates that the number distribution of asteroid shapes is proportional to $(b/a)^2$. Allowing smaller amplitudes produces worse fits and the power of the axis ratio shape distribution moves away from $b/a = 1$. A stepwise distribution in b/a provides a superior fit for $\Delta m > 0.1$ mag and suggests a large contribution ($\sim$75%) from asteroids with round shapes ($b/a \sim 0.8$) while the remaining objects form a distinct group of elongated objects with $b/a \sim 0.3$.

Acknowledgments

The authors are most grateful for the period determinations of the light curves provided by Petr Pravec. We would like to thank the CFHT staff for the hard work they put into scheduling and acquiring the complicated observing cadence required by the TALCS program; in particular, Pierre Martin, Mary Beth Laychak, Peter Forshay, and Adam Draginda. We also would like to thank Mikko Kaasalainen for his help adapting the automated period determination software and for his careful review of the paper. Many helpful comments were also provided by Dan Scheeres , Alan Harris (SSI), and an anonymous reviewer. J.M. was funded for this work under NASA PAST grant NNG06GI46G. J.Ď. was funded from GACR 205/07/P070 of the Czech grant agency and Research Program MSM0021620860 of the Czech Ministry of Education. This research used the facilities of the Canadian Astronomy Data Centre operated by the National Research Council of Canada with the support of the Canadian Space Agency. The authors wish to recognize and acknowledge the very

significant cultural role and reverence that the summit of Mauna Kea has always had within the indigenous Hawaiian community. We are most fortunate to have the opportunity to conduct observations from this sacred mountain.

REFERENCES

Bertin, E. & Arnouts, S., 1996, "SExtractor: Software for source extraction", A&A Supp., 117, 393.

Bottke, W.F., Cellino, A., Paolicchi, P. & Binzel, R.P., 2002, "An Overview of the Asteroids: The Asteroids III Perspective", Asteroids III (W. F. Bottke, Jr. et al., eds.), 3.

Bottke, W.F., Vokrouhlický, D., Rubincam, D.P. & Nesvorný, D., 2006, "The Yarkovsky and YORP Effects: Implications for Asteroid Dynamics", Annu. Rev. Earth Planet. Sci., 34, 157.

Boulade, O., et al., 2000, "Development of MegaCam, the next-generation wide-field imaging camera for the 3.6-m Canada-France-Hawaii Telescope", Proc. SPIE, 4008, 657.

Čapek, D. & Vokrouhlický, D., 2004, "The YORP effect with finite thermal conductivity", Icarus, 172, 526.

Chapman, C.R., 2002, "Cratering on Asteroids from *Galileo* and *NEAR Shoemaker*", Asteroids III (W. F. Bottke, Jr. et al., eds.), 315.

Dermawan, B., 2004, "Spin characteristics of very small main-belt asteroids", Ph. D. thesis, School of Science, University of Tokyo.

Ďurech, J., Kaasalainen, M., Warner, B.D., Fauerbach, M., Marks, S.A., Fauvaud, S., Fauvaud, M., Vugnon, J.-M., Pilcher, F., Bernasconi, L. & Behrend, R., 2009, "Asteroid models from combined sparse and dense photometric data", A&A, 493, 291.

Ďurech, J., Scheirich, P., Kaasalainen, M., Grav, T., Jedicke, R. & Denneau, L., 2007, "Physical models of asteroids from sparse photometric data", Proc. of IAU Symp. 236 (A. Milani, G.B. Valsecchi & D. Vokrouhlický, eds.), 191.

Gottleib, A.D., 2001, "Asymptotic accuracy of the jackknife variance estimator for certain smooth statistics", arXiv:math/0109002.

Gwyn, S.D.J., 2008, "MegaPipe: the MegaCam Image Stacking Pipeline at the Canadian Astronomical Data Centre", PASP, 120, 212.

Harris, A.W., 1996, “The Rotation Rates of Very Small Asteroids: Evidence for ’Rubble Pile’ Structure”, Lunar and Planetary Sci., 27, 493.

Harris, A.W., 2002, “On the Slow Rotation of Asteroids”, Icarus, 156, 184.

Harris, A.W. & Lagerros, J.S.V., 2002, “Asteroids in the Thermal Infrared”, Asteroids III (W. F. Bottke, Jr. et al., eds.), 205.

Harris, A.W. & Young, J.W., 1983, “Asteroid Rotation: IV. 1979 Observations”, Icarus, 54, 59.

Harris, A.W., Young, J.W., Bowell, E., Martin, L.J., Millis, R.L., Poutanen, M., Scarltriti, F., Zappalà, V., Schober, H.J., Debenhogne, H. & Zeigler, K.W., 1989, “Photoelectric Observations of Asteroids 3, 24, 60, 261, and 863”, Icarus, 77, 171.

Henry, J.P., Evrard, A.E., Hoekstra, H., Babul, A. & Mahdavi, A., 2008, “The X-ray cluster normalization of the matter power spectrum”, arXiv:0809.3832.

Holsapple, K.A., 2007, “Spin limits of Solar System bodies: From the small fast-rotators to 2003 EL61”, Icarus, 187, 500.

Ivezic, Z., Tabachnik, S., Rafikov, R. et al., 2001, “Solar System Objects Observed in the Sloan Digital Sky Survey Commissioning Data”, AJ, 122, 2749.

Jedicke, R. & Herron, J.D., 1997, “Observational Constraints on the Centaur Population”, Icarus, 127, 494.

Jedicke, R., Magnier, E.A., Kaiser, N. & Chambers, K.C., 2007, “The next decade of Solar System discovery with Pan-STARRS”, Proc. of IAU Symp. 236 (G.B. Valsecchi & D. Vokrouhlický, eds.), 341.

Kaasalainen, M., 2004, “Physical models of large number of asteroids from calibrated photometry sparse in time”, A&A, 422, L39.

Kaasalainen, M. & Ďurech, J., 2007, “Inverse problems of NEO photometry: Imaging the NEO population”, Proc. of IAU Symp. 236 (A. Milani, G.B. Valsecchi & D. Vokrouhlický, eds.), 151.

Kubica, J., Denneau, L., Grav, T., Heasley, J., Jedicke, R., Masiero, J., Milani, A., Moore, A., Tholen, D. & Wainscoat, R. J., 2005, “Efficient intra- and inter-night linking of asteroid detections using kd-trees”, Icarus, 189, 151.

Lacerda, P. & Jewitt, D., 2007, “Densities of Solar System objects from their rotational light curves”, AJ, 133, 1393.

Lacerda, P. & Luu, J., 2003, “On the detectability of lightcurves of Kuiper belt objects”, Icarus, 161, 174.

Lupton, R., 1993, “Statistics in Theory and Practice”, Princeton University Press, 46.

Megnier, E.A. & Cuillandre, J.-C., 2004, “The Elixir System: Data Characterization and Calibration at the Canada-France-Hawaii Telescope”, PASP, 116, 449.

Milani, A., Gronchi, G.F., Farnocchia, D., Knežević, Z., Jedicke, R., Denneau, L. & Pierfederici, F., 2008, “Topocentric orbit determination: Algorithms for the next generation surveys”, Icarus, 195, 474.

Muinonen, K. 1996. Light Scattering by Gaussian Random Particles. Earth Moon and Planets 72, 339-342.

Muinonen, K. 1998. Introducing the Gaussian shape hypothesis for asteroids and comets. Astronomy and Astrophysics 332, 1087-1098.

Polishook, D. & Brosch, N., 2008, “Photometry and Spin Rate Distribution of Small-Sized Main Belt Asteroids”, arXiv:0811.1223.

Pravec, P. & Harris, A.W., 2000, “Fast and Slow Rotation of Asteroids”, Icarus, 148, 12.

Pravec, P., Harris, A. W., Michałowski, T., 2002, “Asteroid Rotations”, Asteroids III (W. F. Bottke, Jr. et al., eds.), 113.

Pravec, P., Harris, A.W., Scheirich, P., et al., 2005, “Tumbling asteroids”, Icarus, 173, 108.

Pravec, P., Harris, A.W., Vokrouhlický, D., et al., 2008, “Spin rate distribution of small asteroids”, Icarus, 197, 497.

Pope, A.C. & Szapudi, I., 2008, “Shrinkage Estimation of the Power Spectrum Covariance Matrix”, MNRAS, 389, 766.

Rossi, A., Marzari, F. & Scheeres, D.J., “Computing the effects of YORP on the spin rate distribution of the NEO population”, in prep.

Rubincam, D.P., 2000, “Radiative Spin-up and Spin-down of Small Asteroids”, Icarus, 148, 2.

Salo, H., 1987, "Numerical Simulations of Collisions between Rotating Particles", Icarus, 70, 37.

Scheeres, D., 2007, "The dynamical evolution of uniformly rotating asteroids subject to YORP", Icarus, 188, 430.

Scheeres, D., 2007, "Rotational fission of contact binary asteroids", Icarus, 189, 370.

Slivan, S.M., Binzel, R.P., Crespo da Silva, L.D., Kaasalainen, M., Lyndaker, M.M., & Krčo, M., 2003, "Spin vectors in the Koronis family: comprehensive results from two independent analyses of 213 rotation lightcurves", Icarus, 162, 285.

Sullivan, R.J., Thomas, P.C., Murchie, S.L. & Robinson, M.S., 2002, "Asteroid Geology from *Galileo* and *NEAR Shoemaker* Data", Asteroids III (W. F. Bottke, Jr. et al., eds.), 331.

Tedesco, E.F., Cellino, A., Zappalà, V., 2005, "The Statistical Asteroid Model. I. The Main-Belt Population for Diameters Greater than 1 Kilometer", AJ, 129, 2869.

Tedesco, E.F., Noah, P.V., Noah, M. & Price, S.D., 2002, "The Supplemental IRAS Minor Planet Survey", AJ, 123, 1056.

Vokrouhlický, D., Breiter, S., Nesvorný, D. & Bottke, W.F., 2007, "Generalized YORP evolution: Onset of tumbling and new asymptotic states", Icarus, 191, 636.

Vokrouhlický, D. & Čapek, D., 2002, "YORP-Induced Long-Term Evolution of the Spin State of Small Asteroids and Meteoroids: Rubincam's Approximation", Icarus, 159, 449.

Walsh, K.J., Richardson, D.C. & Michel, P., 2008, "Rotational breakup as the origin of small binary asteroids", Nature, 454, 188.

Table 1. TALCS observing log

UT Obs Date	Central RA (hh:mm:ss)	Central Dec (dd:mm:ss)	Pointings	Images per Pointing	Exposure Time (sec)	TTI[a] (min)	Filter
09-14-2006	01:12:22.58	+07:40:08.9	12	17	30	15	g'
09-17-2006	01:10:17.19	+07:27:26.2	12	10	40	17	r'
09-20-2006	01:07:58.57	+07:13:19.4	2/6	35/30	20/30	2/8	g'
09-21-2006	01:07:09.68	+07:08:19.9	12	18	30	15	g'
09-22-2006	01:06:19.55	+07:03:12.3	12	17	30	15	g'
09-28-2006	01:00:56.75	+06:30:01.4	12	6	30	15	g'

[a]Transient Time Interval

Table 2. Asteroids identified in TALCS

TALCS ID[a]	MPC desig.	a (AU)	e	i (deg)	Ω (deg)	ω (deg)	τ_{peri} (mjd)	Epoch (mjd)	H_v (mag)	Orbital Arc (days)	N_{obs}	albedo[b]	Diameter (km)
1	39420	1.96	0.08	21.44	187.6	318.6	54364.16	53995	15.11	8	128	0.20	2.8
2	2006 RJ43	3.12	0.16	5.43	19.9	315.4	53851.05	53995	16.08	14	93	0.04	4.1
3	2006 ST62	3.08	0.17	7.63	187.8	160.2	53909.48	53996	16.22	14	89	0.04	3.8
4	145635	2.77	0.20	9.78	10.5	44.6	54140.97	53995	15.59	8	112	0.08	3.6
6	82495	2.70	0.08	5.48	19.0	353.0	54004.32	53995	16.05	8	77	0.08	2.9
7	2001 VZ123	3.03	0.16	6.10	15.7	21.2	54098.53	53996	16.21	8	64	0.04	3.8
8	70172	2.24	0.21	1.49	161.7	108.4	53740.54	53995	16.24	8	79	0.20	1.7
9	2006 RK43	2.76	0.12	8.94	14.7	237.2	53497.56	53995	16.16	14	85	0.08	2.8
10	2006 RF42	2.37	0.25	5.52	184.1	188.2	54011.22	53995	18.56	8	66	0.20	0.6
11	143096	2.62	0.15	14.33	11.4	105.8	54385.03	53995	15.63	14	119	0.08	3.5
12	135797	2.56	0.23	5.15	7.4	18.1	54044.18	53995	15.95	8	135	0.08	3.0
13	3186	3.12	0.19	0.79	169.7	197.5	53987.13	53995	13.00	8	130	0.04	17
14	4863	2.81	0.11	2.42	24.4	111.4	54541.10	53995	12.33	8	81	0.04	23
15	45302	2.45	0.20	2.66	15.5	1.1	54021.22	53995	15.65	8	61	0.20	2.2
16	2006 RD101	2.42	0.22	4.40	186.8	140.3	53900.42	53995	17.65	8	98	0.20	0.9
17	2006 RB39	2.37	0.15	6.88	11.0	328.0	53920.40	53995	17.51	7	62	0.20	0.9
18	44760	2.30	0.12	5.16	185.5	262.3	54232.91	53995	15.78	14	71	0.20	2.1
19	46603	2.44	0.17	2.00	15.4	81.3	54261.36	53995	15.59	8	130	0.20	2.3
20	138261	2.54	0.20	26.98	11.7	137.2	54492.53	53996	15.67	8	111	0.08	3.5
21	2006 RP42	4.22	0.58	1.44	23.9	86.1	54285.78	53995	15.86	7	64	0.04	4.5
23	2006 RY41	2.44	0.19	0.67	195.4	189.4	54044.39	53995	18.04	14	89	0.20	0.7
24	134527	2.29	0.21	23.32	188.6	73.7	53711.50	53995	15.90	8	73	0.20	2.0
25	2006 SU210	2.27	0.17	4.91	5.8	321.9	53901.41	53996	18.43	8	72	0.20	0.6
26	1999 VE85	2.37	0.22	0.81	197.3	117.8	53871.35	53995	17.77	8	92	0.20	0.8
27	144050	2.40	0.16	2.91	13.9	84.3	54268.30	53995	17.09	8	73	0.20	1.1
28	84478	2.65	0.23	1.59	5.2	27.8	54067.77	53995	15.67	14	95	0.08	3.5
29	2006 SZ48	2.29	0.13	7.23	186.6	195.2	54037.26	53995	17.71	8	72	0.20	0.9
30	107676	2.37	0.15	1.55	23.0	182.7	53407.47	53995	16.54	8	80	0.20	1.5
31	32705	3.11	0.11	16.67	10.5	9.0	54040.04	53995	14.02	8	86	0.04	11
32	85051	2.59	0.19	12.73	7.4	1.4	54001.76	53995	14.93	14	75	0.08	4.9
34	2006 RA39	2.36	0.23	1.82	356.5	307.2	53844.56	53995	17.39	8	47	0.20	1.0
35	8783	2.28	0.17	5.46	193.6	352.9	54608.72	53995	13.97	8	110	0.20	4.8
36	80952	2.54	0.06	8.60	6.3	111.1	54410.60	53995	15.82	8	76	0.08	3.2

Table 2—Continued

TALCS ID[a]	MPC desig.	a (AU)	e	i (deg)	Ω (deg)	ω (deg)	τ_{peri} (mjd)	Epoch (mjd)	H_v (mag)	Orbital Arc (days)	N_{obs}	albedo[b]	Diameter (km)
37	8325	3.20	0.05	6.83	6.3	287.6	53582.09	53995	13.95	14	87	0.04	11
38	139216	2.58	0.25	11.31	190.7	96.6	53769.86	53995	16.39	14	140	0.08	2.5
39	103405	2.41	0.19	0.42	291.8	78.9	54005.39	53995	16.64	14	90	0.20	1.4
41	2002 PM155	2.42	0.19	0.81	0.7	360.0	53980.51	53995	17.82	14	111	0.20	0.8
42	2006 RX91	2.61	0.19	3.03	359.2	329.0	53878.38	53995	17.60	8	73	0.08	1.4
43	2006 RW35	3.16	0.11	5.26	8.4	337.6	53885.16	53995	15.27	14	107	0.04	5.9
44	58477	2.23	0.19	4.97	193.3	92.6	53790.02	53995	15.52	14	81	0.20	2.4
45	103148	2.38	0.16	4.17	194.6	180.9	54018.44	53995	16.45	8	79	0.20	1.5
46	139800	2.78	0.02	6.34	196.0	234.5	54269.26	53995	15.87	14	92	0.08	3.2
49	2006 RJ60	2.66	0.30	2.91	186.4	225.8	54103.03	53995	17.65	14	134	0.08	1.4
51	142519	2.58	0.17	12.37	188.9	167.5	53960.98	53995	16.25	14	137	0.08	2.6
52	1999 TK33	2.31	0.14	6.95	9.4	301.2	53836.13	53996	16.85	8	65	0.20	1.3
53	2006 RD92	2.38	0.20	3.14	191.0	116.2	53839.06	53995	17.92	14	132	0.20	0.8
54	88871	2.95	0.08	1.81	184.1	169.4	53918.86	53995	15.87	8	73	0.04	4.5
55	2002 VA106	2.64	0.17	4.19	6.4	56.7	54166.30	53995	16.54	14	94	0.08	2.3
58	75555	2.46	0.09	6.39	9.8	16.2	54054.03	53995	16.44	8	130	0.20	1.5
59	2002 UB14	2.62	0.16	12.87	189.6	264.0	54279.95	53995	16.02	14	93	0.08	2.9
60	161723	3.15	0.14	5.05	194.5	202.8	54113.48	53995	15.58	14	89	0.04	5.1
62	78293	2.39	0.11	0.14	249.1	135.6	54045.54	53995	16.14	8	129	0.20	1.8
63	2005 GC60	2.27	0.20	22.67	9.1	269.5	53763.59	53995	16.38	8	124	0.20	1.6
100	47993	2.47	0.22	3.34	15.0	241.9	53654.24	53996	15.40	8	58	0.20	2.5
101	2006 RE18	3.96	0.31	10.32	10.5	333.0	53890.45	53998	15.43	8	79	0.04	5.5
102	2006 RC105	3.09	0.28	0.74	41.8	299.6	53916.66	53996	17.46	14	52	0.04	2.1
103	117685	2.38	0.18	2.23	18.6	278.0	53800.80	53996	17.09	14	52	0.20	1.1
104	2006 SN2	3.13	0.12	11.81	187.8	211.9	54127.37	53996	16.03	8	59	0.04	4.1
105	83913	3.04	0.07	2.42	16.6	308.2	53781.68	53997	15.11	14	62	0.04	6.3
106	2006 RC39	2.26	0.18	4.11	181.7	140.2	53886.63	53997	17.83	14	90	0.20	0.8
107	2006 SZ81	2.32	0.25	4.89	180.4	180.3	53985.57	53998	18.49	8	72	0.20	0.6
108	129989	2.35	0.38	1.13	149.5	159.8	53903.33	53996	16.93	14	61	0.20	1.2
109	2006 RO19	2.34	0.12	6.48	16.4	26.5	54094.91	53996	17.67	14	64	0.20	0.9
110	2006 RK39	2.25	0.24	4.87	181.1	190.0	54007.44	53998	18.99	8	82	0.20	0.5
111	2002 UE16	2.60	0.17	9.12	186.2	246.5	54197.47	53998	16.82	5	59	0.08	2.0
112	2005 ED209	2.44	0.19	2.47	33.9	241.7	53717.32	53996	17.13	8	56	0.20	1.1

Table 2—Continued

TALCS ID[a]	MPC desig.	a (AU)	e	i (deg)	Ω (deg)	ω (deg)	τ_{peri} (mjd)	Epoch (mjd)	H_v (mag)	Orbital Arc (days)	N_{obs}	albedo[b]	Diameter (km)
113	2001 RW30	2.79	0.08	1.70	153.0	219.3	54003.41	53996	16.31	8	62	0.08	2.6
114	15124	2.85	0.19	2.20	41.0	228.7	53605.89	53996	14.01	8	56	0.04	11
115	136992	2.51	0.05	5.66	17.3	168.8	54704.07	53998	15.88	11	65	0.08	3.1
116	140037	3.02	0.16	9.63	190.7	250.2	54277.84	53996	15.39	7	45	0.04	5.6
117	2001 XA221	3.10	0.21	3.07	17.1	339.0	53946.63	53996	16.36	14	69	0.04	3.6
118	55430	3.03	0.17	1.55	180.1	128.1	53747.73	53996	14.58	8	50	0.04	8.1
119	17148	3.15	0.19	9.65	187.9	172.1	53955.58	53996	14.05	8	53	0.04	10
120	2001 UL84	3.02	0.14	10.19	13.9	56.2	54240.67	53996	15.68	8	61	0.04	4.9
121	32282	3.12	0.15	0.75	37.4	293.7	53826.95	53996	14.66	8	62	0.04	7.8
122	2006 RY91	3.20	0.10	4.11	194.1	182.5	54022.07	53998	16.04	8	122	0.04	4.1
123	2006 RA43	2.26	0.20	7.28	8.2	325.7	53923.00	53998	18.87	8	111	0.20	0.5
124	2006 UB75	2.68	0.26	5.03	186.3	102.7	53763.35	53998	16.91	8	116	0.08	2.0
125	1995 SH19	3.00	0.05	0.64	186.8	327.4	54731.40	53998	15.64	8	98	0.04	5.0
126	2006 SZ2	2.22	0.25	6.10	8.0	21.2	54043.61	53998	19.01	5	100	0.20	0.5
127	2006 RL40	3.07	0.07	9.83	190.2	216.6	54166.77	53998	15.41	8	69	0.04	5.5
128	116573	2.35	0.21	5.72	185.7	243.3	54150.16	53998	16.79	8	129	0.20	1.3
129	142942	2.62	0.14	4.20	8.9	14.6	54043.58	53998	16.54	8	116	0.08	2.3
130	84045	2.48	0.21	1.11	13.5	342.0	53966.91	53998	16.32	8	127	0.20	1.6
131	46748	2.64	0.32	1.86	182.2	95.3	53755.27	53998	17.01	5	100	0.08	1.9
132	138585	3.16	0.18	11.43	190.7	166.9	53949.24	53997	15.50	8	120	0.04	5.3
133	79493	3.19	0.13	16.62	10.4	191.0	53024.75	53997	14.85	8	133	0.04	7.1
134	2006 RN26	2.67	0.30	4.68	7.8	16.6	54037.84	53998	17.36	8	118	0.08	1.6
135	22988	2.42	0.15	1.58	212.2	24.1	53542.09	53996	15.58	8	54	0.20	2.3
136	142135	2.47	0.06	2.80	356.3	29.5	54058.14	53996	16.41	14	65	0.20	1.6
137	55423	3.15	0.00	9.90	7.8	138.7	54765.62	53996	14.93	14	69	0.04	6.9
138	137598	2.37	0.16	2.91	8.3	130.9	54424.12	53996	16.26	8	77	0.20	1.7
139	2006 SC81	2.61	0.13	1.51	198.2	134.6	53879.69	53997	17.30	8	78	0.08	1.6
140	90050	2.72	0.14	1.21	248.8	80.8	53861.34	53996	16.12	8	57	0.08	2.8
141	79331	2.98	0.12	1.03	263.0	68.0	53835.80	53996	15.53	8	50	0.04	5.2
142	140141	2.96	0.16	1.38	342.1	106.7	54311.54	53998	15.34	8	72	0.04	5.7
143	29019	3.06	0.08	5.39	204.4	284.1	54586.35	53996	14.06	8	55	0.04	10
144	136360	2.41	0.25	4.24	359.7	26.5	54041.29	53998	16.47	8	61	0.20	1.5
145	29760	2.78	0.26	2.44	357.5	149.8	54521.34	53998	14.15	8	64	0.08	7.0

Table 2—Continued

TALCS ID[a]	MPC desig.	a (AU)	e	i (deg)	Ω (deg)	ω (deg)	τ_{peri} (mjd)	Epoch (mjd)	H_v (mag)	Orbital Arc (days)	N_{obs}	albedo[b]	Diameter (km)
146	45115	2.36	0.18	1.39	222.9	106.1	53898.19	53996	15.87	14	61	0.20	2.0
147	138256	2.62	0.06	14.55	192.5	232.4	54212.08	53997	16.79	14	83	0.08	2.1
148	2002 TK139	2.57	0.21	17.41	6.1	25.8	54062.44	53997	17.35	8	73	0.08	1.6
149	140121	3.30	0.33	0.81	251.3	66.0	53835.88	53997	16.52	8	75	0.04	3.3
150	141061	3.19	0.23	4.91	6.2	90.6	54341.36	53997	15.50	8	67	0.04	5.3
151	2006 RB92	2.77	0.04	6.26	7.4	35.6	54135.61	53996	16.55	14	81	0.08	2.3
152	2004 FK93	2.75	0.15	9.15	6.8	129.6	54503.60	53996	15.96	8	54	0.08	3.0
153	143917	2.60	0.18	3.18	2.4	234.9	53494.91	53996	15.64	14	59	0.08	3.5
154	141977	2.40	0.12	6.18	6.6	26.5	54069.87	53996	16.50	14	53	0.20	1.5
155	142567	2.57	0.10	21.83	191.4	246.4	54238.55	53998	16.27	5	69	0.08	2.6
156	136061	2.66	0.21	3.17	2.2	67.5	54178.06	53996	16.11	8	49	0.08	2.8
157	135039	2.76	0.28	6.18	7.6	50.2	54126.71	53998	15.13	7	59	0.08	4.4
158	2001 UA61	2.94	0.08	1.24	222.7	227.2	54350.32	53996	15.84	14	60	0.04	4.5
159	140041	2.94	0.14	1.19	211.2	128.8	53877.92	53995	16.46	8	61	0.04	3.4
160	81345	2.61	0.11	2.99	8.6	67.9	54229.31	53996	15.84	8	62	0.08	3.2
161	113166	2.55	0.20	2.81	190.6	168.1	53970.24	53996	16.49	8	53	0.08	2.4
162	30470	3.03	0.20	3.20	201.3	74.5	53602.66	53996	14.14	8	62	0.04	9.9
163	50317	2.55	0.16	4.59	196.9	336.4	54634.88	53996	15.33	14	69	0.08	4.0
164	27450	2.68	0.05	1.47	209.1	43.0	53488.21	53996	15.49	8	48	0.08	3.8
165	2002 VM59	2.63	0.11	12.59	191.5	280.4	54378.79	53996	16.21	8	55	0.08	2.7
166	2006 TN66	2.69	0.17	7.28	8.4	49.4	54150.94	53996	17.13	7	41	0.08	1.8
200	2001 XV127	3.10	0.16	1.86	195.2	174.9	53999.38	53997	15.81	14	135	0.04	4.6
224	2000 QG136	3.11	0.14	0.63	191.0	171.9	53963.10	53996	15.46	8	82	0.04	5.4
245	57560	3.09	0.15	1.05	176.5	284.3	54402.91	53997	14.86	14	61	0.04	7.1
247	40003	3.20	0.12	1.12	18.7	155.3	54915.62	53998	14.90	14	83	0.04	7.0
248	73727	2.43	0.14	4.66	16.2	124.4	54452.85	53999	16.51	11	44	0.20	1.5
249	2001 XR170	3.15	0.18	0.27	131.4	263.2	54097.83	53999	15.92	11	50	0.04	4.4
250	24215	2.42	0.05	1.68	192.3	107.2	53758.01	53996	15.13	14	51	0.20	2.8
251	137587	2.42	0.09	1.21	23.3	280.3	53785.97	53997	17.45	14	44	0.20	1.0
252	101878	2.23	0.18	0.60	156.4	144.6	53832.73	53996	16.90	14	60	0.20	1.2
253	30427	2.94	0.15	1.76	177.7	155.7	53862.13	53996	14.54	8	46	0.04	8.2
254	12527	2.36	0.14	7.17	184.0	109.3	53775.34	53996	14.29	8	52	0.20	4.1
255	100468	2.25	0.18	5.83	12.1	309.7	53888.96	53998	16.94	5	38	0.20	1.2

Table 2—Continued

TALCS ID[a]	MPC desig.	a (AU)	e	i (deg)	Ω (deg)	ω (deg)	τ_{peri} (mjd)	Epoch (mjd)	H_v (mag)	Orbital Arc (days)	N_{obs}	albedo[b]	Diameter (km)
256	2006 UZ213	2.68	0.13	6.97	16.3	7.1	54045.15	53998	17.17	8	60	0.08	1.7
257	2001 XA147	3.15	0.19	1.37	151.6	263.2	54172.88	53998	15.84	5	46	0.04	4.5
258	27962	2.76	0.20	1.55	26.7	340.6	53993.60	53997	16.18	8	63	0.08	2.7
259	2003 YH137	2.27	0.11	1.79	20.6	56.3	54194.19	53998	17.87	14	80	0.20	0.8
260	65384	2.37	0.18	1.43	67.1	189.9	53650.83	53998	16.25	8	60	0.20	1.7
262	137632	2.31	0.21	1.69	169.4	214.9	54036.23	53997	17.73	8	62	0.20	0.8
263	2006 RU104	3.22	0.14	1.57	151.3	139.4	53608.00	53997	16.02	8	55	0.04	4.2
264	149259	2.59	0.17	3.60	23.9	324.0	53934.99	53998	16.51	5	45	0.08	2.3
265	2006 RD57	2.54	0.28	5.94	12.8	6.4	54024.33	53998	18.25	14	56	0.08	1.1
266	140391	3.01	0.27	0.38	31.5	74.8	54331.91	53998	15.06	5	45	0.04	6.5
267	141641	2.22	0.15	0.43	27.5	238.8	53708.97	53998	17.57	14	109	0.20	0.9
268	2004 BU22	2.33	0.20	2.60	184.4	277.5	54250.10	53998	17.51	8	125	0.20	0.9
269	2004 FQ92	3.05	0.06	7.98	191.6	30.0	53212.51	53996	15.55	14	62	0.04	5.2
270	2006 SF107	3.14	0.27	4.14	5.1	318.6	53846.67	53996	16.95	14	58	0.04	2.7
271	66914	2.40	0.18	1.18	351.4	117.0	54293.03	53997	16.72	8	48	0.20	1.4
272	2006 SW275	3.15	0.07	9.48	190.9	230.4	54246.40	53998	16.06	14	110	0.04	4.1
273	83669	3.01	0.13	12.89	10.4	188.8	53103.46	53997	15.10	14	56	0.04	6.4
274	137987	2.59	0.17	7.95	193.0	343.9	54681.14	53997	16.00	8	53	0.08	3.0
276	33108	2.93	0.26	2.27	357.8	124.7	54418.60	53998	14.13	5	36	0.04	9.9
277	138167	2.59	0.05	2.10	351.5	28.7	54040.12	53996	16.39	8	80	0.08	2.5
278	2002 PY87	2.44	0.20	1.35	225.2	105.3	53903.26	53998	17.54	11	38	0.20	0.9
279	2006 RZ59	2.61	0.26	3.67	353.4	323.9	53869.80	53996	17.46	8	39	0.08	1.5
280	55523	3.08	0.10	11.17	7.6	287.1	53641.27	53997	14.13	14	62	0.04	9.9
281	2006 RP32	2.57	0.18	8.65	193.3	175.1	53999.97	53998	17.34	11	54	0.08	1.6
282	2006 RF93	3.31	0.01	1.37	329.5	87.8	54271.09	53996	15.32	14	62	0.04	5.7
283	142659	2.58	0.27	3.16	353.2	322.6	53868.41	53998	16.65	8	41	0.08	2.2
284	2002 XW31	2.71	0.18	3.80	358.4	357.7	53959.08	53998	16.94	5	45	0.08	1.9
285	2006 RG92	2.98	0.15	0.81	357.0	44.2	54115.52	53996	16.59	14	78	0.04	3.2
287	2004 BW95	2.33	0.23	22.76	9.1	105.3	54279.26	53996	16.63	8	78	0.20	1.4
288	2001 YH142	3.13	0.11	0.94	337.2	19.8	53932.69	53996	16.12	14	52	0.04	4.0
289	2006 RC06	2.42	0.25	4.25	1.5	337.6	53934.15	53997	17.67	8	58	0.20	0.9
290	83391	2.86	0.03	1.20	341.1	174.5	54693.33	53997	15.10	8	54	0.04	6.4
291	25186	2.53	0.15	13.53	10.4	240.9	53570.93	53997	14.72	14	80	0.08	5.4

Table 2—Continued

TALCS ID[a]	MPC desig.	a (AU)	e	i (deg)	Ω (deg)	ω (deg)	τ_{peri} (mjd)	Epoch (mjd)	H_v (mag)	Orbital Arc (days)	N_{obs}	albedo[b]	Diameter (km)
292	141258	3.09	0.07	2.01	8.7	349.7	53932.58	53996	15.24	14	81	0.04	5.9
293	79782	2.53	0.26	8.83	8.4	14.9	54034.24	53997	15.88	14	62	0.08	3.1
294	1999 TK176	2.31	0.17	2.61	2.7	331.0	53910.04	53996	17.88	14	65	0.20	0.8
295	144093	2.35	0.08	0.52	256.1	163.0	54154.07	53998	17.40	5	44	0.20	1.0
307	81326	2.57	0.14	0.61	1.9	74.3	54213.76	53999	16.22	14	84	0.08	2.7
357	755	3.17	0.15	3.25	177.3	40.1	53152.66	53999	10.13	14	85	0.04	62
359	22319	2.39	0.19	1.84	41.6	250.6	53784.15	54000	15.54	14	56	0.20	2.3
374	74642	2.26	0.11	1.88	179.2	186.3	53994.73	54002	17.20	7	41	0.20	1.1
375	81802	2.83	0.09	2.44	184.5	53.3	53401.91	54002	15.93	7	41	0.04	4.3
376	2002 TE241	2.53	0.20	4.54	11.6	19.7	54063.79	54002	17.87	7	33	0.08	1.3
377	2006 SO384	2.76	0.21	8.33	13.5	315.1	53876.65	54002	17.63	7	37	0.08	1.4
378	136805	2.47	0.14	1.21	175.8	130.1	53799.15	54000	17.66	14	81	0.20	0.9
379	2001 GG01	2.27	0.13	3.05	21.3	68.6	54227.40	54001	17.92	14	87	0.20	0.8
381	20571	2.24	0.10	2.09	188.2	53.5	53594.61	54002	15.49	14	92	0.20	2.4
382	138284	2.60	0.08	2.77	186.8	314.0	54521.28	54001	16.56	14	71	0.08	2.3
383	57802	3.21	0.11	4.93	12.0	161.8	54921.82	54002	15.08	14	115	0.04	6.4
384	2006 SO2	2.54	0.21	0.84	355.0	14.8	54003.43	54000	18.26	14	116	0.08	1.1
385	2002 UN65	2.52	0.02	13.32	192.7	160.2	53935.40	54001	16.97	14	75	0.08	1.9
386	2006 RV41	3.20	0.29	4.96	8.7	316.5	53860.85	54000	17.45	14	69	0.04	2.2
387	2006 UO213	3.47	0.11	9.61	8.3	333.7	53845.52	54000	15.93	14	54	0.04	4.3
388	44770	2.30	0.19	5.03	198.0	35.0	53575.82	54000	16.19	14	68	0.20	1.7
389	76949	2.21	0.22	4.20	7.9	353.3	53989.09	54001	16.46	14	49	0.20	1.5
390	55924	3.11	0.03	10.52	11.5	88.5	54477.48	54002	15.20	7	42	0.04	6.1
391	103914	2.63	0.21	5.47	4.4	333.2	53914.74	53999	15.71	14	50	0.08	3.4
392	142278	2.49	0.17	2.39	199.4	242.8	54219.02	54002	16.84	7	39	0.20	1.3
393	2005 JZ15	2.54	0.11	2.00	194.9	131.8	53859.11	54000	17.64	14	48	0.08	1.4
395	81308	2.56	0.17	3.04	352.5	43.8	54081.53	54002	15.94	7	42	0.08	3.1
396	45776	3.03	0.18	0.98	285.7	330.7	53486.99	53999	14.98	14	57	0.04	6.7
397	2006 UJ47	2.41	0.08	6.83	5.6	94.6	54307.01	53999	17.48	14	71	0.20	1.0
1034	2006 SP81	2.39	0.17	5.22	186.7	176.1	53985.73	53996	19.42	14	93	0.20	0.4
1035	2006 RM113	3.10	0.09	10.43	185.7	189.0	54012.67	53996	17.30	8	41	0.04	2.3
1049	2006 SK147	2.46	0.23	2.99	204.0	252.8	54242.39	53997	18.30	8	50	0.20	0.7
1050	2006 RT41	2.76	0.08	4.14	5.5	22.0	54071.42	53997	17.68	14	35	0.08	1.4

Table 2—Continued

TALCS ID[a]	MPC desig.	a (AU)	e	i (deg)	Ω (deg)	ω (deg)	τ_{peri} (mjd)	Epoch (mjd)	H_v (mag)	Orbital Arc (days)	N_{obs}	albedo[b]	Diameter (km)
1051	2006 SV242	3.02	0.03	2.78	200.7	188.0	54091.13	53997	17.25	14	49	0.04	2.4
1054	173974	3.12	0.18	1.81	195.2	163.8	53956.98	53997	15.89	8	113	0.04	4.4
1063	2006 SP177	2.98	0.20	1.50	34.6	320.1	53943.95	53997	17.96	8	53	0.04	1.7
1068	2006 RT117	2.76	0.15	8.17	14.5	192.0	53256.63	53997	17.23	14	56	0.08	1.7
1071	2006 RQ106	2.36	0.22	4.74	357.8	298.1	53815.08	53996	19.54	8	43	0.20	0.4
1073	2006 RB57	2.64	0.17	3.75	179.4	243.6	54165.25	53996	17.10	8	64	0.08	1.8
1076	2006 SD65	3.21	0.17	3.57	357.2	89.4	54327.05	53996	17.04	8	48	0.04	2.6
1077	2006 SE242	2.55	0.13	10.26	9.0	323.4	53878.23	53996	18.63	8	52	0.08	0.9
1079	2006 RY112	2.29	0.21	0.98	45.6	241.5	53793.04	53996	20.00	14	43	0.20	0.3
1083	2006 RR110	2.81	0.05	3.08	188.8	78.7	53527.61	53996	17.43	14	54	0.04	2.2
1087	2006 RJ109	3.16	0.13	1.72	191.2	260.3	54373.73	53996	18.01	8	71	0.04	1.7
1093	2006 RY110	2.33	0.19	5.70	13.8	162.8	54570.24	53996	18.67	8	45	0.20	0.6
1094	2006 RV92	3.21	0.21	3.41	211.2	231.1	54289.55	53996	16.78	8	41	0.04	2.9
1098	2006 SR2	2.57	0.15	0.40	244.5	180.8	54175.48	53996	18.80	8	37	0.08	0.8
1100	2006 SP242	2.43	0.21	2.17	352.4	25.8	54026.03	53996	19.34	8	42	0.20	0.4
1105	2006 RK113	3.02	0.12	2.13	25.2	302.5	53814.14	53996	18.17	8	55	0.04	1.5
1109	2006 RH108	3.10	0.18	8.75	192.0	78.4	53554.02	53996	18.03	8	47	0.04	1.7
1110	8906	3.20	0.20	1.38	146.7	263.6	54151.65	53996	13.09	8	49	0.04	16
1112	2006 RS111	3.17	0.26	2.26	44.6	85.6	54507.50	53996	17.72	8	29	0.04	1.9
1113	2006 SY146	3.05	0.09	9.25	194.5	207.6	54136.57	53996	18.25	8	50	0.04	1.5
1117	2006 SH242	2.82	0.09	1.34	216.2	225.7	54292.08	53996	17.68	8	36	0.04	1.9
1118	2006 RC110	3.20	0.12	4.32	8.3	86.4	54398.34	53996	18.01	14	45	0.04	1.7
1119	2006 RJ111	3.06	0.10	3.38	186.0	70.8	53425.76	53996	17.44	8	38	0.04	2.2
1120	2006 SA107	2.68	0.08	5.33	190.4	204.1	54089.04	53996	17.17	14	85	0.08	1.7
1125	2006 RK108	2.74	0.09	7.30	191.8	9.4	53230.63	53996	17.35	8	51	0.08	1.6
1127	2006 SP2	2.93	0.21	12.51	193.0	253.3	54271.99	53996	18.36	14	43	0.04	1.4
1132	2006 RM43	2.94	0.24	6.90	16.6	13.0	54059.07	53996	18.04	8	48	0.04	1.6
1138	148471	2.35	0.14	1.61	146.5	70.8	53464.19	53996	17.89	14	45	0.20	0.8
1144	2005 KO01	2.74	0.21	4.59	187.4	78.1	53617.72	53996	16.70	8	65	0.08	2.1
1154	2006 RN112	2.72	0.15	5.03	15.6	76.7	54297.20	53996	17.96	8	56	0.08	1.2
1168	2006 RP92	3.09	0.07	1.14	300.5	60.5	53953.33	53996	16.38	8	46	0.04	3.5
1170	2006 SQ177	3.08	0.16	1.43	159.3	115.5	53565.44	53996	16.62	8	51	0.04	3.2
1172	2006 SN147	2.39	0.17	0.47	246.4	153.2	54083.99	53996	19.47	8	34	0.20	0.4

Table 2—Continued

TALCS ID[a]	MPC desig.	a (AU)	e	i (deg)	Ω (deg)	ω (deg)	τ_{peri} (mjd)	Epoch (mjd)	H_v (mag)	Orbital Arc (days)	N_{obs}	albedo[b]	Diameter (km)
1177	2006 SJ147	2.91	0.10	0.97	270.3	167.4	54287.74	53996	16.91	8	38	0.04	2.8
1179	2006 RG108	2.35	0.19	1.22	342.2	43.5	54043.89	53996	21.01	8	34	0.20	0.2
1181	2006 SH177	2.40	0.17	0.93	168.0	244.4	54117.56	53996	19.12	14	90	0.20	0.5
1184	2006 SQ2	2.98	0.11	0.52	304.1	181.5	54527.10	53996	16.77	14	58	0.04	2.9
1185	2006 SS147	2.84	0.09	1.20	334.4	8.0	53886.82	53996	18.01	14	48	0.04	1.7
1191	2006 RX115	3.03	0.28	1.45	8.9	3.9	54011.07	53996	19.64	8	61	0.04	0.8
1195	2006 RL109	3.20	0.19	3.46	186.3	214.9	54119.37	53996	18.38	14	72	0.04	1.4
1200	2006 RD115	3.15	0.10	1.76	3.8	348.6	53916.35	53996	17.75	8	44	0.04	1.9
1206	2006 RR108	2.63	0.11	2.30	355.5	154.3	54563.51	53996	18.32	8	48	0.08	1.0
1209	2006 SC107	2.80	0.07	5.04	193.9	212.3	54143.23	53996	17.79	14	53	0.04	1.8
1218	2006 RE113	3.10	0.11	1.37	154.9	39.0	53012.48	53996	17.45	14	49	0.04	2.2
1222	2006 SG107	2.39	0.18	0.46	242.0	106.5	53949.46	53996	19.10	8	54	0.20	0.5
1224	2006 RO110	3.01	0.19	3.97	188.2	324.1	54653.22	53996	16.77	8	59	0.04	2.9
1227	2006 RO92	3.11	0.11	10.80	197.7	85.8	53585.07	53998	16.59	5	22	0.04	3.2
1229	2006 RK107	2.30	0.15	6.19	193.3	168.5	53984.73	53996	20.62	8	32	0.20	0.2
1235	2001 UG87	3.07	0.08	2.00	38.2	314.4	53909.21	53996	16.72	8	39	0.04	3.0
1238	2006 RP105	2.37	0.12	0.41	262.8	321.0	53480.24	53996	18.40	8	42	0.20	0.6
1239	2006 RJ107	2.80	0.09	4.07	354.7	345.6	53881.46	53996	18.13	8	47	0.08	1.1
1250	2006 RW91	2.35	0.21	0.80	324.1	55.6	54027.11	53996	19.26	8	48	0.20	0.4
1252	2006 RK105	2.70	0.07	2.32	192.2	252.9	54295.22	53996	18.76	14	47	0.08	0.8
1257	2004 EZ63	2.96	0.12	1.44	205.1	26.9	53316.50	53996	16.76	8	44	0.04	3.0
1258	2006 SW147	2.56	0.22	3.23	201.1	184.5	54044.94	53996	19.17	14	54	0.08	0.7
1265	2006 RZ107	2.55	0.16	0.65	286.1	86.6	54012.20	53996	19.15	8	48	0.08	0.7
1266	2006 SD242	2.68	0.06	1.38	3.4	230.7	53409.59	53996	17.73	8	54	0.08	1.3
1269	2006 RE109	2.47	0.19	1.05	180.0	244.0	54153.54	53996	19.58	14	63	0.20	0.4
1273	2006 RQ109	2.31	0.17	3.87	11.4	244.7	53663.94	53996	18.81	8	72	0.20	0.5
1275	2006 RV111	2.32	0.22	2.43	25.7	4.7	54050.58	53996	19.92	14	43	0.20	0.3
1278	2006 RN111	2.59	0.15	2.47	13.9	236.4	53549.28	53999	17.69	14	50	0.08	1.4
1283	171677	3.13	0.16	0.62	190.9	162.2	53924.36	53999	15.54	14	82	0.04	5.2
1285	2006 RE106	3.08	0.06	1.14	208.1	246.2	54412.93	53999	18.06	14	56	0.04	1.6
1300	2005 GZ145	2.30	0.07	3.12	358.6	258.7	53629.68	53999	17.77	14	69	0.20	0.8
1302	2006 RS92	3.13	0.09	8.78	197.1	235.3	54297.74	53999	17.12	14	67	0.04	2.5
1303	81444	2.55	0.18	2.92	355.4	43.5	54087.15	53999	16.45	14	88	0.08	2.4

Table 2—Continued

TALCS ID[a]	MPC desig.	a (AU)	e	i (deg)	Ω (deg)	ω (deg)	τ_{peri} (mjd)	Epoch (mjd)	H_v (mag)	Orbital Arc (days)	N_{obs}	albedo[b]	Diameter (km)
1304	2006 RT92	2.68	0.09	3.41	204.5	199.7	54128.51	53999	17.21	14	83	0.08	1.7
1308	2005 GE79	2.54	0.17	5.39	196.8	65.5	53639.16	53999	17.39	14	53	0.08	1.6
1310	2006 RX108	2.25	0.11	2.00	193.9	26.1	53509.92	53999	18.15	14	65	0.20	0.7
1313	2006 SY80	2.61	0.17	1.62	193.0	213.0	54115.15	54000	18.46	14	55	0.08	1.0
1327	2006 SA213	2.42	0.19	3.09	11.5	38.3	54107.52	53999	19.27	14	75	0.20	0.4
1330	2005 EK177	2.64	0.22	4.26	192.3	87.0	53708.97	53999	17.24	14	97	0.08	1.7
1332	2006 SV81	3.18	0.11	5.52	15.7	149.1	54835.38	53999	15.91	14	90	0.04	4.4
1335	2006 RS110	3.22	0.08	9.31	191.2	279.0	54517.31	53999	17.11	14	55	0.04	2.5
1342	2006 RW111	2.79	0.08	4.27	20.2	60.2	54286.56	53999	18.05	14	59	0.08	1.2
1345	2006 RX110	2.37	0.13	5.64	187.1	88.6	53704.71	53999	18.95	14	55	0.20	0.5
1347	2006 RB106	3.03	0.03	8.42	192.2	190.5	54051.97	53999	17.31	14	76	0.04	2.3
1350	2006 RL113	2.64	0.04	3.15	23.9	223.5	53479.58	53999	17.94	14	65	0.08	1.2
1352	2006 RW110	2.75	0.23	7.46	185.4	251.8	54202.82	53999	19.19	14	60	0.08	0.7
1353	1981 EO33	2.77	0.15	15.62	190.4	354.5	54792.92	53999	16.03	14	108	0.08	2.9
1367	2006 RQ113	3.07	0.17	4.31	187.3	12.4	53077.30	53999	16.82	14	53	0.04	2.9
1369	2006 RL108	2.42	0.17	2.50	191.7	72.7	53674.17	53999	18.28	14	50	0.20	0.7
1374	2006 RS113	2.95	0.11	8.37	11.7	358.7	54001.25	54000	17.97	14	62	0.04	1.7
1376	2006 SJ81	2.69	0.13	2.50	178.1	65.9	53489.09	54000	17.23	14	39	0.08	1.7
1380	2006 RH114	2.76	0.08	0.54	127.0	274.3	54122.89	54000	18.09	14	74	0.08	1.1
1381	2006 SU146	3.05	0.08	9.33	10.2	78.1	54363.35	53998	17.17	14	82	0.04	2.4
1382	2006 RP111	2.67	0.09	6.25	15.7	359.2	54015.41	54001	19.36	14	43	0.08	0.6
1384	2006 RJ42	3.16	0.11	5.62	16.3	132.8	54727.40	54000	16.12	14	66	0.04	4.0
1386	2006 RZ92	2.73	0.06	5.64	195.1	200.3	54103.71	53998	17.36	14	65	0.08	1.6
1387	2006 SW106	2.70	0.09	4.57	196.1	187.8	54050.65	53998	17.30	14	64	0.08	1.6
1394	2006 SZ80	2.22	0.22	0.86	193.1	139.9	53928.39	54000	20.02	14	58	0.20	0.3
1396	2006 SG241	2.33	0.18	1.42	356.3	55.0	54106.58	53999	19.20	14	36	0.20	0.4
1400	2006 RH115	2.27	0.23	2.36	10.6	322.7	53927.83	54000	19.51	14	49	0.20	0.4
1401	2006 RF118	2.87	0.08	14.90	194.3	356.9	54878.57	54001	17.53	14	47	0.04	2.1
1402	2006 RD112	3.01	0.06	10.31	18.5	186.1	53118.80	53998	17.88	14	40	0.04	1.8
1404	2006 SQ146	2.78	0.03	0.81	329.6	330.4	53680.17	53998	17.15	14	52	0.08	1.8
1406	2006 SV146	2.58	0.04	0.93	193.9	263.3	54345.13	53999	17.84	14	86	0.08	1.3
1407	2006 SE81	2.76	0.08	6.02	13.2	325.5	53876.18	54000	18.16	14	49	0.08	1.1
1408	2006 RW112	2.84	0.15	1.69	156.4	10.1	54711.20	54000	17.74	14	45	0.04	1.9

Table 2—Continued

TALCS ID[a]	MPC desig.	a (AU)	e	i (deg)	Ω (deg)	ω (deg)	τ_{peri} (mjd)	Epoch (mjd)	H_v (mag)	Orbital Arc (days)	N_{obs}	albedo[b]	Diameter (km)
1416	2006 SJ385	2.42	0.19	0.45	265.8	136.1	54089.58	54001	19.27	11	40	0.20	0.4
1417	2006 SR81	2.70	0.07	3.52	183.8	144.6	53834.77	54001	17.70	14	71	0.08	1.4
1421	2006 RQ110	2.56	0.19	1.54	188.4	221.7	54113.61	54000	19.40	14	51	0.08	0.6
1422	2006 RS42	2.65	0.07	1.18	35.7	241.6	53628.98	54000	17.72	14	58	0.08	1.3
1423	2006 RN113	2.90	0.05	2.28	39.5	5.9	54153.12	54000	18.10	14	36	0.04	1.6
1426	2006 RG93	2.32	0.18	2.15	209.4	40.3	53635.87	54001	17.84	14	53	0.20	0.8
1427	2006 ST385	3.13	0.20	10.09	12.9	19.0	54080.66	54001	18.48	11	34	0.04	1.3
1429	2006 SH385	2.92	0.08	1.11	324.7	128.9	54374.91	54001	17.71	11	49	0.04	1.9
1430	2006 RE116	3.15	0.08	10.33	194.2	183.0	54024.33	54001	17.77	14	62	0.04	1.9
1433	2006 SV106	3.14	0.22	9.61	192.8	254.5	54295.46	54000	17.25	14	92	0.04	2.4
1435	2006 RE42	2.61	0.19	0.57	127.7	310.2	54211.78	54000	18.47	14	41	0.08	1.0
1436	2006 SD81	3.13	0.21	4.88	185.3	180.1	53985.02	54000	18.39	14	42	0.04	1.4
1440	2004 GB67	3.10	0.05	12.94	15.7	301.9	53722.65	53998	16.36	14	56	0.04	3.6
1442	2006 RM114	2.47	0.16	1.14	175.9	270.3	54230.75	54000	19.26	14	61	0.20	0.4
1443	2006 RW108	2.48	0.15	5.93	188.8	162.8	53950.41	53998	20.09	14	51	0.20	0.3
1444	2006 RN42	2.65	0.06	1.06	147.6	25.9	54704.06	54000	17.57	14	55	0.08	1.4
1450	2006 SR242	2.78	0.06	4.76	199.8	95.6	53677.35	54000	18.04	14	37	0.08	1.2
1451	2006 SG81	3.09	0.17	4.32	183.9	141.2	53821.17	54000	17.18	14	48	0.04	2.4
1452	2006 SV275	2.67	0.12	4.15	197.5	200.9	54099.80	54001	17.33	14	57	0.08	1.6
1455	2006 RR105	2.25	0.13	1.75	213.3	347.1	53424.07	54000	18.97	14	46	0.20	0.5
1456	2006 SM385	2.55	0.19	9.35	188.5	112.6	53792.90	54001	18.75	14	80	0.08	0.8
1458	2006 RS112	3.18	0.08	7.54	17.5	198.9	53126.40	53998	16.32	14	60	0.04	3.6
1461	1995 SK10	3.05	0.09	2.16	15.9	306.6	53777.38	54000	17.58	14	77	0.04	2.0
1462	2006 SA81	3.16	0.14	10.15	189.6	99.7	53622.59	54000	17.17	14	62	0.04	2.5
1463	2006 SO275	2.84	0.09	0.48	350.3	285.3	53587.53	53998	16.91	14	63	0.04	2.8
1467	2006 SO81	3.12	0.13	12.14	189.9	300.2	54586.33	53998	16.36	14	60	0.04	3.6
1471	2006 SY212	3.16	0.19	25.69	11.9	258.0	53545.61	54000	16.51	14	94	0.04	3.3
1473	2006 RR92	2.17	0.22	5.80	192.3	150.2	53950.66	54001	19.77	11	32	0.20	0.3
1474	2006 RE115	3.10	0.21	0.35	164.3	254.9	54183.89	54000	17.82	14	60	0.04	1.8
1476	2006 RD113	2.77	0.07	1.03	64.6	236.6	53706.65	54001	18.57	14	39	0.08	0.9
1477	2006 RX119	3.05	0.17	1.23	40.8	352.2	54086.24	54001	18.06	14	35	0.04	1.6
1482	2006 RK110	2.91	0.03	0.72	31.8	172.4	53157.11	53998	17.03	14	101	0.04	2.6
1486	2006 RO115	2.41	0.17	0.75	184.1	242.3	54160.33	54000	19.19	14	64	0.20	0.4

Table 2—Continued

TALCS ID[a]	MPC desig.	a (AU)	e	i (deg)	Ω (deg)	ω (deg)	τ_{peri} (mjd)	Epoch (mjd)	H_v (mag)	Orbital Arc (days)	N_{obs}	albedo[b]	Diameter (km)
1487	2006 RU119	2.57	0.04	13.71	15.6	213.2	53413.04	54001	18.15	14	37	0.08	1.1
1488	2006 SB243	2.75	0.12	2.45	356.2	323.9	53815.27	53998	17.36	14	51	0.08	1.6
1490	2006 ST242	3.18	0.22	15.79	194.1	114.2	53761.87	54001	16.96	11	36	0.04	2.7
1493	2006 RV42	3.17	0.08	12.12	13.7	43.1	54220.19	54000	16.50	14	75	0.04	3.3
1498	2006 RG114	2.89	0.10	2.07	173.9	262.0	54275.16	54000	18.10	14	47	0.04	1.6
1502	2006 RT106	2.36	0.22	0.60	319.0	0.6	53882.33	54000	18.77	14	49	0.20	0.5
1503	2006 RO112	2.26	0.11	1.62	41.2	177.4	53499.05	54000	18.69	14	44	0.20	0.5
1505	2006 SD147	3.14	0.11	6.41	193.1	55.1	53353.58	53999	15.86	14	66	0.04	4.5
1518	2006 RL118	2.75	0.53	1.10	210.2	289.8	54320.26	53996	17.48	8	43	0.08	1.5
1524	2006 RY92	2.99	0.07	9.85	196.5	99.4	53647.71	53996	17.10	14	56	0.04	2.5
1526	2006 RQ115	2.32	0.24	4.00	179.4	168.8	53960.21	53996	20.70	7	31	0.20	0.2
1533	2006 RX118	2.63	0.23	2.25	161.7	187.1	53945.68	53996	17.69	7	30	0.08	1.4
1540	2006 SB147	3.10	0.19	19.33	11.2	303.0	53773.41	53995	17.98	8	87	0.04	1.7
1558	2006 RM107	2.72	0.16	4.40	355.6	35.2	54069.95	53995	18.92	8	42	0.08	0.8
1566	173147	2.38	0.14	3.29	20.2	155.5	54598.30	53995	16.78	8	61	0.20	1.3
1571	2005 GQ48	2.24	0.09	3.85	181.2	53.5	53564.70	53996	18.55	8	65	0.20	0.6
1579	2006 RH93	2.66	0.10	1.03	304.0	81.5	54054.84	53996	17.93	8	50	0.08	1.2
1586	2006 RG43	3.16	0.19	5.61	181.6	273.7	54355.15	53996	16.26	14	54	0.04	3.7
1587	2006 RX90	3.06	0.11	2.29	197.4	293.5	54571.79	53996	16.28	8	45	0.04	3.7
1588	2006 SC148	3.07	0.09	4.24	0.0	281.1	53562.79	53996	16.27	14	58	0.04	3.7
1592	2005 GX169	2.54	0.12	4.14	24.5	246.9	53645.17	53996	17.21	8	46	0.08	1.7
1593	2006 RH92	3.08	0.14	5.18	197.7	150.4	53901.20	53997	17.04	14	47	0.04	2.6
1597	2003 BX84	3.02	0.18	1.08	211.6	296.9	54633.10	53997	16.56	14	68	0.04	3.2
1599	2006 RK112	2.27	0.04	7.61	17.6	131.4	54469.43	53996	18.46	14	55	0.20	0.6
1601	2002 TN37	2.54	0.21	5.27	186.0	250.5	54187.69	53996	17.38	8	50	0.08	1.6
1603	2006 SG242	2.61	0.28	13.30	10.3	293.2	53828.83	53997	18.30	14	65	0.08	1.0
1611	2006 RY65	2.59	0.14	5.00	1.7	357.2	53968.87	53996	18.21	14	52	0.08	1.1
1612	147908	2.75	0.04	6.22	10.3	9.1	54031.87	53996	16.64	14	70	0.08	2.2
1616	2006 RL110	2.30	0.21	0.98	23.9	337.3	53984.63	53998	20.29	14	57	0.20	0.3
1617	2006 RO113	3.14	0.19	1.54	45.6	340.2	54055.42	53998	18.36	14	49	0.04	1.4
1622	2004 BX02	2.48	0.06	1.28	17.3	173.9	53288.06	53996	17.68	8	104	0.20	0.9
1625	2006 RW41	2.37	0.20	2.46	177.6	208.0	54045.10	53996	18.78	8	37	0.20	0.5
1629	2006 RQ118	3.03	0.15	1.77	23.9	55.4	54278.24	53996	18.48	8	43	0.04	1.3

Table 2—Continued

TALCS ID[a]	MPC desig.	a (AU)	e	i (deg)	Ω (deg)	ω (deg)	τ_{peri} (mjd)	Epoch (mjd)	H_v (mag)	Orbital Arc (days)	N_{obs}	albedo[b]	Diameter (km)
1635	2006 RH111	3.86	0.54	0.45	52.1	74.4	54376.67	53995	16.68	8	42	0.04	3.1
1636	2006 RE119	2.20	0.09	4.53	185.7	297.7	54342.45	53996	19.60	14	42	0.20	0.4
1637	2006 RS105	2.45	0.14	2.00	353.4	118.5	54330.72	53995	18.11	8	38	0.20	0.7
1639	2006 RK117	3.07	0.10	2.09	44.4	21.1	54245.77	53996	18.19	8	35	0.04	1.5
1640	2006 SS146	2.76	0.05	0.88	227.7	63.9	53655.20	53995	18.15	14	51	0.08	1.1
1641	2006 SX145	3.14	0.23	13.70	10.4	3.0	54006.92	53998	18.06	8	48	0.04	1.6
1642	2006 RR109	2.16	0.06	3.21	190.5	72.1	53678.54	53996	19.43	14	61	0.20	0.4
1643	2006 RJ118	3.21	0.11	10.76	7.5	43.1	54183.30	53996	18.24	8	38	0.04	1.5
1644	2006 RC111	3.09	0.15	8.22	188.9	255.8	54313.03	53996	18.17	8	37	0.04	1.6
1646	2006 RS109	2.72	0.03	8.50	192.0	340.5	54728.39	53996	17.97	14	65	0.08	1.2
1647	2006 RA113	2.66	0.02	2.74	20.4	176.4	53233.53	53996	18.06	8	52	0.08	1.2
1649	2006 RF119	2.94	0.18	1.96	17.8	297.3	53796.55	53997	18.71	8	53	0.04	1.2
1652	2006 RR117	2.47	0.19	3.98	10.3	318.7	53893.31	53996	19.70	14	46	0.20	0.3
1655	2006 RG116	2.27	0.22	1.48	201.5	79.1	53775.89	53996	19.68	8	58	0.20	0.3
1656	2006 RR42	3.15	0.02	9.22	185.6	102.4	53535.98	53995	16.29	8	32	0.04	3.7
1664	2006 RL114	2.52	0.20	3.42	9.5	359.6	54001.61	53996	19.96	14	47	0.08	0.5
1669	2006 RF106	2.58	0.08	3.08	198.8	105.5	53753.42	53996	18.51	8	43	0.08	0.9
1670	2006 RH109	3.17	0.04	14.80	191.2	65.8	53362.38	53995	17.01	14	74	0.04	2.6
1673	2006 RE107	2.62	0.08	3.85	194.0	167.9	53969.09	53996	19.23	14	52	0.08	0.7
1674	2006 SX106	2.40	0.13	6.97	192.3	336.3	54569.78	53996	17.36	14	84	0.20	1.0
1676	2006 RF113	3.10	0.08	9.54	15.2	13.4	54078.84	53995	17.74	14	67	0.04	1.9
1684	2006 SA242	2.34	0.18	2.93	195.7	220.6	54121.43	53996	19.19	14	67	0.20	0.4
1688	2006 RQ112	2.76	0.06	4.39	180.5	138.5	53782.12	53996	18.91	14	39	0.08	0.8
1692	2006 RA115	2.66	0.16	6.83	187.3	186.0	54015.18	53996	19.41	14	41	0.08	0.6
1696	2006 RS106	2.55	0.19	2.61	352.3	25.2	54023.89	53996	20.37	8	27	0.08	0.4
1698	2006 SY81	2.77	0.05	5.52	15.9	73.2	54337.65	53995	17.46	8	45	0.08	1.5
1699	173885	2.99	0.23	1.38	220.3	255.0	54402.38	53997	15.91	8	48	0.04	4.4
1700	2006 SM147	2.60	0.15	1.56	229.3	142.6	54008.94	53996	18.01	8	42	0.08	1.2
1704	2006 SE241	2.28	0.14	7.00	12.0	174.1	54602.11	53995	18.20	14	46	0.20	0.7
1705	2006 RZ108	2.17	0.08	3.10	2.7	123.0	54351.02	53995	19.61	14	46	0.20	0.4
1706	2005 KP08	2.22	0.14	0.93	8.1	158.1	54502.02	53995	16.97	8	64	0.20	1.2
1708	2004 DM56	2.45	0.10	2.27	182.4	288.5	54351.95	53996	18.32	8	49	0.20	0.6
1711	2006 RG113	2.77	0.02	4.10	175.5	98.8	53554.54	53996	18.55	8	36	0.08	0.9

Table 2—Continued

TALCS ID[a]	MPC desig.	a (AU)	e	i (deg)	Ω (deg)	ω (deg)	τ_{peri} (mjd)	Epoch (mjd)	H_v (mag)	Orbital Arc (days)	N_{obs}	albedo[b]	Diameter (km)
1716	2006 RA107	3.13	0.07	10.24	7.3	143.5	54745.54	53995	17.23	8	42	0.04	2.4
1719	2006 RJ116	2.53	0.24	4.79	197.6	354.1	53265.05	53996	17.89	8	46	0.08	1.2
1720	2006 RW105	2.34	0.10	2.33	194.0	214.9	54116.97	53996	19.99	14	45	0.20	0.3
1721	2006 RP112	3.92	0.22	2.93	20.3	8.1	54080.67	53995	18.06	8	49	0.04	1.6
1722	2006 RX117	3.76	0.42	0.72	29.0	281.2	53817.62	53996	18.06	8	40	0.04	1.6
1723	2006 RP117	2.92	0.06	2.26	169.5	111.5	53573.21	53996	17.46	14	58	0.04	2.1
1724	2006 RJ114	2.54	0.24	12.65	7.7	65.3	54170.44	53996	19.22	8	71	0.08	0.7
1725	2006 RB110	3.20	0.26	14.99	8.8	334.3	53908.19	53996	19.08	8	48	0.04	1.0
1726	2006 RJ110	2.34	0.09	1.25	5.4	164.0	54559.14	53996	18.83	8	70	0.20	0.5
1728	2006 RG110	2.72	0.09	4.01	183.4	156.8	53882.68	53996	19.39	14	34	0.08	0.6
1732	2006 RK109	3.09	0.18	0.64	23.2	293.0	53784.12	53995	18.12	14	81	0.04	1.6
1734	2006 RO118	3.21	0.31	0.41	224.1	232.8	54300.87	53996	18.28	8	39	0.04	1.5
1735	2006 RA118	2.53	0.14	0.52	188.4	169.1	53965.86	53997	19.39	14	59	0.08	0.6
1737	2006 RB111	2.56	0.05	6.35	11.3	237.6	53509.87	53995	19.03	14	44	0.08	0.7
1739	2006 RL117	3.03	0.12	1.46	43.6	193.2	53326.30	53996	17.64	8	44	0.04	2.0
1744	2006 RW106	2.83	0.11	3.17	203.0	91.1	53686.30	53996	18.13	8	61	0.04	1.6
1746	2006 RP106	3.04	0.15	10.01	192.5	124.9	53779.66	53995	18.61	14	64	0.04	1.3
1749	2006 RB116	2.90	0.09	1.45	201.8	156.4	53940.80	53996	17.49	8	49	0.04	2.1
1750	2006 RO106	3.10	0.20	11.03	197.5	10.6	53127.00	53995	17.17	14	45	0.04	2.5
1761	2006 RT112	2.57	0.11	2.39	32.6	226.1	53581.47	53996	18.78	8	32	0.08	0.8
1763	2006 SV176	2.31	0.10	5.31	184.4	295.2	54352.36	53996	17.93	8	44	0.20	0.8
1764	2006 RP118	4.04	0.55	1.26	23.0	93.8	54328.40	53996	17.64	8	52	0.04	2.0
1769	2006 RY118	2.67	0.19	3.24	10.5	358.6	54000.89	53996	19.45	14	49	0.08	0.6
1771	2006 RV115	2.79	0.11	3.61	16.6	17.2	54091.70	53996	19.22	8	34	0.08	0.7
1774	2006 RT108	2.66	0.08	6.14	6.1	75.7	54275.88	53996	19.02	8	41	0.08	0.7
1775	2006 RW107	2.65	0.07	0.97	277.4	231.2	54576.48	53996	17.67	8	44	0.08	1.4
1777	2006 RP116	2.69	0.04	1.09	264.7	45.8	53749.23	53996	18.80	8	36	0.08	0.8
1783	2006 ST146	2.86	0.11	1.75	342.6	78.8	54201.44	53996	17.93	8	46	0.04	1.7
1786	2006 RN114	2.87	0.07	2.05	176.8	215.7	54093.54	53995	18.52	14	57	0.04	1.3
1800	173638	2.35	0.19	1.82	6.8	180.4	54634.16	53997	17.32	8	54	0.20	1.0
1803	2006 RG112	2.75	0.03	5.78	18.5	275.5	53652.23	53996	18.64	14	34	0.08	0.9
1813	2006 RR113	3.18	0.19	0.70	166.3	261.0	54229.65	53995	18.35	14	41	0.04	1.4
1816	2006 RF109	2.89	0.11	1.79	13.5	334.5	53910.24	53995	18.15	8	75	0.04	1.6

Table 2—Continued

TALCS ID[a]	MPC desig.	a (AU)	e	i (deg)	Ω (deg)	ω (deg)	τ_{peri} (mjd)	Epoch (mjd)	H_v (mag)	Orbital Arc (days)	N_{obs}	albedo[b]	Diameter (km)
1817	2006 RP113	3.01	0.02	2.09	14.6	65.3	54352.12	53996	18.35	8	43	0.04	1.4
1819	2006 RB43	2.87	0.08	12.74	11.2	4.2	54017.72	53996	16.86	14	99	0.04	2.8
1827	2006 SR146	2.33	0.16	0.88	204.5	217.1	54140.53	53996	19.56	14	90	0.20	0.4
1832	2006 RD43	3.10	0.19	1.76	30.8	271.7	53723.38	53996	16.83	8	66	0.04	2.9
1837	2006 RM106	2.41	0.13	1.60	334.3	242.4	53443.54	53996	18.35	8	40	0.20	0.6
1838	2006 RA106	2.32	0.16	1.01	342.6	278.2	53670.98	53995	18.90	14	51	0.20	0.5
1840	2006 RB120	2.77	0.08	5.71	195.2	245.9	54290.65	53996	18.78	14	48	0.08	0.8
1844	2006 RR118	3.07	0.16	5.86	11.7	344.2	53939.90	53996	18.46	14	49	0.04	1.4
1850	2006 RL106	2.33	0.24	0.64	231.8	66.9	53835.69	53996	20.38	8	36	0.20	0.3
1856	2006 RO43	2.79	0.14	3.46	28.9	275.1	53746.84	53997	17.76	8	47	0.08	1.3
1858	2006 RE112	2.74	0.08	1.37	130.7	203.5	53852.28	53995	18.69	8	41	0.08	0.9
1859	2006 RS108	2.38	0.19	0.63	206.7	165.3	54010.36	53996	19.88	8	85	0.20	0.3
1865	2006 RX105	2.61	0.25	3.81	202.9	298.7	54448.15	53996	18.05	8	42	0.08	1.2
1869	2006 RP107	2.84	0.15	1.16	231.9	81.4	53790.38	53996	19.00	8	38	0.04	1.1
1876	2006 RZ118	3.05	0.16	0.91	171.0	230.8	54122.25	53996	18.01	8	88	0.04	1.7
1878	1995 SO81	2.38	0.22	0.68	27.4	260.8	53787.64	53996	18.30	14	64	0.20	0.7
1880	2006 RO114	2.27	0.22	1.92	176.3	173.1	53961.23	53996	20.44	14	58	0.20	0.2
1890	2006 RW42	3.08	0.08	9.79	187.5	179.0	53976.04	53996	17.30	14	60	0.04	2.3
1891	2005 MR03	2.81	0.15	4.69	183.8	102.9	53671.38	53995	17.38	14	49	0.04	2.2
1894	2006 RH116	2.41	0.12	1.57	203.1	4.3	53389.41	53996	17.92	14	61	0.20	0.8
1895	2006 SP146	2.27	0.14	4.10	199.5	243.1	54202.77	53995	19.08	8	38	0.20	0.5
1896	2006 RE111	3.13	0.15	17.65	14.4	139.8	54723.70	53996	17.74	14	28	0.04	1.9
1897	2006 RN105	2.31	0.24	2.88	1.9	334.4	53929.43	53996	20.07	8	40	0.20	0.3
1902	2006 RP109	2.19	0.07	3.39	189.8	22.3	53490.25	53996	18.06	14	100	0.20	0.7
1905	2005 HO02	2.29	0.19	1.80	30.0	155.6	54605.88	53996	17.44	8	62	0.20	1.0
1908	2001 XZ148	3.11	0.31	1.48	176.8	264.7	54229.71	53995	17.32	14	49	0.04	2.3
1909	2006 RT105	2.75	0.13	7.60	5.6	163.6	54694.82	53996	18.11	8	30	0.08	1.1
1910	2006 RS116	3.04	0.17	12.06	190.9	217.5	54146.90	53996	17.92	14	80	0.04	1.7
1911	2006 RK116	2.98	0.11	8.75	195.0	139.6	53847.08	53996	18.39	14	63	0.04	1.4
1913	2006 RE110	3.12	0.24	0.84	174.7	144.6	53817.64	53995	18.86	8	64	0.04	1.1
1916	2006 RV117	2.76	0.07	0.95	62.1	293.3	53939.36	53996	18.82	8	29	0.08	0.8
1917	2006 RM105	2.60	0.12	1.41	193.3	312.8	54520.62	53995	18.08	14	43	0.08	1.1
1929	2006 RA111	2.73	0.21	8.09	9.1	18.2	54050.01	53996	18.85	8	66	0.08	0.8

Table 2—Continued

TALCS ID[a]	MPC desig.	a (AU)	e	i (deg)	Ω (deg)	ω (deg)	τ_{peri} (mjd)	Epoch (mjd)	H_v (mag)	Orbital Arc (days)	N_{obs}	albedo[b]	Diameter (km)
1938	2006 RU118	2.60	0.07	7.06	185.4	85.5	53601.88	53996	18.44	8	46	0.08	1.0
1939	2006 RU115	3.09	0.13	4.18	188.3	217.7	54151.73	53995	18.02	14	62	0.04	1.7
1945	2006 RQ114	2.96	0.14	4.56	182.5	252.4	54258.27	53996	17.50	14	53	0.04	2.1
1948	32842	3.03	0.26	4.29	180.0	239.8	54158.23	53998	14.28	14	74	0.04	9.3
1954	2006 RR111	3.04	0.19	5.87	16.0	0.2	54018.68	53996	17.86	14	54	0.04	1.8
1967	2006 RZ119	2.90	0.14	14.74	191.3	265.3	54343.53	53996	18.02	8	40	0.04	1.7
1968	2006 SA147	2.31	0.23	4.20	2.2	335.3	53933.14	53996	19.10	8	43	0.20	0.5
1971	2006 RD109	2.90	0.07	2.68	0.3	89.2	54353.45	53996	18.35	8	47	0.04	1.4
1975	2006 RM110	3.17	0.05	9.46	191.9	108.0	53613.04	53995	17.86	14	46	0.04	1.8
1977	2006 RZ109	2.39	0.16	1.26	178.5	94.3	53705.85	53996	18.49	14	79	0.20	0.6
1991	173140	3.14	0.13	0.56	185.9	115.8	53676.38	53998	15.87	14	88	0.04	4.5
1992	2006 RB107	2.45	0.17	3.89	0.3	326.0	53880.45	53995	19.09	8	59	0.20	0.5
1996	2006 RQ108	2.25	0.23	9.09	183.9	154.9	53940.31	53995	19.98	8	46	0.20	0.3
2002	2001 WP90	3.09	0.15	7.13	6.4	69.8	54276.89	53996	16.33	8	50	0.04	3.6
2005	2006 RA109	2.72	0.11	5.26	6.1	300.3	53757.74	53998	18.89	14	66	0.08	0.8
2007	2001 FT83	2.45	0.19	1.72	352.3	242.3	53538.69	53996	18.20	8	49	0.20	0.7
2008	2006 RK42	2.38	0.07	7.28	189.0	288.0	54370.10	53998	17.89	14	82	0.20	0.8
2009	2006 RG107	2.56	0.11	13.97	191.6	323.1	54560.61	53996	17.26	14	95	0.08	1.7
2015	2006 RB113	2.22	0.15	1.45	164.0	288.2	54222.77	53996	19.01	8	52	0.20	0.5
2019	2006 RR106	2.44	0.05	4.43	194.6	229.2	54191.51	53996	19.23	14	60	0.20	0.4
2020	2006 SO147	2.49	0.19	5.14	359.5	285.4	53745.73	53996	18.36	8	64	0.20	0.6
2022	2006 SO154	2.69	0.04	3.39	354.6	122.6	54456.36	53996	17.92	8	49	0.08	1.2
2023	2006 RV91	2.37	0.13	2.12	196.8	303.3	54432.88	53998	17.70	14	92	0.20	0.9
2024	2006 RC43	2.55	0.14	8.99	187.2	133.8	53844.33	53997	18.13	14	94	0.08	1.1
2025	2006 RC106	2.26	0.14	6.63	189.0	168.5	53970.20	53997	18.72	14	66	0.20	0.5
2026	2006 RE108	2.73	0.30	9.46	186.5	189.5	54019.75	53998	20.77	14	49	0.08	0.3
2027	2006 SW241	2.31	0.16	2.87	360.0	33.5	54064.90	53996	18.84	14	73	0.20	0.5
2029	2006 RY119	3.11	0.18	5.38	189.1	110.6	53701.68	54000	17.94	14	40	0.04	1.7
2030	2006 SR147	2.57	0.16	3.59	354.1	357.7	53949.27	53996	18.24	8	42	0.08	1.1
2032	2006 RV108	2.67	0.13	5.90	4.6	249.2	53541.76	53996	17.53	14	62	0.08	1.5
2034	2006 RK119	2.78	0.08	1.76	1.7	133.4	54543.94	53997	17.79	14	66	0.08	1.3
2036	2006 SN275	2.64	0.14	0.67	349.4	349.4	53901.12	53998	17.83	14	73	0.08	1.3
2041	2006 RN107	2.55	0.13	14.31	6.1	141.8	54523.37	53996	17.53	8	45	0.08	1.5

Table 2—Continued

TALCS ID[a]	MPC desig.	a (AU)	e	i (deg)	Ω (deg)	ω (deg)	τ_{peri} (mjd)	Epoch (mjd)	H_v (mag)	Orbital Arc (days)	N_{obs}	albedo[b]	Diameter (km)
2044	2006 RY42	2.40	0.05	3.20	18.4	241.5	53605.26	53998	17.62	14	70	0.20	0.9
2049	2006 RN43	2.39	0.15	2.44	168.5	293.0	54275.18	53996	18.37	8	46	0.20	0.6
2051	2006 SK381	2.63	0.06	0.37	154.2	148.4	53730.72	53996	17.93	14	90	0.08	1.2
2052	2006 SF345	3.04	0.11	10.51	11.4	348.1	53947.56	53999	17.41	14	55	0.04	2.2
2054	2006 SJ241	3.99	0.20	2.65	6.1	20.6	54071.08	53999	16.54	14	72	0.04	3.3
2057	2006 SC242	2.56	0.23	3.21	3.3	356.3	53976.35	53998	19.33	14	65	0.08	0.6
2063	2006 RD42	2.62	0.16	7.57	10.6	248.1	53596.53	53999	17.17	14	50	0.08	1.7
2065	2006 RF117	2.64	0.05	1.47	180.8	178.8	53954.35	53999	18.54	14	64	0.08	0.9
2070	75422	2.36	0.13	4.88	20.9	69.1	54239.71	53999	16.60	11	36	0.20	1.4
2071	2006 RM42	2.41	0.11	2.24	18.1	49.3	54180.27	54000	18.02	14	61	0.20	0.7
2077	2006 RN116	2.66	0.05	4.47	200.9	236.2	54273.06	54000	18.66	14	53	0.08	0.9
2078	2006 ST80	2.79	0.06	4.05	10.7	249.6	53512.79	53998	17.45	14	50	0.08	1.5
2081	2006 SX81	2.31	0.20	3.02	22.4	282.7	53842.84	54001	18.88	11	36	0.20	0.5
2082	2006 RD114	2.47	0.18	3.35	186.3	12.2	53333.37	53998	18.10	14	53	0.20	0.7
2086	2006 RD107	2.40	0.07	4.54	197.5	242.9	54237.93	53997	18.53	14	49	0.20	0.6
2087	2006 RF107	2.39	0.09	4.35	194.7	325.5	54538.91	54000	18.83	14	40	0.20	0.5
2093	15579	2.70	0.15	3.67	29.4	93.3	54426.10	54001	14.42	7	29	0.08	6.1
2094	2006 SZ242	2.63	0.21	1.07	321.6	81.9	54098.25	54001	19.11	14	67	0.08	0.7
2096	2006 RG106	2.75	0.06	4.24	7.9	338.2	53894.64	53998	18.79	14	54	0.08	0.8
2098	2006 RC119	2.56	0.15	14.70	191.6	301.4	54439.34	53998	18.74	14	39	0.08	0.8
2100	2006 SL147	2.35	0.17	4.95	200.0	242.0	54202.94	53996	18.79	14	29	0.20	0.5
2105	2006 RA112	2.41	0.19	1.68	30.9	313.2	53936.00	54000	20.51	14	42	0.20	0.2
2106	2006 RB119	2.76	0.08	5.17	185.4	265.5	54333.35	54000	18.66	14	35	0.08	0.9
2107	2006 RU108	2.43	0.09	0.52	316.6	266.2	53458.16	53996	18.40	14	33	0.20	0.6
2108	2006 RW113	2.31	0.27	1.38	9.8	308.5	53898.70	53998	19.76	14	67	0.20	0.3
2109	2006 SQ385	2.20	0.10	5.51	17.6	205.1	53535.38	54001	18.83	11	31	0.20	0.5
2110	2006 UY66	3.06	0.10	5.39	192.0	321.6	54727.05	54001	16.06	14	106	0.04	4.1
2111	2006 RO42	3.12	0.08	8.18	12.9	357.7	53997.54	53997	16.98	14	55	0.04	2.7
2114	2006 SU106	3.06	0.13	10.46	194.0	210.0	54138.62	53997	17.82	14	63	0.04	1.8
2115	2004 DE41	2.78	0.09	11.32	12.1	171.1	54802.99	53998	16.66	14	64	0.08	2.2
2116	2006 RQ105	2.25	0.20	1.62	208.8	79.9	53799.36	53998	20.10	14	44	0.20	0.3
2117	2006 RE114	2.80	0.04	0.30	80.9	69.2	54645.04	53998	17.59	14	66	0.08	1.4
2118	2005 EL87	2.44	0.22	0.67	123.3	164.4	53776.44	53997	18.12	14	37	0.20	0.7

Table 2—Continued

TALCS ID[a]	MPC desig.	a (AU)	e	i (deg)	Ω (deg)	ω (deg)	τ_{peri} (mjd)	Epoch (mjd)	H_v (mag)	Orbital Arc (days)	N_{obs}	albedo[b]	Diameter (km)
2120	2006 RD102	3.06	0.14	8.95	196.5	183.7	54038.32	54001	16.49	11	38	0.04	3.3
2121	2006 RN117	3.16	0.06	4.83	179.4	356.2	54920.31	54001	16.39	14	36	0.04	3.5
2128	2006 RU114	2.85	0.12	2.59	175.4	337.3	54641.42	54000	17.88	14	46	0.04	1.8
2131	2006 RU106	3.04	0.14	5.56	4.4	333.1	53863.15	54001	18.46	14	55	0.04	1.4
2132	2006 RC107	2.64	0.03	1.77	343.8	37.9	54044.06	53999	18.75	14	47	0.08	0.8
2134	2006 RX112	3.04	0.05	9.25	14.4	272.7	53575.76	54000	17.87	14	52	0.04	1.8
2136	2006 RH110	2.38	0.16	12.09	8.8	246.0	53633.68	53996	18.77	14	58	0.20	0.5
2140	2006 SV385	2.70	0.14	7.14	15.1	152.1	54674.53	54002	17.78	11	29	0.08	1.3
2142	2006 RU112	2.87	0.03	2.08	167.9	252.6	54230.77	54001	19.03	14	29	0.04	1.0
2143	2006 RG118	3.06	0.15	1.86	210.4	99.6	53738.97	54000	18.64	14	34	0.04	1.2
2144	2006 RU109	2.66	0.12	7.53	6.4	306.1	53794.36	53998	18.63	14	51	0.08	0.9
2148	2006 RQ116	2.57	0.06	7.46	195.6	140.5	53874.93	54001	18.49	14	39	0.08	0.9
2150	2006 RQ92	2.29	0.16	6.86	194.8	94.4	53784.81	54000	18.76	14	44	0.20	0.5
2151	2006 RO108	2.63	0.26	5.06	7.0	101.9	54300.92	54000	18.58	14	57	0.08	0.9
2152	2006 SY385	2.52	0.25	0.83	197.2	285.8	54336.23	54001	18.18	11	38	0.08	1.1
2156	2006 RC118	3.02	0.13	2.51	18.3	158.6	54856.01	54000	17.19	14	50	0.04	2.4
2157	2006 RU105	2.39	0.15	3.20	0.3	146.4	54460.61	53998	18.11	14	42	0.20	0.7
2159	2006 RV119	3.00	0.20	4.43	182.0	282.2	54364.47	54001	17.52	14	54	0.04	2.1
2161	2006 RP119	3.15	0.03	11.55	190.3	310.0	54709.77	54001	18.04	14	28	0.04	1.6
2165	2006 SP147	3.23	0.11	4.69	202.8	115.4	53743.67	53997	16.68	14	55	0.04	3.1
2167	2006 RF115	2.58	0.11	3.02	10.4	57.7	54206.42	53998	18.85	14	35	0.08	0.8
2168	2006 RS118	3.10	0.05	9.16	191.9	88.3	53514.46	53998	17.57	14	51	0.04	2.0
2170	2006 RL107	2.69	0.22	1.37	323.4	16.2	53917.72	54000	19.67	14	43	0.08	0.6
2174	2006 RB93	2.67	0.25	6.38	3.9	66.5	54169.22	53998	17.79	14	73	0.08	1.3
2177	2006 SS289	2.57	0.21	4.66	184.7	231.6	54134.05	54000	19.82	14	42	0.08	0.5
2178	2006 SR385	2.92	0.03	11.38	16.2	156.4	54807.59	54001	17.22	11	28	0.04	2.4
2183	2006 RH107	2.39	0.11	1.77	211.1	100.9	53821.22	53997	19.76	14	27	0.20	0.3
2187	2006 RT119	3.19	0.20	13.62	9.1	11.2	54037.64	54000	18.40	14	58	0.04	1.4
2189	144410	2.90	0.14	6.57	186.3	351.1	54813.22	54001	16.07	11	36	0.04	4.1
2190	2006 RD117	2.61	0.12	3.50	8.9	20.1	54061.97	53999	19.79	14	48	0.08	0.5
2192	2006 RW117	2.74	0.05	4.47	12.5	303.2	53775.52	54001	18.70	14	49	0.08	0.9
2193	2006 SO177	2.75	0.19	3.56	179.3	145.0	53851.89	54000	18.86	14	49	0.08	0.8
2194	2006 RY109	2.28	0.09	2.54	7.4	84.0	54251.16	53998	19.76	14	42	0.20	0.3

Table 2—Continued

TALCS ID[a]	MPC desig.	a (AU)	e	i (deg)	Ω (deg)	ω (deg)	τ_{peri} (mjd)	Epoch (mjd)	H_v (mag)	Orbital Arc (days)	N_{obs}	albedo[b]	Diameter (km)
2196	2006 SL385	2.63	0.20	12.77	6.6	116.2	54389.57	54001	18.90	11	27	0.08	0.8
2197	2006 RK115	3.14	0.13	2.86	186.1	262.4	54356.63	53997	18.23	14	46	0.04	1.5
2199	2006 RF105	2.44	0.07	5.52	191.8	149.6	53902.66	53998	19.17	14	47	0.20	0.4
2200	2004 GX46	3.18	0.06	1.10	152.3	128.0	53511.00	53998	16.44	14	31	0.04	3.4
2201	2006 RE117	2.39	0.09	3.18	189.6	42.6	53504.40	53999	18.97	14	46	0.20	0.5
2203	2006 SU81	2.91	0.17	0.68	160.9	275.6	54245.29	54000	17.70	14	62	0.04	1.9
2205	173991	3.15	0.19	0.26	130.4	245.9	54026.42	54001	16.08	11	40	0.04	4.0
2206	2006 SO385	2.34	0.13	2.27	174.0	323.1	54409.19	54002	18.94	11	38	0.20	0.5
2207	144333	2.69	0.15	13.06	8.3	348.7	53960.57	54000	16.13	14	68	0.08	2.8
2210	2006 RJ117	2.68	0.05	6.54	11.9	313.9	53812.62	54001	18.66	14	46	0.08	0.9
2212	173878	2.96	0.09	0.23	130.8	268.1	54122.59	53998	16.92	14	59	0.04	2.7
2214	2006 RQ06	2.70	0.15	14.27	192.3	173.2	53983.19	54002	16.34	7	34	0.08	2.5
2218	2006 RG109	3.21	0.13	11.76	189.5	246.0	54297.08	53998	18.20	14	46	0.04	1.5
2220	2006 RM117	2.25	0.07	4.76	19.5	305.8	53866.96	54001	20.35	14	33	0.20	0.3
2225	2006 ST81	3.08	0.06	9.83	188.0	200.1	54081.17	54000	17.03	14	48	0.04	2.6
2226	2006 RP110	2.36	0.15	2.51	17.2	236.4	53630.15	54000	18.68	14	72	0.20	0.5
2229	2006 SV241	2.34	0.18	1.97	207.4	107.0	53858.50	54001	20.00	14	35	0.20	0.3
2231	2006 RV109	3.10	0.23	15.50	10.5	72.4	54268.96	54001	18.28	14	59	0.04	1.5
2236	2006 RH112	2.38	0.14	2.32	160.3	35.8	53351.49	54001	18.42	14	43	0.20	0.6
2237	2006 RF108	2.78	0.16	13.44	191.6	313.2	54564.08	54001	17.64	14	49	0.08	1.4
2239	2006 RO111	2.81	0.05	0.58	104.7	192.8	53668.46	53998	18.26	14	49	0.04	1.5
2245	104193	2.63	0.10	2.42	198.0	152.0	53932.13	53998	16.05	14	46	0.08	2.9
2249	2006 RK111	2.63	0.17	3.73	16.2	67.2	54235.13	54000	19.16	14	38	0.08	0.7
2250	2006 RV112	2.33	0.39	2.64	17.5	260.2	53830.29	53998	20.00	14	40	0.20	0.3
2251	2006 RZ105	2.40	0.27	2.00	208.5	329.3	54585.92	53998	18.08	14	31	0.20	0.7
2253	2006 SP385	3.93	0.24	3.87	181.8	145.1	53777.54	54001	17.48	11	45	0.04	2.1
2254	2006 SX385	2.71	0.01	6.28	19.1	196.6	53295.80	54001	18.04	11	31	0.08	1.2
2255	2006 RY105	3.18	0.21	9.95	192.5	179.7	54003.32	53997	18.70	14	63	0.04	1.2
2257	2006 RM115	2.86	0.10	15.03	9.4	112.3	54492.40	54000	16.70	14	68	0.04	3.0
2258	2006 SQ147	2.30	0.13	1.71	221.5	306.1	54536.74	54001	17.68	14	61	0.20	0.9
2262	2006 SC241	2.30	0.20	3.87	193.0	278.1	54273.93	54001	18.56	14	52	0.20	0.6
2265	2006 RD106	2.61	0.09	0.80	221.8	183.3	54122.21	54001	19.36	14	48	0.08	0.6
2266	2006 RW119	2.40	0.15	1.03	166.1	296.5	54283.56	54001	18.72	14	46	0.20	0.5

Table 2—Continued

TALCS ID[a]	MPC desig.	a (AU)	e	i (deg)	Ω (deg)	ω (deg)	τ_{peri} (mjd)	Epoch (mjd)	H_v (mag)	Orbital Arc (days)	N_{obs}	albedo[b]	Diameter (km)
2269	2006 RM109	2.99	0.08	9.49	190.7	112.6	53689.06	53998	18.42	14	51	0.04	1.4
2271	1995 SB09	2.35	0.10	1.43	5.8	140.1	54467.43	54001	17.75	14	68	0.20	0.8
2277	2006 RU110	2.41	0.19	1.21	15.6	258.2	53714.50	53998	18.63	14	86	0.20	0.6
2278	2006 SF385	2.63	0.19	13.81	193.7	352.6	54749.09	54001	17.27	11	37	0.08	1.7
2286	2006 RV113	3.18	0.15	1.07	180.5	167.1	53903.56	53998	18.78	14	59	0.04	1.2
2287	2006 SQ242	2.20	0.16	1.92	200.6	194.1	54066.18	53998	18.79	14	50	0.20	0.5
2288	2006 RS114	2.63	0.08	2.30	28.1	82.9	54395.33	54000	18.79	14	41	0.08	0.8
2293	137468	2.37	0.10	1.52	200.0	325.7	54547.21	54000	16.62	14	50	0.20	1.4
2296	2006 RC113	3.38	0.03	9.85	187.3	245.7	54359.24	54000	17.64	14	49	0.04	2.0
2297	2006 RR114	3.17	0.13	1.53	167.8	327.1	54626.13	54000	17.52	14	49	0.04	2.1
2298	2006 RE118	3.02	0.06	1.86	23.1	353.5	54028.35	54000	18.56	14	37	0.04	1.3
2299	2006 RX113	3.07	0.17	0.91	172.3	133.8	53738.87	53998	18.85	14	42	0.04	1.1
2301	2006 SS385	3.14	0.06	1.27	159.1	12.6	54888.75	54001	17.73	11	30	0.04	1.9
2302	2006 SK385	2.89	0.10	1.36	354.3	55.0	54163.25	54001	17.97	11	32	0.04	1.7
2303	2006 RU92	2.41	0.26	1.73	201.5	204.9	54086.38	53997	18.99	14	65	0.20	0.5
2308	2006 SW385	2.34	0.15	2.14	17.8	222.5	53572.64	54001	19.17	11	25	0.20	0.4
2312	2006 SH147	2.24	0.05	3.62	357.7	136.1	54409.81	54001	18.84	14	44	0.20	0.5
2314	2006 SW242	3.19	0.23	11.61	6.7	302.7	53768.98	53998	17.46	14	45	0.04	2.1
2316	2006 RT107	2.33	0.19	6.64	192.2	168.2	53982.05	53998	19.24	14	69	0.20	0.4
2318	2006 RH43	2.41	0.17	2.80	27.6	60.7	54225.82	54000	18.54	14	48	0.20	0.6
2319	2006 SC147	2.83	0.04	0.33	276.5	57.4	53830.35	53998	17.71	14	63	0.04	1.9
2321	2006 SZ212	3.04	0.22	2.55	5.4	350.9	53954.98	53999	17.95	14	110	0.04	1.7
2324	2006 RF43	2.26	0.17	1.47	154.4	182.0	53921.21	53997	18.73	14	55	0.20	0.5
2326	2006 OU20	2.79	0.12	1.47	165.6	271.9	54256.39	53999	16.84	14	66	0.08	2.0
2330	2006 RD93	2.31	0.09	3.72	194.2	310.3	54454.40	54000	17.94	14	90	0.20	0.8
2331	2006 RD110	2.60	0.28	6.02	8.7	44.6	54106.01	53999	19.62	14	94	0.08	0.6
2332	2006 RJ115	2.69	0.05	5.14	8.6	315.1	53810.35	53999	17.67	14	57	0.08	1.4
2341	2003 AZ72	2.99	0.17	4.60	8.1	153.2	54727.41	54000	16.21	14	64	0.04	3.8
2343	79193	2.66	0.25	13.12	192.1	229.6	54143.14	54003	15.88	7	28	0.08	3.1
2344	2006 RY116	2.27	0.10	5.50	3.5	324.3	53881.51	53999	20.52	14	38	0.20	0.2
2351	2006 RZ115	3.00	0.10	8.51	194.3	194.5	54071.08	53995	18.64	8	35	0.04	1.2
2362	2006 RK92	2.34	0.26	0.08	174.1	267.8	54166.43	53995	18.29	8	65	0.20	0.7
2363	145056	2.27	0.10	2.81	178.9	55.0	53561.71	53996	17.70	7	28	0.20	0.9

Table 2—Continued

TALCS ID[a]	MPC desig.	a (AU)	e	i (deg)	Ω (deg)	ω (deg)	τ_{peri} (mjd)	Epoch (mjd)	H_v (mag)	Orbital Arc (days)	N_{obs}	albedo[b]	Diameter (km)
2366	2006 RE06	3.09	0.02	11.99	191.7	214.6	54177.90	53996	15.55	8	34	0.04	5.2
2376	2006 RN110	2.67	0.25	13.65	186.7	158.1	53936.42	53994	18.33	8	62	0.08	1.0
2378	2006 RO116	2.74	0.15	9.01	193.7	276.8	54380.93	53996	17.96	14	61	0.08	1.2
2381	2006 RL112	3.20	0.28	2.00	32.3	270.2	53755.65	53994	18.60	8	33	0.04	1.3
2387	2006 RZ47	2.64	0.11	7.00	184.0	174.5	53960.63	53994	16.81	8	38	0.08	2.0
2394	2006 RP108	2.25	0.05	2.81	4.8	152.7	54495.76	53995	19.10	14	55	0.20	0.5
2399	147490	2.32	0.21	2.24	212.7	229.9	54187.80	53996	17.79	14	59	0.20	0.8
2400	2006 SS177	3.05	0.02	9.45	186.4	116.6	53634.64	53997	17.10	8	44	0.04	2.5
2401	2006 RW114	2.98	0.12	1.45	162.1	205.3	53986.45	53995	18.94	8	30	0.04	1.1
2404	2006 RG115	2.62	0.20	12.11	185.9	190.6	54023.16	53995	19.34	8	45	0.08	0.6
2405	2006 SE177	2.42	0.17	1.73	21.5	38.1	54138.82	53996	18.78	14	59	0.20	0.5
2412	2006 RH118	2.69	0.24	3.97	195.5	253.0	54231.59	53995	19.16	14	36	0.08	0.7
2415	2006 RA110	2.74	0.08	4.12	189.2	203.5	54085.80	53995	18.65	14	84	0.08	0.9
2421	2006 RQ107	2.37	0.16	0.53	281.7	111.5	54067.00	53995	20.24	8	32	0.20	0.3
2422	2006 RX109	2.86	0.18	9.65	8.3	352.1	53966.72	53996	19.53	14	44	0.04	0.8
2424	2006 RM119	2.61	0.21	3.45	178.7	156.1	53904.53	53996	20.12	14	25	0.08	0.4
2425	2006 RH119	2.78	0.04	1.27	221.5	213.3	54277.37	53996	18.78	8	28	0.08	0.8
2426	2006 RY111	2.77	0.08	0.95	62.7	51.7	54435.73	53997	17.93	14	48	0.08	1.2
2427	2006 RV107	2.67	0.24	3.75	201.1	121.6	53871.67	53996	19.44	8	39	0.08	0.6
2428	2006 RL119	2.66	0.15	9.31	188.9	51.9	53480.37	53996	18.18	14	30	0.08	1.1
2430	2006 RL111	3.05	0.19	10.51	15.3	216.3	53312.53	53996	17.40	14	30	0.04	2.2
2432	2006 RR112	2.26	0.09	6.30	182.5	61.7	53595.67	53996	19.79	8	31	0.20	0.3
2439	2006 RD108	3.43	0.04	10.10	9.1	134.5	54825.50	53996	16.91	14	40	0.04	2.8
2440	2006 RX111	2.56	0.15	8.40	11.9	331.0	53917.06	53996	19.92	14	50	0.08	0.5
2442	2006 RZ106	2.47	0.08	0.98	214.2	32.3	53543.76	53996	18.73	8	50	0.20	0.5
2445	2005 GN86	2.35	0.19	1.64	8.3	224.1	53548.12	53996	17.88	8	40	0.20	0.8
2446	2006 SL81	2.22	0.15	3.82	181.0	178.5	53980.13	53995	18.93	8	35	0.20	0.5
2448	2006 RC116	2.99	0.13	1.55	5.9	317.9	53801.47	53996	17.64	8	49	0.04	2.0
2450	2006 RJ106	2.45	0.16	0.89	323.0	303.8	53672.01	53995	18.35	8	44	0.20	0.6
2452	2006 SJ106	3.07	0.01	11.73	14.6	17.7	54103.16	53996	17.11	8	36	0.04	2.5
2455	2006 RZ114	3.24	0.18	1.28	21.3	227.1	53379.77	53995	16.54	8	43	0.04	3.3
2462	2006 RJ119	2.91	0.06	4.43	8.8	90.0	54407.59	53998	17.48	14	84	0.04	2.1
2464	2006 SV80	2.74	0.06	0.32	14.7	336.8	53926.69	53995	18.05	14	40	0.08	1.2

Table 2—Continued

TALCS ID[a]	MPC desig.	a (AU)	e	i (deg)	Ω (deg)	ω (deg)	τ_{peri} (mjd)	Epoch (mjd)	H_v (mag)	Orbital Arc (days)	N_{obs}	albedo[b]	Diameter (km)
2476	2002 RC160	2.47	0.20	2.26	354.7	17.7	54011.51	53995	17.55	8	69	0.20	0.9
2477	2006 SR177	2.63	0.06	2.55	169.2	149.7	53797.42	53995	18.63	8	39	0.08	0.9
2481	2006 RW109	3.11	0.18	1.05	15.2	79.5	54349.63	53996	17.72	14	63	0.04	1.9
2487	2006 SU385	3.11	0.15	0.92	43.1	2.3	54147.25	53998	18.14	5	31	0.04	1.6
2490	2006 RN119	2.98	0.13	4.77	194.5	281.3	54468.38	53996	18.14	14	46	0.04	1.6
2497	2006 RP115	2.32	0.27	5.53	5.9	294.9	53852.93	53995	19.65	8	53	0.20	0.4
2498	2006 RR116	2.72	0.17	3.04	356.7	305.3	53769.21	53996	18.95	14	47	0.08	0.8
2499	2004 DF64	2.66	0.28	13.26	11.9	161.3	54649.58	53996	16.85	14	68	0.08	2.0
2500	2006 RU116	3.10	0.16	4.81	7.7	25.9	54093.50	53996	18.42	8	71	0.04	1.4
2503	2006 SX163	2.92	0.06	0.84	264.1	77.1	53860.78	53995	17.58	8	47	0.04	2.0
2504	2006 RU107	2.59	0.18	1.27	241.6	6.8	53563.91	53995	18.55	8	37	0.08	0.9
2506	2006 RV114	2.73	0.09	4.44	18.2	156.5	54731.58	53995	17.66	8	52	0.08	1.4
2510	2006 RT116	2.36	0.21	1.06	197.4	143.6	53937.56	53996	20.51	8	67	0.20	0.2
2512	2006 RW116	2.38	0.19	1.39	10.6	294.8	53831.28	53996	18.74	14	93	0.20	0.5
2522	2006 RF116	3.39	0.12	5.52	7.5	316.8	53753.35	53996	17.99	14	48	0.04	1.7
2539	2006 RO109	2.99	0.18	1.00	14.7	154.9	54777.48	53995	16.95	8	63	0.04	2.7
2545	2006 RT111	2.74	0.06	2.98	170.5	277.3	54320.30	53995	18.53	8	37	0.08	0.9
2546	2006 RD119	2.44	0.21	9.48	185.6	140.0	53892.24	53995	20.45	8	31	0.20	0.2
2549	2006 RZ111	2.31	0.15	11.60	11.3	30.9	54088.37	53996	20.33	14	39	0.20	0.3
2556	2006 RD118	3.04	0.04	11.15	11.2	307.2	53736.13	53996	17.43	14	56	0.04	2.2
2561	2006 RZ110	2.34	0.08	1.50	25.3	183.0	53419.22	53995	18.99	8	45	0.20	0.5
2562	2006 RY108	4.01	0.34	3.62	188.1	146.4	53858.04	53996	18.59	14	55	0.04	1.3
2573	2619 P-L	3.18	0.03	7.74	11.0	34.2	54186.70	53995	15.03	8	56	0.04	6.6
2582	2006 RT113	2.57	0.15	7.95	12.6	97.3	54346.32	53995	18.89	8	32	0.08	0.8
2590	2006 RF114	2.75	0.19	8.61	11.2	242.0	53546.83	53996	17.54	14	77	0.08	1.5
2595	2006 RS107	3.07	0.28	14.42	189.7	130.2	53846.88	53995	19.45	14	46	0.04	0.9
2601	2006 RT115	2.63	0.17	6.20	7.2	14.0	54037.26	53996	19.90	8	45	0.08	0.5
2609	2006 RQ111	2.47	0.19	1.85	30.5	16.4	54100.70	53996	20.21	14	44	0.20	0.3
2614	2006 RN106	3.07	0.21	8.05	4.9	86.3	54310.25	53996	17.62	8	38	0.04	2.0
2616	2006 RB108	2.33	0.20	1.09	333.7	35.9	54005.54	53995	20.10	8	36	0.20	0.3
2621	2006 RB115	3.02	0.04	0.60	181.5	349.6	54844.29	53996	18.18	8	32	0.04	1.5
2622	2006 RM116	2.59	0.19	4.00	196.9	99.6	53777.86	53997	19.26	8	29	0.08	0.7
2624	2006 RY113	2.98	0.13	2.32	17.3	11.4	54073.08	53996	18.17	8	53	0.04	1.6

Table 2—Continued

TALCS ID[a]	MPC desig.	a (AU)	e	i (deg)	Ω (deg)	ω (deg)	τ_{peri} (mjd)	Epoch (mjd)	H_v (mag)	Orbital Arc (days)	N_{obs}	albedo[b]	Diameter (km)
2632	2006 RK114	2.68	0.19	5.11	11.1	25.4	54081.78	53995	19.63	14	53	0.08	0.6
2633	2006 RL105	2.58	0.14	4.22	194.3	338.5	54646.14	53995	18.11	14	46	0.08	1.1
2636	2006 RJ113	2.64	0.30	13.18	7.9	337.7	53948.20	53995	19.88	8	81	0.08	0.5
2639	2006 RB117	3.33	0.34	1.07	31.9	100.1	54496.11	53996	17.24	8	44	0.04	2.4
2643	2006 RZ42	3.21	0.18	3.02	24.0	319.5	53888.00	53996	17.06	8	66	0.04	2.6
2646	2006 RR115	2.73	0.09	0.96	153.5	230.7	54056.25	53996	19.17	14	38	0.08	0.7
2653	2006 SX146	2.92	0.08	11.68	193.2	171.3	53970.07	53995	17.64	14	50	0.04	2.0
2657	2006 RD111	2.70	0.11	3.79	184.7	189.8	54012.17	53996	18.75	8	33	0.08	0.8
2659	2006 RM112	3.08	0.09	10.61	17.0	27.6	54149.11	53996	17.94	8	41	0.04	1.7
2669	2006 RQ117	2.36	0.24	4.23	6.4	315.2	53894.74	53996	20.57	14	44	0.20	0.2
2679	2006 RN108	3.13	0.10	0.39	343.1	328.7	53718.54	53995	17.39	8	57	0.04	2.2
2683	2006 RC109	2.29	0.17	0.36	256.2	52.5	53846.63	53995	20.38	8	50	0.20	0.3
2703	137451	2.28	0.09	1.55	43.0	336.7	54029.43	53996	16.90	14	48	0.20	1.2
2722	2006 RV105	3.19	0.09	1.25	233.9	289.7	54835.14	53996	17.33	8	38	0.04	2.3
2727	2006 RC120	2.56	0.09	9.61	11.3	1.5	54008.36	53996	19.89	14	36	0.08	0.5
2728	2006 RV110	2.55	0.09	8.63	188.7	125.4	53797.74	53996	19.37	14	35	0.08	0.6
2745	2006 RG105	2.58	0.14	1.66	2.5	272.2	53656.97	53996	18.49	14	50	0.08	0.9
2748	2006 RE120	2.75	0.21	3.54	181.3	182.0	53982.51	53995	19.66	14	47	0.08	0.6
2770	2006 RK118	2.71	0.06	3.04	350.0	284.0	53593.48	53996	18.86	14	40	0.08	0.8
2774	2006 RA108	3.17	0.15	10.24	8.9	189.9	53024.73	53995	15.83	8	42	0.04	4.5
2782	2005 GK75	2.54	0.24	1.98	209.3	71.4	53743.00	53996	19.01	8	44	0.08	0.7
2791	2006 RD120	3.04	0.08	9.99	186.0	136.9	53772.85	53996	18.62	14	27	0.04	1.3
2800	2006 RC115	2.39	0.14	1.24	180.5	87.3	53679.95	53995	19.32	14	34	0.20	0.4
2826	2006 RA117	3.18	0.11	1.08	176.1	193.5	53990.80	53996	18.30	8	47	0.04	1.5
2849	2006 RX116	2.58	0.10	9.47	188.8	142.6	53865.57	53996	18.96	14	74	0.08	0.8
2858	2006 SY106	2.16	0.11	5.34	7.9	262.3	53718.84	53997	19.11	14	46	0.20	0.5
2869	2006 RY107	3.09	0.16	16.58	189.1	129.8	53791.03	53996	18.03	8	42	0.04	1.6
2871	2006 SM177	2.29	0.19	0.65	158.7	254.5	54108.02	53998	19.42	14	55	0.20	0.4
2873	2006 SA243	2.99	0.24	9.27	3.9	305.2	53793.29	53995	17.82	8	47	0.04	1.8
2877	2006 RZ113	2.26	0.05	2.69	11.5	179.5	53386.59	53998	18.72	14	73	0.20	0.5
2881	2006 RW115	2.58	0.17	1.93	18.7	301.1	53851.37	53998	18.95	14	46	0.08	0.8
2889	2006 RT109	2.22	0.19	2.25	358.7	50.1	54093.89	53996	20.81	8	50	0.20	0.2
2894	2006 RH117	3.13	0.17	9.11	188.9	129.6	53779.07	53996	18.49	8	35	0.04	1.3

Table 2—Continued

TALCS ID[a]	MPC desig.	a (AU)	e	i (deg)	Ω (deg)	ω (deg)	τ_{peri} (mjd)	Epoch (mjd)	H_v (mag)	Orbital Arc (days)	N_{obs}	albedo[b]	Diameter (km)
2902	2006 RY114	2.67	0.35	2.17	183.2	146.2	53923.19	53997	19.41	14	49	0.08	0.6
2904	2006 SY242	2.78	0.21	3.84	3.3	23.6	54054.95	53996	18.04	14	81	0.08	1.2
2910	2006 RZ117	3.24	0.10	5.09	188.7	125.3	53720.35	53998	17.92	14	47	0.04	1.7
2911	2006 RO117	3.02	0.11	1.24	47.1	260.1	53718.54	53996	17.30	8	50	0.04	2.3
2920	2006 SZ241	2.32	0.29	2.82	5.1	279.1	53807.67	53996	19.32	14	54	0.20	0.4
2925	2006 RO105	2.64	0.21	3.07	5.5	320.4	53869.53	53996	19.58	8	37	0.08	0.6
2926	2006 RX114	2.77	0.04	1.50	194.2	198.8	54099.40	53999	17.46	14	42	0.08	1.5
2927	2006 UR254	2.63	0.05	1.85	11.4	259.1	53593.33	53996	17.25	8	43	0.08	1.7
2930	175047	2.75	0.14	9.05	6.7	130.3	54513.30	53996	15.93	8	51	0.08	3.1
2932	2006 RX41	2.84	0.07	1.55	353.4	342.4	53853.81	53996	17.33	14	54	0.04	2.3
2942	2006 RL115	2.26	0.15	3.56	8.1	343.6	53960.41	53998	19.76	14	61	0.20	0.3
2943	147887	2.35	0.12	6.77	182.7	179.2	53980.59	53996	16.89	8	43	0.20	1.3
2944	2005 JN113	2.21	0.04	4.41	190.6	322.5	54470.87	53997	18.33	14	83	0.20	0.6
2946	2006 SB213	2.31	0.16	4.57	12.7	31.0	54089.51	53998	19.78	14	53	0.20	0.3
2948	2006 ST145	2.60	0.09	0.98	2.6	303.7	53763.10	53997	17.87	14	59	0.08	1.3
2949	2006 RH106	2.62	0.02	3.19	199.4	305.3	54565.61	53998	18.60	14	44	0.08	0.9
2951	2006 SM241	2.40	0.18	2.36	198.0	65.4	53669.00	53999	18.00	14	43	0.20	0.8
2956	2006 UZ66	2.76	0.27	5.66	192.0	266.7	54267.67	53999	18.21	14	83	0.08	1.1
2960	2006 RY115	2.16	0.11	4.21	189.9	127.9	53866.18	53999	20.76	14	39	0.20	0.2
2965	2006 SN385	3.16	0.11	12.44	17.7	234.9	53381.69	53999	16.00	11	35	0.04	4.2
2966	2006 RZ112	2.29	0.10	0.68	94.2	182.3	53714.34	53999	19.95	14	44	0.20	0.3
2969	2006 SW80	3.07	0.02	12.80	188.1	277.7	54509.32	53995	16.67	7	32	0.04	3.1
2971	2006 SH107	2.64	0.16	9.64	192.2	148.1	53909.18	53996	18.78	14	48	0.08	0.8
2983	2006 RS115	3.33	0.19	0.96	173.9	140.5	53754.21	53994	18.49	8	44	0.04	1.3
2985	2006 RQ119	2.99	0.10	7.97	184.4	223.9	54156.71	53996	17.37	8	34	0.04	2.2
2991	2006 RJ112	3.07	0.05	12.59	15.3	16.1	54093.23	53995	17.66	8	36	0.04	2.0
2997	2000 EC102	2.75	0.19	7.87	183.0	77.3	53581.67	53995	16.90	7	30	0.08	2.0
2998	2006 RB42	2.74	0.02	5.88	191.9	160.8	53923.02	53995	17.30	14	52	0.08	1.6
2999	2006 RT114	2.31	0.24	3.30	11.5	280.6	53818.69	53997	19.35	14	63	0.20	0.4
3009	2006 RB109	2.74	0.23	4.42	188.7	164.4	53955.25	53996	20.28	14	48	0.08	0.4
3024	2006 RG117	3.17	0.06	8.65	12.9	160.0	54899.81	53996	16.99	14	54	0.04	2.7
3026	2006 RX92	2.32	0.04	1.98	205.1	236.9	54243.31	53995	18.55	8	59	0.20	0.6
3035	2006 RC112	2.86	0.09	6.41	181.6	226.4	54148.21	53996	18.05	8	37	0.04	1.6

Table 2—Continued

TALCS ID[a]	MPC desig.	a (AU)	e	i (deg)	Ω (deg)	ω (deg)	τ_{peri} (mjd)	Epoch (mjd)	H_v (mag)	Orbital Arc (days)	N_{obs}	albedo[b]	Diameter (km)
3040	2006 RB112	1.95	0.10	19.59	8.3	103.4	54253.62	53996	20.35	8	58	0.20	0.3
3045	2006 RO107	2.74	0.04	1.86	231.7	330.4	53225.94	53995	17.95	14	43	0.08	1.2
3050	2006 RL116	3.05	0.23	1.34	332.4	178.6	54636.76	53996	17.28	14	35	0.04	2.3
3054	2006 RU113	3.13	0.10	0.73	24.6	253.4	53538.79	53996	17.77	8	43	0.04	1.9
3058	2006 RG111	3.12	0.11	11.58	191.5	281.2	54482.24	53996	17.99	8	35	0.04	1.7
3060	2006 RT110	3.09	0.15	8.47	189.2	205.5	54093.87	53995	18.54	14	48	0.04	1.3
3065	2006 RZ91	3.02	0.06	9.97	193.6	184.3	54028.28	53996	16.98	14	47	0.04	2.7
3066	2006 RJ108	1.92	0.23	5.22	188.9	39.4	53674.86	53995	19.45	8	38	0.20	0.4
3069	137187	3.19	0.20	9.28	186.9	78.7	53521.57	53995	15.17	8	40	0.04	6.2
3070	2006 RA114	3.05	0.09	10.58	186.6	227.6	54197.00	53996	18.75	8	32	0.04	1.2
3075	136673	2.45	0.22	1.29	29.2	267.8	53804.59	53997	18.26	8	62	0.20	0.7
3083	2006 SD3	3.24	0.20	0.33	187.6	137.5	53809.42	53995	16.88	8	48	0.04	2.8
3085	2006 RR107	2.61	0.16	1.28	237.6	107.8	53926.67	53996	19.41	8	43	0.08	0.6
3091	2006 RF111	2.96	0.02	9.44	189.1	306.9	54628.02	53995	17.59	8	38	0.04	2.0
3117	2001 FH159	2.38	0.15	6.47	195.0	7.8	53386.70	53994	18.04	8	49	0.20	0.7
3119	2006 RF120	2.90	0.07	1.78	180.3	120.6	53691.47	53998	18.32	14	28	0.04	1.4
3177	2006 RA116	3.02	0.19	0.19	334.1	48.6	54039.59	53996	19.20	8	30	0.04	1.0
3205	2006 RZ116	2.67	0.02	6.22	8.0	60.0	54245.89	53995	18.55	8	45	0.08	0.9
3230	2006 RF110	2.34	0.10	5.61	7.4	104.8	54327.77	53996	19.63	14	40	0.20	0.4
3247	30075	2.69	0.10	13.54	13.3	177.9	54796.14	53995	14.59	14	47	0.08	5.7
3271	2006 RV116	2.14	0.13	5.45	188.6	131.2	53880.46	53997	20.26	14	78	0.20	0.3
3276	2006 RX106	3.02	0.03	11.59	7.6	21.2	54085.97	53995	17.16	8	41	0.04	2.5
3278	2006 RH113	2.64	0.14	8.70	184.7	255.7	54240.37	53996	19.03	8	34	0.08	0.7
3282	2006 RU111	3.05	0.15	1.58	149.7	222.6	54003.25	53995	18.18	8	43	0.04	1.5
3287	137013	2.53	0.22	4.29	14.8	51.4	54152.72	53997	16.61	14	66	0.08	2.2
3289	2006 RN115	2.76	0.02	4.46	185.8	101.8	53628.00	53996	18.05	14	46	0.08	1.2
3292	2006 SC243	2.58	0.15	15.73	8.4	348.8	53962.58	53997	19.43	14	74	0.08	0.6
3298	2006 RU117	2.83	0.37	2.23	11.0	356.0	53998.40	53997	21.03	14	61	0.04	0.4
3299	2006 RS119	2.35	0.16	1.33	9.7	75.7	54215.15	53998	18.30	14	103	0.20	0.7
3308	2006 RM111	3.05	0.04	11.36	15.1	181.3	53048.54	53996	17.58	14	49	0.04	2.0
3315	2006 RC114	2.91	0.02	5.86	15.1	79.8	54408.18	53996	17.93	8	54	0.04	1.7
3317	2006 RJ105	2.58	0.11	4.35	190.6	229.2	54167.36	53999	19.67	14	36	0.08	0.6
3318	2006 SA82	2.78	0.08	4.46	179.1	189.7	53990.79	53997	18.30	14	46	0.08	1.0

Table 2—Continued

TALCS ID[a]	MPC desig.	a (AU)	e	i (deg)	Ω (deg)	ω (deg)	τ_{peri} (mjd)	Epoch (mjd)	H_v (mag)	Orbital Arc (days)	N_{obs}	albedo[b]	Diameter (km)
3320	2006 SN81	2.97	0.19	3.17	180.6	197.8	54030.14	53999	18.27	14	38	0.04	1.5
3325	2006 RX107	2.63	0.21	11.95	190.3	50.6	53529.30	53999	17.72	14	32	0.08	1.3
3326	2006 SF81	3.01	0.12	0.20	315.2	18.5	53847.96	53996	16.99	8	57	0.04	2.7
3327	75191	2.39	0.13	2.06	338.7	149.9	54392.90	53996	16.51	8	29	0.20	1.5
3335	2006 SF241	2.43	0.18	1.12	356.6	51.1	54102.01	53999	19.63	14	41	0.20	0.4
3337	2006 RW118	3.04	0.29	2.72	25.1	83.4	54338.96	53996	18.31	8	47	0.04	1.5
3338	173412	2.63	0.11	2.70	359.1	196.2	53236.57	53996	16.76	8	33	0.08	2.1
3339	2006 RG119	2.57	0.02	5.37	197.6	334.4	54669.29	53996	19.09	14	40	0.08	0.7
3346	2006 RV106	3.16	0.12	10.93	7.7	150.4	54777.59	53996	17.45	8	31	0.04	2.2
3348	2006 RM108	3.06	0.01	0.49	259.7	171.3	54318.35	53995	17.93	8	42	0.04	1.7
3352	2006 RR119	2.23	0.02	7.18	2.8	111.8	54350.38	53996	19.51	8	39	0.20	0.4
3358	2006 RN118	3.16	0.29	13.21	189.2	266.0	54295.31	53996	18.42	14	47	0.04	1.4
3359	2006 RA120	2.45	0.18	2.52	8.8	283.3	53770.64	53996	19.37	14	41	0.20	0.4
3366	2006 RO119	3.02	0.25	1.03	228.8	256.3	54456.44	53996	17.48	8	34	0.04	2.1
3367	2006 RB118	3.03	0.26	1.56	22.3	65.3	54267.24	53997	19.02	8	27	0.04	1.0
3373	2006 RH105	2.31	0.20	3.52	6.2	252.5	53679.86	53996	19.09	14	50	0.20	0.5
3383	2006 SZ385	2.38	0.16	7.42	8.8	345.7	53964.77	53998	20.21	5	21	0.20	0.3
3384	2006 SG385	2.90	0.09	6.19	202.4	287.7	54546.49	53996	18.22	5	25	0.04	1.5
3386	2006 RC117	2.39	0.18	1.18	172.5	171.5	53934.78	53996	20.29	8	41	0.20	0.3
3393	2006 RM118	2.70	0.11	4.93	6.1	86.8	54315.69	53996	18.22	8	52	0.08	1.1
3397	2006 RS117	2.46	0.09	3.07	18.7	152.4	54612.67	53996	18.77	14	42	0.20	0.5
3412	2006 RD116	2.51	0.08	1.47	206.2	339.5	54697.82	53996	18.30	14	53	0.08	1.0
3434	2006 SB386	2.70	0.03	5.79	197.7	188.6	54064.69	53999	18.57	8	30	0.08	0.9
3442	2006 RF112	2.87	0.08	2.10	167.5	134.0	53690.24	53994	18.27	8	38	0.04	1.5
3445	2006 RA119	2.53	0.11	6.50	10.1	248.3	53593.70	53996	19.32	14	31	0.08	0.6
3447	2006 RC108	2.62	0.07	4.78	193.4	318.1	54584.27	53996	18.77	14	32	0.08	0.8
3459	2006 RV118	2.31	0.29	4.82	184.2	114.7	53852.30	53995	19.33	8	30	0.20	0.4
3463	2006 RY117	2.89	0.08	1.72	7.4	334.3	53879.25	53996	19.05	8	29	0.04	1.0
3468	2006 RB114	3.17	0.02	2.06	169.6	248.5	54255.04	53994	17.74	8	36	0.04	1.9
3492	2006 RY106	3.28	0.13	3.39	201.2	106.4	53687.56	53995	17.95	8	50	0.04	1.7
3511	2006 RN109	2.92	0.04	1.87	17.2	298.8	53738.00	53996	18.35	14	55	0.04	1.4
3517	2006 RT118	3.18	0.04	10.55	190.0	175.2	53959.49	53996	17.95	14	55	0.04	1.7
3518	2006 RK106	2.58	0.13	1.07	247.6	330.9	53387.49	53995	17.83	14	48	0.08	1.3

Table 2—Continued

TALCS ID[a]	MPC desig.	a (AU)	e	i (deg)	Ω (deg)	ω (deg)	τ_{peri} (mjd)	Epoch (mjd)	H_v (mag)	Orbital Arc (days)	N_{obs}	albedo[b]	Diameter (km)
3520	2006 RP114	2.61	0.09	11.37	9.8	15.2	54053.75	53997	18.81	14	48	0.08	0.8
3521	2006 SX241	2.39	0.21	2.42	7.5	328.2	53921.49	53997	19.68	14	93	0.20	0.3
3525	2006 SJ177	2.15	0.08	0.91	47.7	43.0	54231.01	53999	19.58	14	40	0.20	0.4

[a]numbering and order are arbitrary and derive from the survey processing methods. [b]assumed from semimajor axis, see text.

Table 3. Fitted Light Curve Parameters

TALCS ID	MPC desig.	period (hr)	amplitude (mag)	$g' - r'$ color (mag)	U[a]
1	39420	$105. \pm 21.$	1.18	1.913 ± 0.50	2
2	2006 RJ43	...	...	0.576 ± 0.05	0
3	2006 ST62	...	...	0.462 ± 0.02	0
4	145635	6.905 ± 0.002	0.30	0.556 ± 0.03	3
6	82495	10.95 ± 0.02	0.16	0.607 ± 0.02	2
7	2001 VZ123	19.46 ± 0.03	0.85	0.329 ± 0.03	3
8	70172	5.7394 ± 0.0004	1.02	0.588 ± 0.01	3
9	2006 RK43	...	...	0.539 ± 0.04	0
10	2006 RF42	2.590 ± 0.002	0.11	0.525 ± 0.02	2
11	143096	...	...	0.576 ± 0.03	0
12	135797	12.09 ± 2.4	0.07	0.582 ± 0.01	2
13	3186	18.147 ± 0.005	0.30	0.408 ± 0.01	3
14	4863	8.616 ± 0.001	0.45	0.564 ± 0.01	3
15	45302	9.911 ± 0.003	0.26	0.611 ± 0.01	3
16	2006 RD101	2.341 ± 0.001	0.14	0.594 ± 0.02	2
17	2006 RB39	2.514 ± 0.001	0.14	0.541 ± 0.02	2
18	44760	26.6 ± 5.2	0.09	0.620 ± 0.02	2
19	46603	...	...	0.460 ± 0.02	0
20	138261	3.558 ± 0.002	0.17	0.564 ± 0.01	2
21	2006 RP42	$40. \pm 8.$	0.50	0.500 ± 0.20	2
23	2006 RY41	2.0950 ± 0.0008	0.13	0.567 ± 0.02	1
24	134527	$80. \pm 16.$	0.40	0.600 ± 0.20	2
25	2006 SU210	26.5 ± 5.3	0.40	0.600 ± 0.20	2
26	1999 VE85	3.143 ± 0.001	0.20	0.522 ± 0.02	2
27	144050	...	...	0.361 ± 0.03	0
28	84478	3.3167 ± 0.0001	0.53	0.491 ± 0.01	3
29	2006 SZ48	5.254 ± 0.004	0.18	0.552 ± 0.02	2
30	107676	...	...	0.593 ± 0.03	0
31	32705	$98. \pm 19.6$	0.50	0.500 ± 0.20	2
32	85051	5.9318 ± 0.0003	0.50	0.594 ± 0.01	3
34	2006 RA39	...	...	0.608 ± 0.02	0
35	8783	5.6951 ± 0.0007	0.67	0.591 ± 0.01	3
36	80952	2.7775 ± 0.0008	0.18	0.559 ± 0.01	2
37	8325	32.35 ± 0.07	0.24	0.637 ± 0.02	2
38	139216	6.151 ± 0.002	0.25	0.412 ± 0.02	3
39	103405	$260. \pm 52.$	0.40	0.500 ± 0.20	2
41	2002 PM155	3.281 ± 0.001	0.14	0.575 ± 0.02	2
42	2006 RX91	0.9086 ± 0.0002	0.16	0.379 ± 0.02	1[b]
43	2006 RW35	11.13 ± 0.01	0.20	0.377 ± 0.02	2
44	58477	5.1371 ± 0.0001	0.92	0.600 ± 0.02	3
45	103148	...	...	0.589 ± 0.02	0
46	139800	5.126 ± 0.001	0.30	0.604 ± 0.01	3
49	2006 RJ60	2.6421 ± 0.0007	0.13	0.341 ± 0.02	2
51	142519	2.2380 ± 0.0002	0.23	0.637 ± 0.02	3
52	1999 TK33	5.846 ± 0.008	0.19	0.589 ± 0.02	2

Table 3—Continued

TALCS ID	MPC desig.	period (hr)	amplitude (mag)	$g' - r'$ color (mag)	U[a]
53	2006 RD92	...	...	0.437 ± 0.03	0
54	88871	...	...	0.633 ± 0.04	0
55	2002 VA106	2.246 ± 0.001	0.06	0.436 ± 0.02	1
58	75555	7.22 ± 0.01	0.07	0.549 ± 0.01	2
59	2002 UB14	2.7985 ± 0.0005	0.16	0.521 ± 0.02	2
60	161723	$45. \pm 10.$	0.26	...	2
62	78293	15.02 ± 0.03	0.13	0.403 ± 0.02	2
63	2005 GC60	8.903 ± 0.005	0.40	0.385 ± 0.02	3
100	47993	23.18 ± 0.05	0.33	0.540 ± 0.01	2
101	2006 RE18	4.327 ± 0.005	0.08	0.465 ± 0.01	2
102	2006 RC105	...	...	0.334 ± 0.03	0
103	117685	$70. \pm 20.$	0.80	0.400 ± 0.50	2
104	2006 SN2	...	...	...	0
105	83913	4.6673 ± 0.0008	1.05	0.446 ± 0.05	3
106	2006 RC39	$116. \pm 30.$	0.60	...	2
107	2006 SZ81	$40. \pm 20.$	0.20	...	2
108	129989	6.408 ± 0.001	0.18	0.424 ± 0.02	2
109	2006 RO19	...	...	0.575 ± 0.02	0
110	2006 RK39	3.366 ± 0.003	0.12	0.510 ± 0.02	2
111	2002 UE16	$34. \pm 8.$	0.70	0.500 ± 0.10	2
112	2005 ED209	3.788 ± 0.003	0.14	0.591 ± 0.02	1
113	2001 RW30	5.2962 ± 0.0007	0.87	0.605 ± 0.01	3
114	15124	9.488 ± 0.004	0.18	0.416 ± 0.01	3
115	136992	$119. \pm 40.$	0.40	0.500 ± 0.10	2
116	140037	4.9630 ± 0.0006	0.66	0.550 ± 0.01	3
117	2001 XA221	3.9904 ± 0.0009	0.20	0.302 ± 0.04	2
118	55430	3.0244 ± 0.0008	0.22	0.579 ± 0.02	3
119	17148	2.7778 ± 0.0002	0.31	0.496 ± 0.02	3
120	2001 UL84	...	...	0.586 ± 0.03	0
121	32282	$95. \pm 30.$	0.50	0.500 ± 0.20	2
122	2006 RY91	5.951 ± 0.005	0.40	0.414 ± 0.04	2
123	2006 RA43	$61. \pm 1.$	0.40	0.530 ± 0.20	2
124	2006 UB75	7.51 ± 0.01	0.10	0.549 ± 0.02	2
125	1995 SH19	$84. \pm 20.$	0.60	0.400 ± 0.30	2
126	2006 SZ2	15.9 ± 0.2	0.44	0.626 ± 0.30	2
127	2006 RL40	...	...	0.400 ± 0.20	0
128	116573	9.55 ± 0.02	0.12	0.543 ± 0.02	2
129	142942	3.000 ± 0.001	0.18	0.502 ± 0.01	2
130	84045	$240. \pm 100.$	0.70	0.500 ± 1.00	2
131	46748	2.698 ± 0.002	0.35	0.604 ± 0.04	2
132	138585	5.5287 ± 0.0005	1.01	0.486 ± 0.05	3
133	79493	2.777 ± 0.002	0.13	0.487 ± 0.03	2
134	2006 RN26	2.3274 ± 0.0006	0.23	0.518 ± 0.01	3
135	22988	24.90 ± 0.06	0.28	0.557 ± 0.02	2
136	142135	$46. \pm 5.$	0.23	0.600 ± 0.20	2

Table 3—Continued

TALCS ID	MPC desig.	period (hr)	amplitude (mag)	$g' - r'$ color (mag)	U[a]
137	55423	$37.5 \pm 5.$	0.25	0.400 ± 0.50	2
138	137598	9.24 ± 0.03	0.14	0.512 ± 0.10	2
139	2006 SC81	$80. \pm 40.$	0.40	0.400 ± 0.50	2
140	90050	$17.3 \pm 4.$	0.12	0.609 ± 0.10	2
141	79331	11.44 ± 0.04	0.15	0.472 ± 0.02	2
142	140141	8.91 ± 0.04	0.08	0.529 ± 0.03	2
143	29019	$160. \pm 50.$	0.30	0.400 ± 1.00	2
144	136360	8.00 ± 0.03	0.08	0.530 ± 0.02	1
145	29760	...	...	0.356 ± 0.01	0
146	45115	4.7178 ± 0.0004	0.29	0.619 ± 0.01	3
147	138256	12.048 ± 0.01	0.66	0.551 ± 0.02	3
148	2002 TK139	6.142 ± 0.001	0.64	...	3
149	140121	19.32 ± 0.08	0.15	...	2
150	141061	5.019 ± 0.001	0.34	0.381 ± 0.02	3
151	2006 RB92	...	...	0.400 ± 0.50	0
152	2004 FK93	3.490 ± 0.002	0.17	0.546 ± 0.02	2
153	143917	5.199 ± 0.004	0.25	0.525 ± 0.03	2
154	141977	19.59 ± 0.06	0.18	0.548 ± 0.02	2
155	142567	$61. \pm 10.$	0.60	0.500 ± 0.20	2
156	136061	5.681 ± 0.006	0.23	0.413 ± 0.03	2
157	135039	4.2057 ± 0.0006	0.20	0.466 ± 0.01	3
158	2001 UA61	5.034 ± 0.005	0.18	0.531 ± 0.03	1
159	140041	2.910 ± 0.002	0.17	0.521 ± 0.01	2
160	81345	3.3735 ± 0.0004	0.40	0.629 ± 0.01	3
161	113166	5.6467 ± 0.0007	0.84	0.584 ± 0.02	3
162	30470	23.02 ± 0.02	0.75	0.431 ± 0.02	3
163	50317	2.6785 ± 0.0005	0.20	0.559 ± 0.01	3
164	27450	4.748 ± 0.005	0.12	0.658 ± 0.02	2
165	2002 VM59	2.196 ± 0.002	0.13	0.591 ± 0.02	1
166	2006 TN66	1.4959 ± 0.0002	0.33	0.539 ± 0.02	1[b]
200	2001 XV127	18.52 ± 0.05	0.15	0.466 ± 0.02	2
224	2000 QG136	7.528 ± 0.004	0.22	0.449 ± 0.02	2
245	57560	9.913 ± 0.001	0.65	0.410 ± 0.02	3
247	40003	6.842 ± 0.007	0.12	0.425 ± 0.02	2
248	73727	$17.5 \pm 3.$	0.20	0.400 ± 0.20	2
249	2001 XR170	9.132 ± 0.005	0.26	0.400 ± 0.10	2
250	24215	11.036 ± 0.006	0.30	0.400 ± 1.00	2
251	137587	...	...	...	0
252	101878	5.4128 ± 0.0005	0.85	0.543 ± 0.02	3
253	30427	$24. \pm 1.$	0.10	0.400 ± 0.20	1
254	12527	7.613 ± 0.004	0.10	0.516 ± 0.01	2
255	100468	5.458 ± 0.008	0.10	0.586 ± 0.02	2
256	2006 UZ213	...	...	0.639 ± 0.10	0
257	2001 XA147	...	...	0.338 ± 0.03	0
258	27962	5.291 ± 0.006	0.08	0.603 ± 0.01	2

Table 3—Continued

TALCS ID	MPC desig.	period (hr)	amplitude (mag)	$g' - r'$ color (mag)	U[a]
259	2003 YH137	...	...	0.347 ± 0.03	0
260	65384	$50. \pm 5.$	0.30	0.500 ± 0.50	2
262	137632	5.263 ± 0.004	0.11	0.571 ± 0.02	2
263	2006 RU104	3.743 ± 0.003	0.16	0.347 ± 0.02	2
264	149259	11.50 ± 0.02	1.16	0.526 ± 0.04	3
265	2006 RD57	...	...	0.462 ± 0.04	0
266	140391	5.084 ± 0.008	0.09	0.361 ± 0.02	2
267	141641	3.691 ± 0.001	0.18	0.566 ± 0.02	2
268	2004 BU22	6.50 ± 0.01	0.18	0.518 ± 0.03	1
269	2004 FQ92	...	...	0.539 ± 0.03	0
270	2006 SF107	6.267 ± 0.006	0.18	0.465 ± 0.03	2
271	66914	...	...	0.400 ± 1.00	0
272	2006 SW275	5.850 ± 0.003	0.59	0.391 ± 0.06	3
273	83669	6.252 ± 0.004	0.21	...	2
274	137987	$40. \pm 4.$	0.20	0.500 ± 0.50	2
276	33108	$155. \pm 50.$	0.40	0.500 ± 1.00	2
277	138167	15.22 ± 0.05	0.80	0.583 ± 0.03	3
278	2002 PY87	...	...	0.600 ± 0.30	0
279	2006 RZ59	2.920 ± 0.001	0.14	0.689 ± 0.07	2
280	55523	$46. \pm 4.$	0.20	...	2
281	2006 RP32	$94. \pm 10.$	0.30	0.500 ± 0.20	2
282	2006 RF93	...	...	0.510 ± 0.02	0
283	142659	14.7 ± 0.5	0.20	0.500 ± 0.30	2
284	2002 XW31	$38. \pm 5.$	0.40	0.500 ± 0.50	2
285	2006 RG92	$220. \pm 20.$	0.40	0.500 ± 0.50	2
287	2004 BW95	5.791 ± 0.008	0.10	0.380 ± 0.02	2
288	2001 YH142	4.436 ± 0.002	0.12	0.411 ± 0.02	2
289	2006 RC06	9.96 ± 0.03	0.09	0.395 ± 0.02	2
290	83391	4.666 ± 0.005	0.10	0.496 ± 0.03	2
291	25186	6.4233 ± 0.0007	0.42	0.642 ± 0.01	3
292	141258	6.68 ± 0.01	0.07	0.443 ± 0.02	2
293	79782	$150. \pm 20.$	0.50	0.500 ± 1.00	2
294	1999 TK176	7.029 ± 0.006	0.10	0.553 ± 0.02	2
295	144093	5.652 ± 0.002	1.06	0.553 ± 0.02	3
307	81326	...	...	0.579 ± 0.03	0
357	755	4.5521 ± 0.0002	0.42	0.478 ± 0.01	3
359	22319	17.698 ± 0.008	0.24	0.567 ± 0.02	2
374	74642	7.471 ± 0.003	0.76	...	3
375	81802	8.49 ± 0.01	0.50	...	2
376	2002 TE241	5.099 ± 0.007	0.24	...	2
377	2006 SO384	...	...	...	0
378	136805	4.766 ± 0.002	0.40	0.442 ± 0.05	2
379	2001 GG01	...	...	0.332 ± 0.06	0
381	20571	$450. \pm 50.$	0.40	0.500 ± 1.00	2
382	138284	...	...	...	0

Table 3—Continued

TALCS ID	MPC desig.	period (hr)	amplitude (mag)	$g' - r'$ color (mag)	U[a]
383	57802	3.571 ± 0.002	0.22	...	2
384	2006 SO2	2.799 ± 0.002	0.14	0.601 ± 0.04	2
385	2002 UN65	4.466 ± 0.002	0.80	0.454 ± 0.02	2
386	2006 RV41	3.361 ± 0.002	0.15	0.325 ± 0.04	2
387	2006 UO213	11.23 ± 0.05	0.70	0.460 ± 0.30	2
388	44770	...	...	0.600 ± 0.50	0
389	76949	...	...	0.542 ± 0.05	0
390	55924	4.81 ± 0.02	0.33	...	3
391	103914	7.905 ± 0.001	0.28	...	3
392	142278	7.47 ± 0.01	0.21	...	2
393	2005 JZ15	4.452 ± 0.004	0.22	0.532 ± 0.03	2
395	81308	...	...	...	0
396	45776	14.90 ± 0.03	0.12	0.440 ± 0.03	2
397	2006 UJ47	0.64190 ± 0.0001	0.16	...	1
1034	2006 SP81	5.077 ± 0.004	0.36	0.676 ± 0.07	2
1049	2006 SK147	6.055 ± 0.006	0.39	0.568 ± 0.10	2
1050	2006 RT41	1.2976 ± 0.0003	0.32	0.479 ± 0.05	1[b]
1051	2006 SV242	5.034 ± 0.002	0.70	0.618 ± 0.05	2
1054	173974	18.43 ± 0.05	0.18	0.465 ± 0.01	2
1063	2006 SP177	19.88 ± 0.05	0.30	0.400 ± 0.20	2
1073	2006 RB57	19.16 ± 0.05	0.20	0.500 ± 0.20	1
1076	2006 SD65	11.52 ± 0.05	0.40	0.590 ± 0.05	1
1077	2006 SE242	18.5 ± 0.5	0.50	0.500 ± 0.20	1
1094	2006 RV92	6.03 ± 0.05	0.30	0.400 ± 0.20	1
1098	2006 SR2	...	...	0.453 ± 0.50	0
1100	2006 SP242	6.41 ± 0.05	0.70	0.584 ± 0.20	2
1110	8906	6.758 ± 0.003	0.17	0.389 ± 0.01	2
1132	2006 RM43	...	...	0.600 ± 0.30	0
1144	2005 KO01	5.743 ± 0.005	0.22	0.600 ± 0.20	1
1168	2006 RP92	9.076 ± 0.002	0.84	0.532 ± 0.10	3
1177	2006 SJ147	...	...	0.563 ± 0.30	0
1222	2006 SG107	...	...	0.473 ± 0.04	0
1235	2001 UG87	2.9 ± 0.1	0.22	0.641 ± 0.10	1
1283	171677	7.533 ± 0.002	0.23	0.439 ± 0.03	2
1303	81444	...	...	0.591 ± 0.05	0
1304	2006 RT92	$30. \pm 5.$	0.24	0.600 ± 0.10	2
1330	2005 EK177	$8.8 \pm 1.$	0.19	0.550 ± 0.10	1
1387	2006 SW106	...	...	0.494 ± 0.20	0
1452	2006 SV275	...	...	0.552 ± 0.10	0
1463	2006 SO275	3.0477 ± 0.0009	0.36	0.577 ± 0.04	2
1473	2006 RR92	...	...	0.549 ± 0.20	0
1488	2006 SB243	...	...	0.400 ± 0.30	0
1490	2006 ST242	...	...	0.550 ± 0.10	0
1493	2006 RV42	5.128 ± 0.002	0.51	0.487 ± 0.10	2
1505	2006 SD147	8.133 ± 0.005	0.90	0.360 ± 0.10	2

Table 3—Continued

TALCS ID	MPC desig.	period (hr)	amplitude (mag)	$g' - r'$ color (mag)	U[a]
1566	173147	6.847 ± 0.009	0.32	0.432 ± 0.05	2
1586	2006 RG43	6.3 ± 0.1	0.24	0.423 ± 0.10	1
1588	2006 SC148	3.254 ± 0.001	0.19	0.362 ± 0.02	2
1592	2005 GX169	$45. \pm 5.$	0.40	...	2
1593	2006 RH92	$49. \pm 5.$	0.40	...	2
1601	2002 TN37	3.481 ± 0.002	0.16	0.568 ± 0.02	2
1612	147908	...	...	...	0
1625	2006 RW41	1.5421 ± 0.0007	0.19	0.573 ± 0.03	1
1699	173885	$10. \pm 1.$	0.10	0.530 ± 0.04	0
1700	2006 SM147	...	...	0.500 ± 0.20	0
1706	2005 KP08	...	...	0.601 ± 0.05	0
1819	2006 RB43	...	...	0.431 ± 0.10	0
1878	1995 SO81	$58. \pm 20.$	0.30	...	2
1908	2001 XZ148	2.774 ± 0.002	0.18	0.668 ± 0.03	2
1948	32842	79.3 ± 0.5	0.50	0.390 ± 0.10	2
1968	2006 SA147	0.34529 ± 0.0001	0.30	0.621 ± 0.05	1
1991	173140	$59. \pm 5.$	0.60	0.500 ± 0.10	2
2002	2001 WP90	3.032 ± 0.005	0.10	0.343 ± 0.05	1
2036	2006 SN275	...	...	0.546 ± 0.10	0
2044	2006 RY42	6.054 ± 0.005	0.24	0.322 ± 0.10	1
2063	2006 RD42	5.241 ± 0.004	0.26	0.547 ± 0.05	2
2070	75422	11.33 ± 0.05	0.12	0.546 ± 0.05	1
2071	2006 RM42	9.25 ± 0.02	0.38	0.626 ± 0.10	1
2093	15579	2.810 ± 0.002	0.14	...	2
2115	2004 DE41	4.376 ± 0.001	0.18	0.487 ± 0.05	2
2120	2006 RD102	11.48 ± 0.02	0.37	0.530 ± 0.10	2
2174	2006 RB93	17.26 ± 0.02	0.30	0.389 ± 0.10	1
2189	144410	8.25 ± 0.05	0.24	0.603 ± 0.10	1
2205	173991	11.214 ± 0.009	0.53	0.425 ± 0.05	2
2207	144333	15.18 ± 0.02	0.23	0.629 ± 0.05	2
2212	173878	2.974 ± 0.002	0.15	0.528 ± 0.10	1
2214	2006 RQ06	$46 \pm 10.$	0.10	...	2
2245	104193	2.7065 ± 0.0009	0.08	0.678 ± 0.02	2
2287	2006 SQ242	$51.6 \pm 1.$	0.59	...	2
2293	137468	3.116 ± 0.001	0.23	0.578 ± 0.05	2
2303	2006 RU92	6.88 ± 0.05	0.22	0.538 ± 0.10	1
2326	2006 OU20	2.24 ± 0.05	0.32	0.448 ± 0.10	1
2343	79193	3.202 ± 0.001	0.33	...	2
2362	2006 RK92	$51. \pm 2.$	0.70	0.500 ± 0.20	2
2366	2006 RE06	...	...	0.400 ± 0.20	0
2387	2006 RZ47	11.5 ± 0.5	0.13	0.353 ± 0.05	1
2399	147490	29.9 ± 0.5	0.29	0.549 ± 0.10	1
2446	2006 SL81	13.17 ± 0.02	0.92	0.423 ± 0.02	2
2476	2002 RC160	7.30 ± 0.01	0.17	0.523 ± 0.05	1
2573	2619 P-L	$64. \pm 5.$	0.10	0.500 ± 0.20	1

Table 3—Continued

TALCS ID	MPC desig.	period (hr)	amplitude (mag)	$g' - r'$ color (mag)	U[a]
2703	137451	10.07 ± 0.05	0.17	0.591 ± 0.05	1
2930	175047	3.256 ± 0.002	0.14	0.548 ± 0.10	2
2943	147887	4.6566 ± 0.0003	0.80	0.633 ± 0.01	3
3069	137187	...	...	...	0
3083	2006 SD3	...	...	0.305 ± 0.10	0
3247	30075	$41.5 \pm 2.$	0.20	...	2
3287	137013	...	...	0.527 ± 0.05	0
3327	75191	...	...	0.647 ± 0.10	0

[a]Light-curve fit reliability code as defined by Harris & Young (1983); see text for details. [b]Detailed analysis of these objects indicates that their reliability code is more likely 1 than the initially determined 2; see text for details. A value of "..." for period or color indicate insufficient data to make a measurement.

Table 4. Followup Light Curve Periods

TALCS ID	MPC desig.	initial period (hr)	U[a]	new period (hr)	amplitude (mag)
1	39420	$105. \pm 21.$	2	$>> 70$	> 0.5
31	32705	$98. \pm 19.6$	2	$>> 70$	> 0.5
59	2002 UB14	2.7985 ± 0.0005	2	2.8 ± 0.1	0.2
131	46748	2.698 ± 0.002	2	2.7 ± 0.1	0.4
248	73727	$17.5 \pm 3.$	2	14.2 ± 0.1	0.3
250	24215	11.036 ± 0.006	2	11.2 ± 0.1	0.2
254	12527	7.613 ± 0.004	2	... [b]	≥ 0.3
274	137987	$40. \pm 4.$	2	... [c]	...
280	55523	$46. \pm 4.$	2	... [c]	...
390	55924	4.81 ± 0.02	3	4.8 ± 0.1	0.3

[a]Light-curve fit reliability code as defined by Harris & Young (1983); see text for details.
[b]Insufficient phase coverage to measure a full period.
[c]No observed variation above noise level.

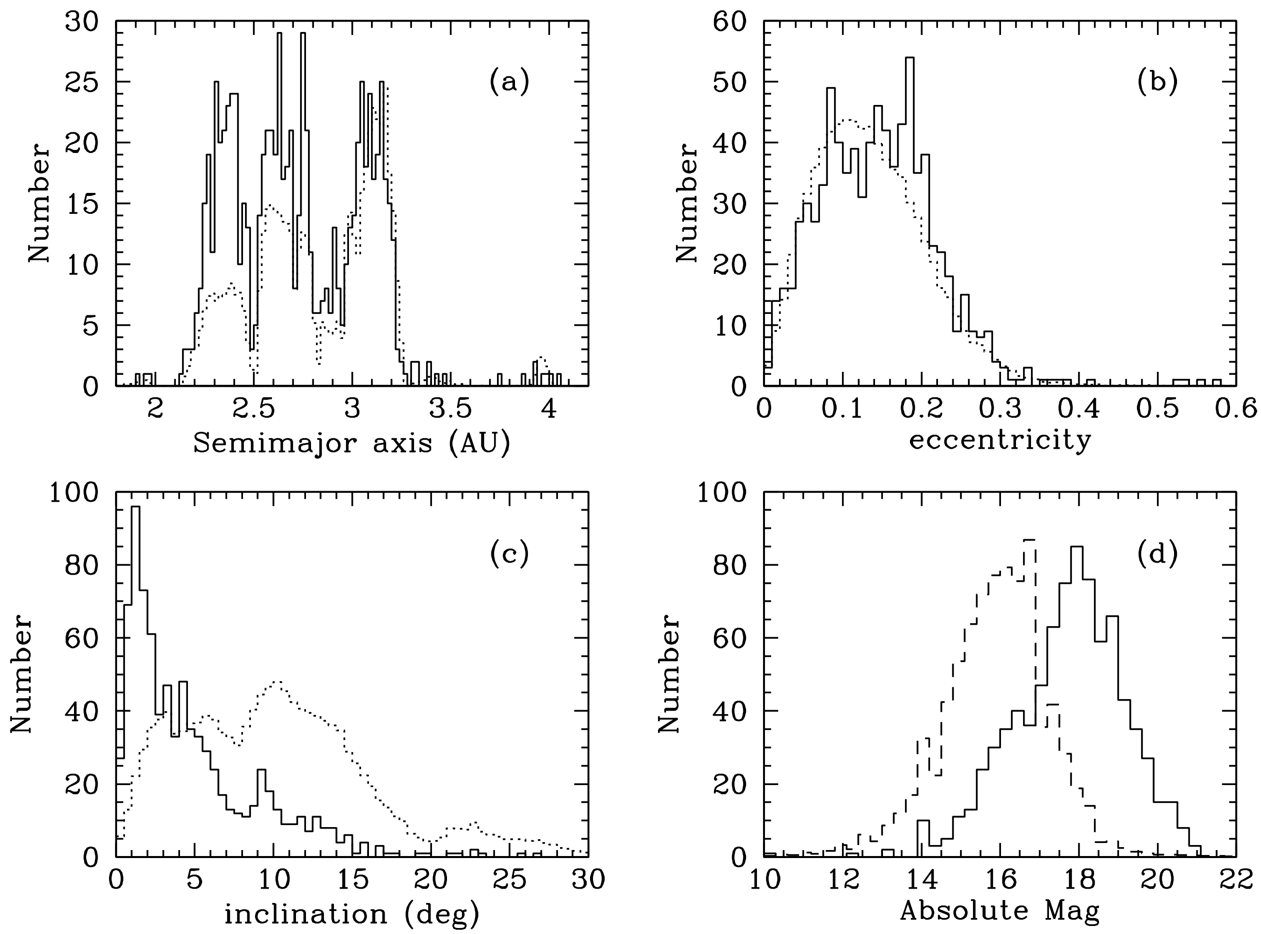

Fig. 1.— The solid lines show the number distributions of TALCS asteroids for a) semimajor axis (0.02 AU bins), b) eccentricity (0.01 bins), c) inclination (0.5° bins), and d) absolute magnitude (0.3 mag bins). The dotted lines show the arbitrarily normalized distributions of all known Main Belt asteroids with $H_v < 15$ for comparison while the dashed line is the arbitrarily normalized distribution for all known Main Belt asteroids.

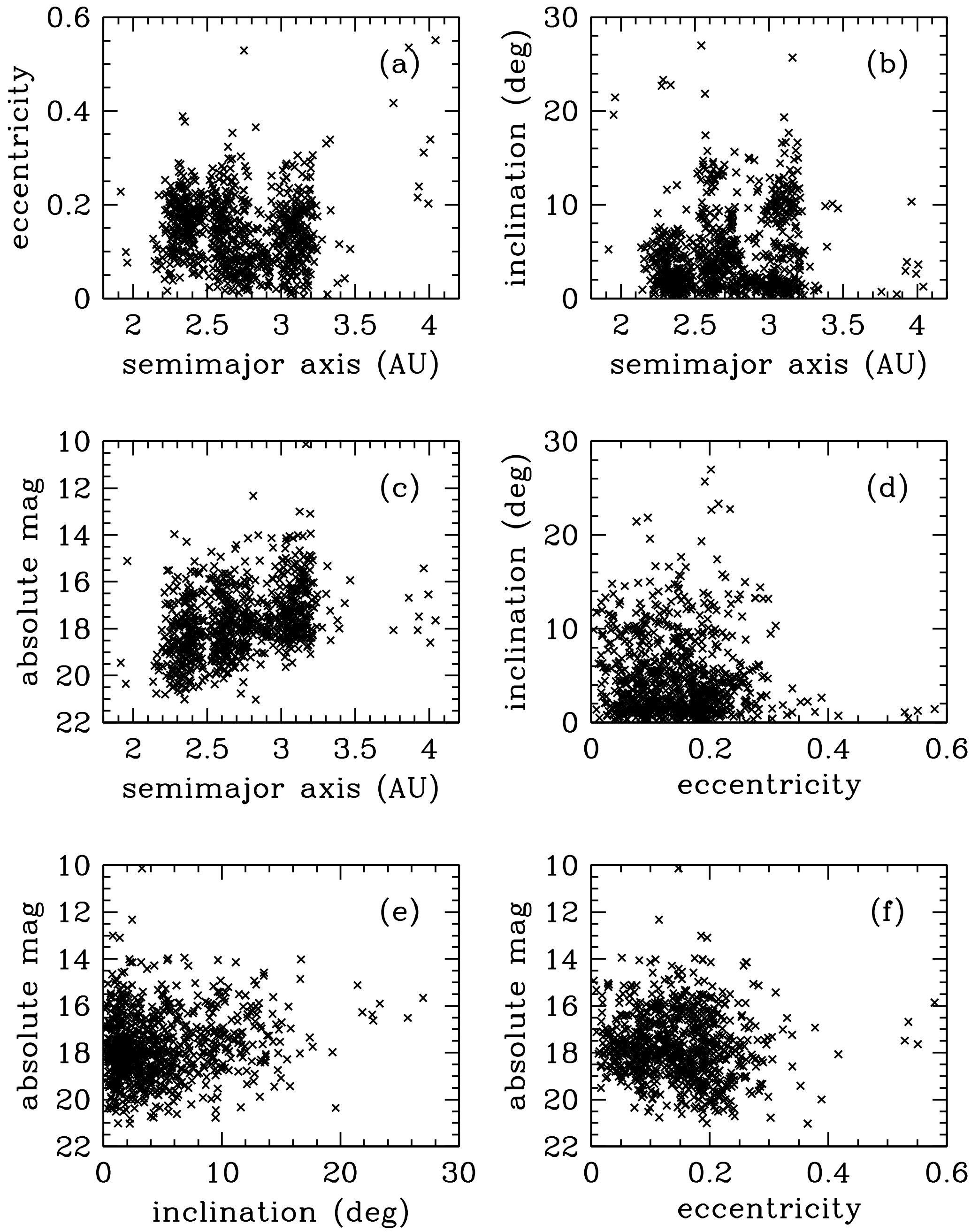

Fig. 2.— Scatter plots for the TALCS objects of: a) eccentricity vs semimajor axis, b) inclination vs semimajor axis, c) absolute magnitude vs semimajor axis, d) inclination vs eccentricity, e) absolute magnitude vs inclination, and f) absolute magnitude vs eccentricity.

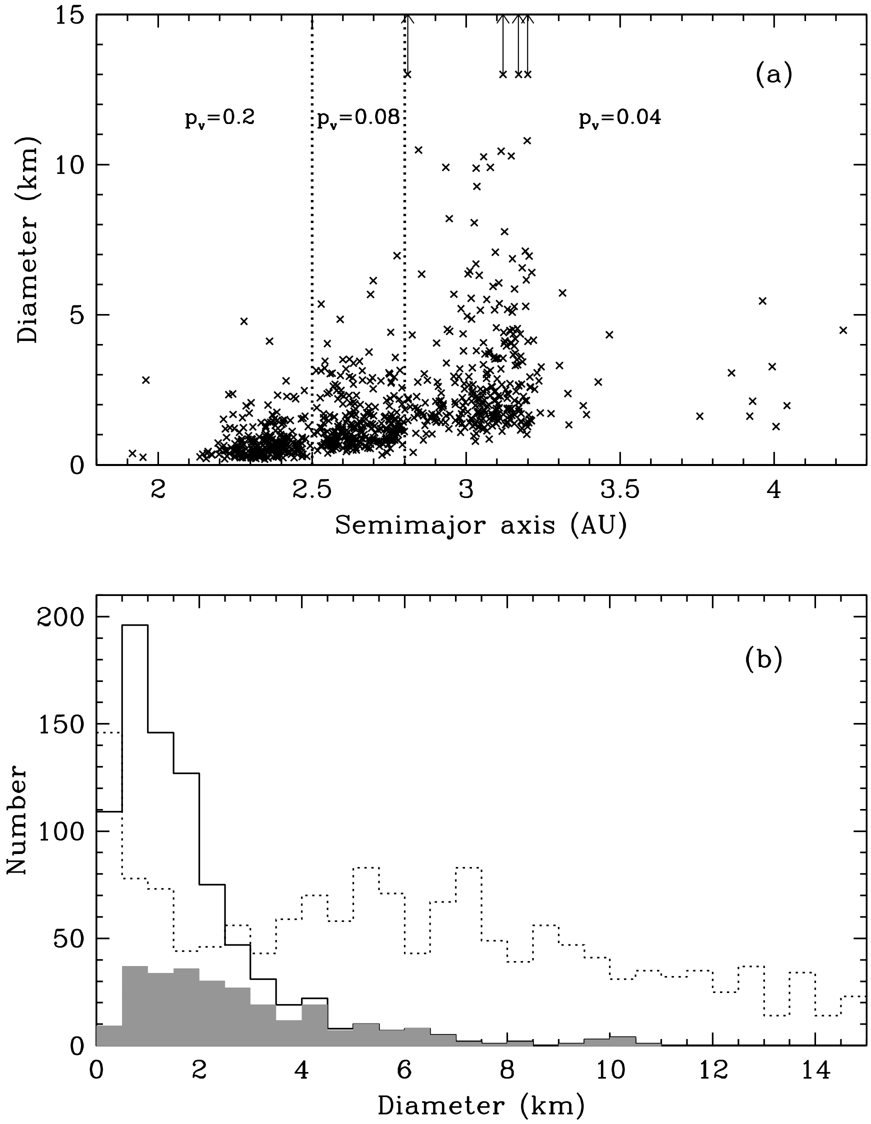

Fig. 3.— a) The derived diameter vs. semimajor axis for the TALCS population. Dotted lines indicate the semi-major axis ranges for assigning albedos (p_v). Four asteroids in our survey ((755) Quintilla, (3186) Manuilova, (4863) Yasutani, and (8906) Yano) have diameters beyond the range of the figure and are indicated by x's with arrows at the appropriate semimajor axis. b) The solid line provides the number distribution for all TALCS objects as a function of their diameter (0.5 km bins) while the shaded region shows the distribution only for those TALCS objects with measured light curves. The four objects with $D > 15$ km are not shown in this histogram. The dotted line shows the diameter distribution of all objects with measured rotation periods and $D < 15$ km as compiled by A.W. Harris, et al. (*http://www.minorplanetobserver.com/astlc/LightcurveParameters.htm).*

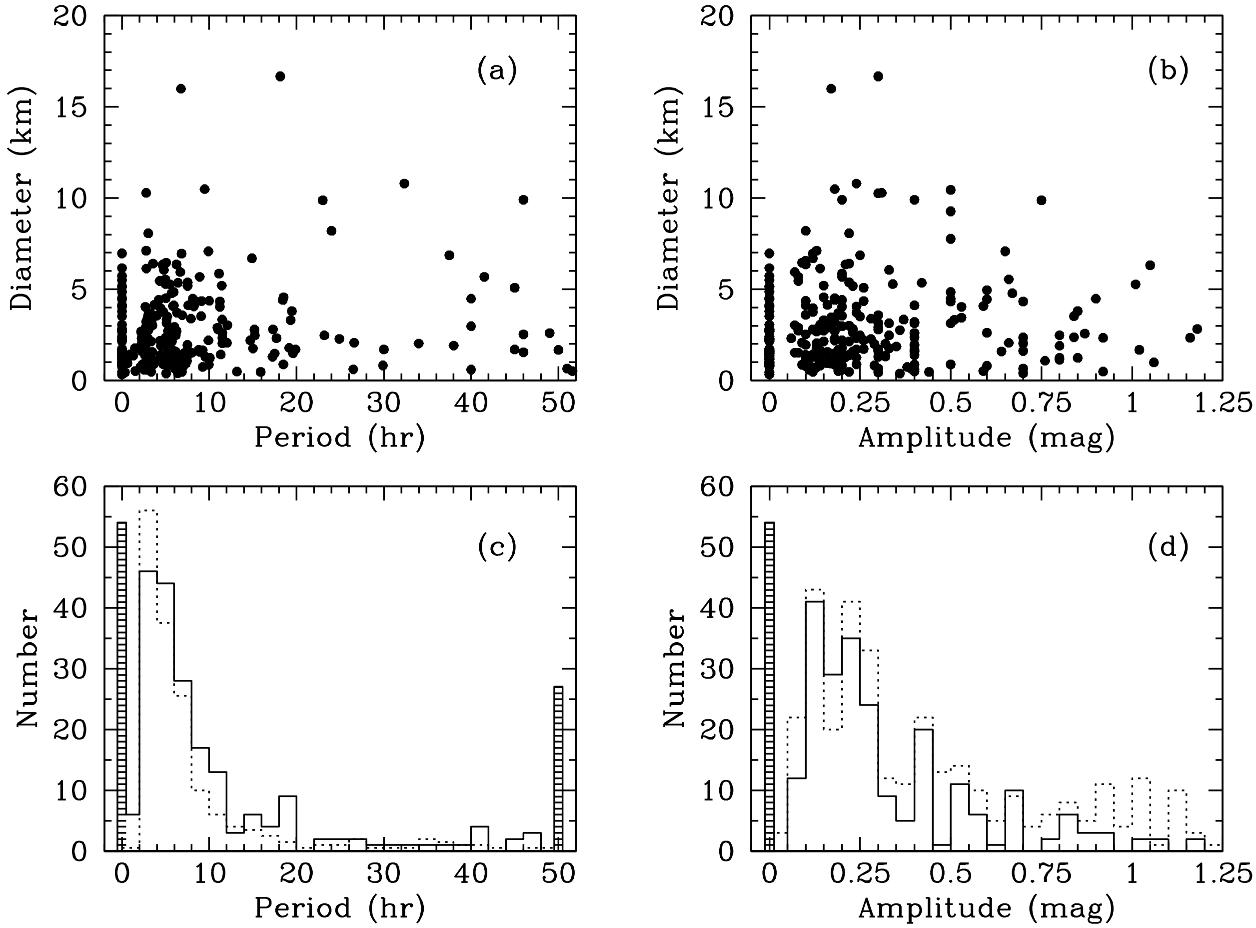

Fig. 4.— a) Diameter vs. period for all light curve-fitted objects. b) same as (a) but vs. light curve amplitude (mag). c) Number distribution of fitted periods of TALCS objects (2 hr bins). The shaded bar at $P = 0$ hr represents all objects with no detectable light curve while the shaded bar at $P = 50$ hr includes all objects with $P > 50$ hr. d) The number distribution of light curve amplitudes (0.05 mag bins). The shaded bar at $P = 0$ hr represents all objects with no detectable light curve. The dotted line in (c) and (d) shows the distribution of previously known light curve periods and amplitudes for asteroids in the same size range as the TALCS objects.

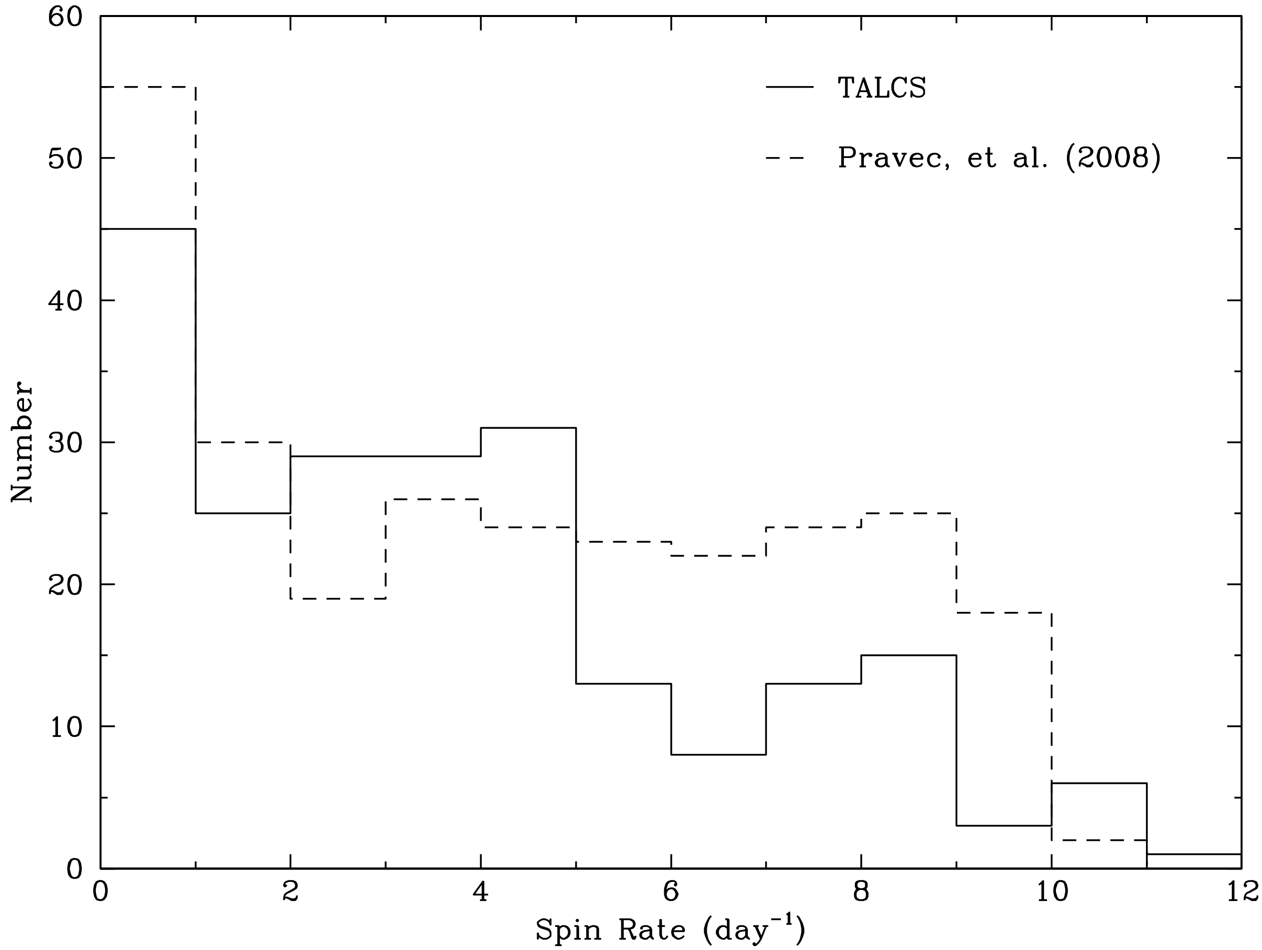

Fig. 5.— Raw spin rate distribution for TALCS objects (solid) compared to the data presented by Pravec et al. (2008, dashed).

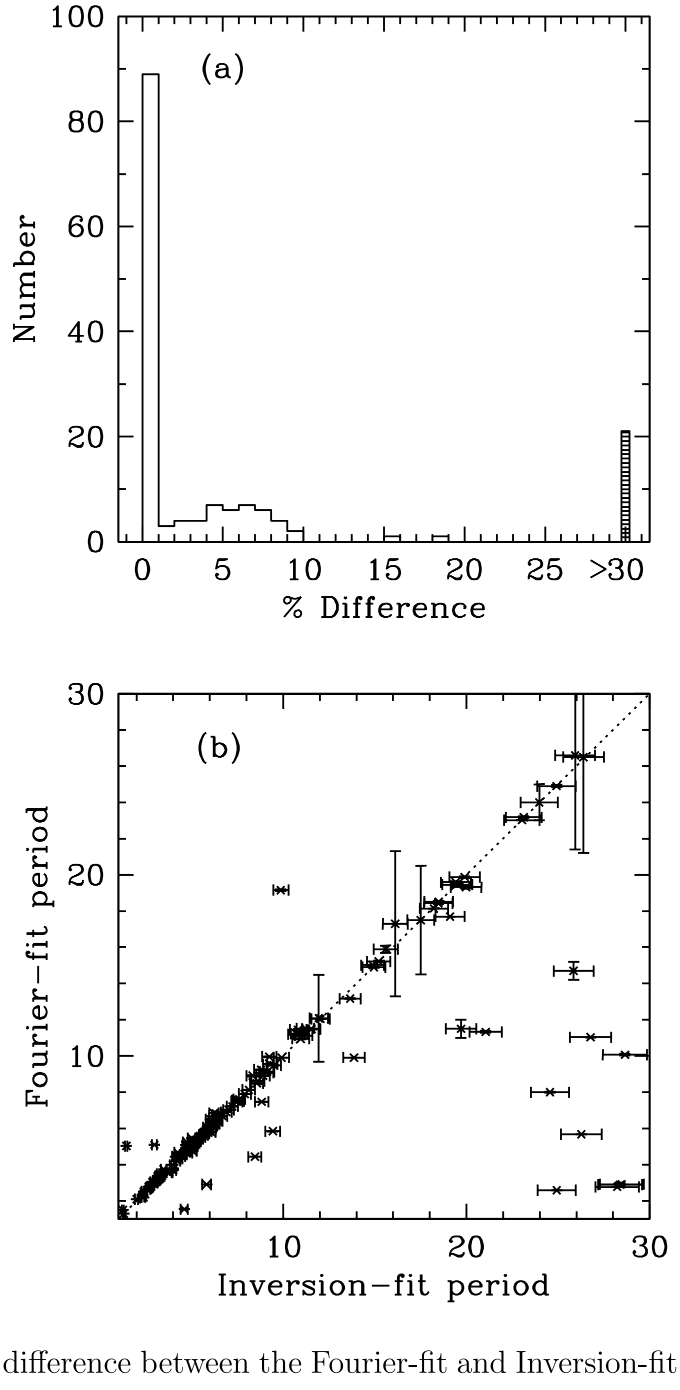

Fig. 6.— a) Percent difference between the Fourier-fit and Inversion-fit periods. The shaded bar at 30% represents all objects with errors greater than this value. The median error was $\sim 0.2\%$. b) Comparison between periods found for the Fourier-fit light curve fitting method and the Inversion (automated) fitting technique over the period range to be debiased. Errors on the inversion periods were set to the $1-\sigma$ error level found in (a).

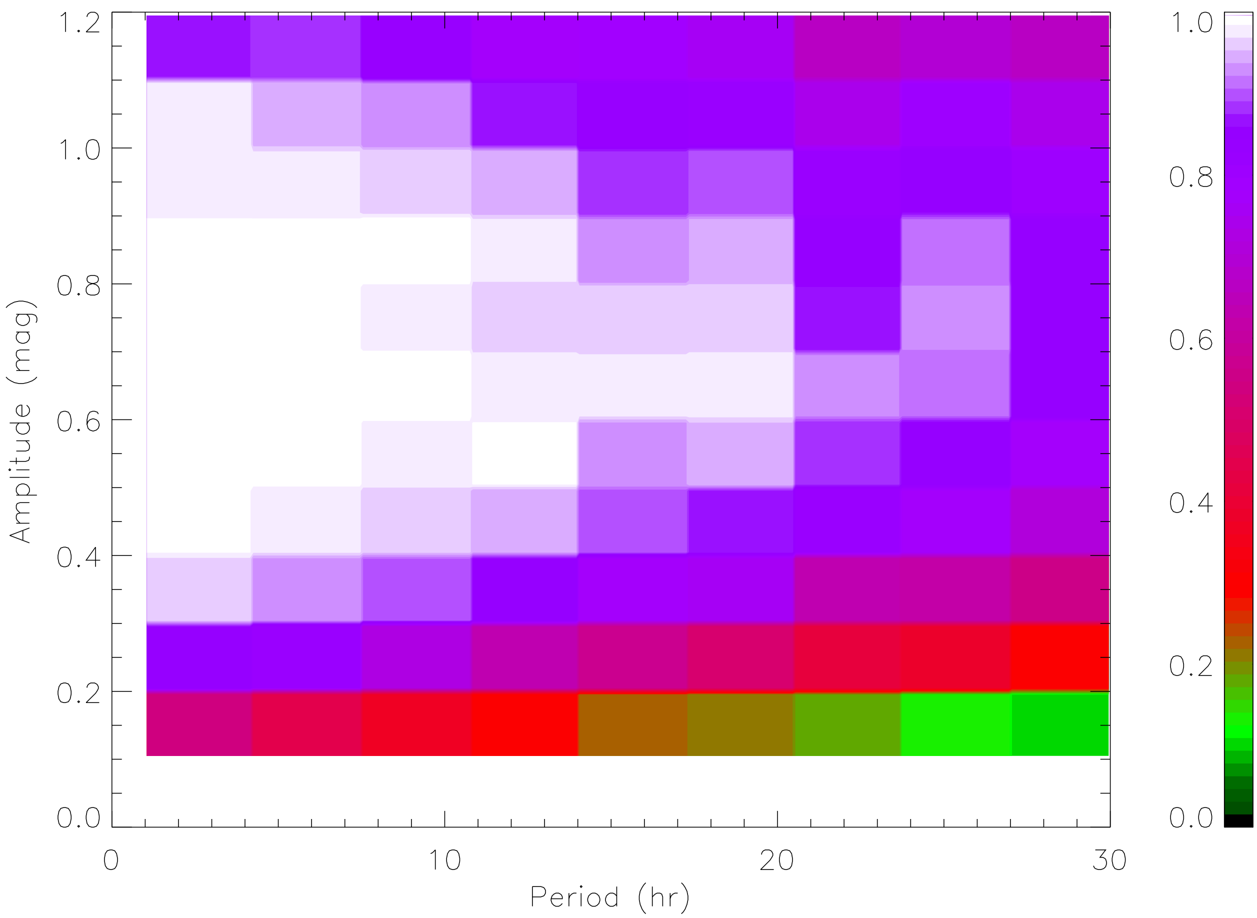

Fig. 7.— Light curve fitting efficiency as determined from our test using 100,000 synthetic objects. The colorbar scale on the right shows the fraction of correctly measured synthetic light curves. Errors on the efficiency in each bin were less than 0.02 in all cases.

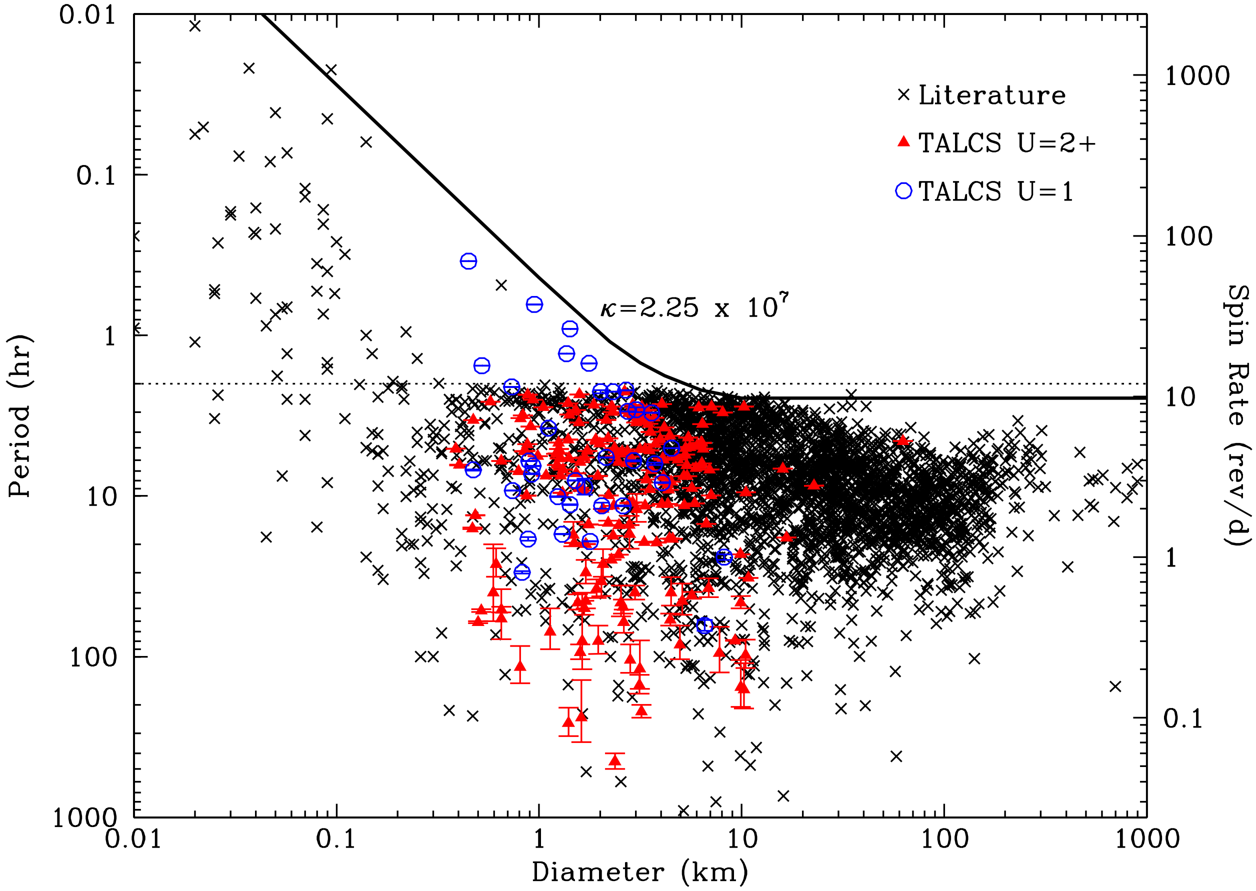

Fig. 8.— Asteroid rotation periods and spin rates vs. diameter. The black x's are known values compiled by A. W. Harris, et al. current as of Nov 2008 (*http://www.minorplanetobserver.com/astlc/LightcurveParameters.htm*). Only light curves with a quality parameter (U) greater than 2 were selected, resulting in a sample of 1442 objects. The red filled triangles are the TALCS data for all objects with fitted periods and U$\geq$ 2 (287 Main Belt asteroids) while the open blue circles are the U= 1 TALCS objects (36 MBAs). The dotted line shows a two-hour period: the spin limit for a gravitationally bound body (Pravec & Harris 2000). The thick solid line is the envelope from a size-dependent strength with $\kappa = 2.25 \times 10^7$ dynes cm$^{-3/2}$ reproduced from Fig. 5 of Holsapple (2007).

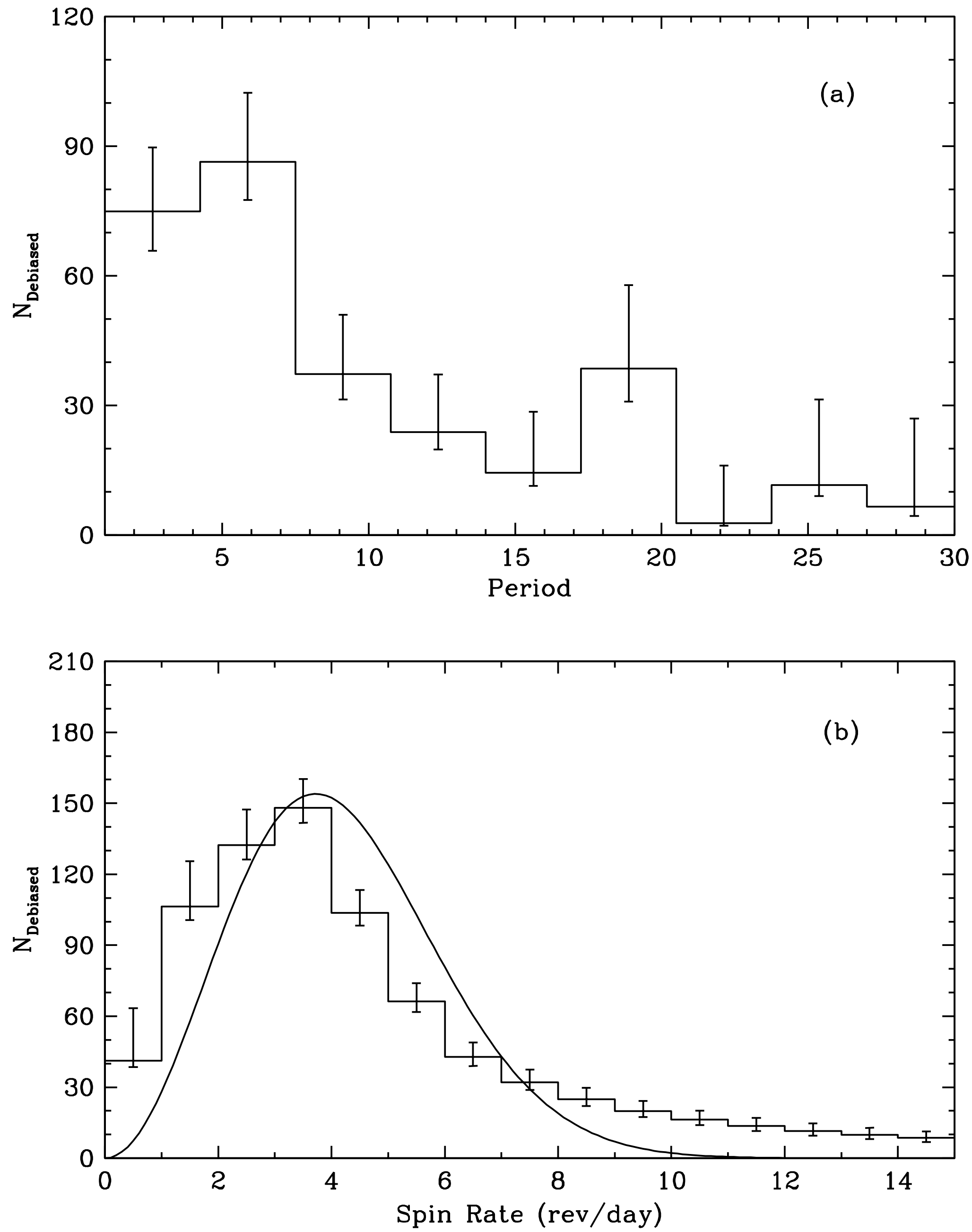

Fig. 9.— (a) Debiased TALCS period distribution for the Main Belt (3.25 hr bins). (b) Debiased TALCS spin rate distribution. The solid curve is the best-fit Maxwellian distribution with a mean rotation rate of 4.19 rev day^{-1}.

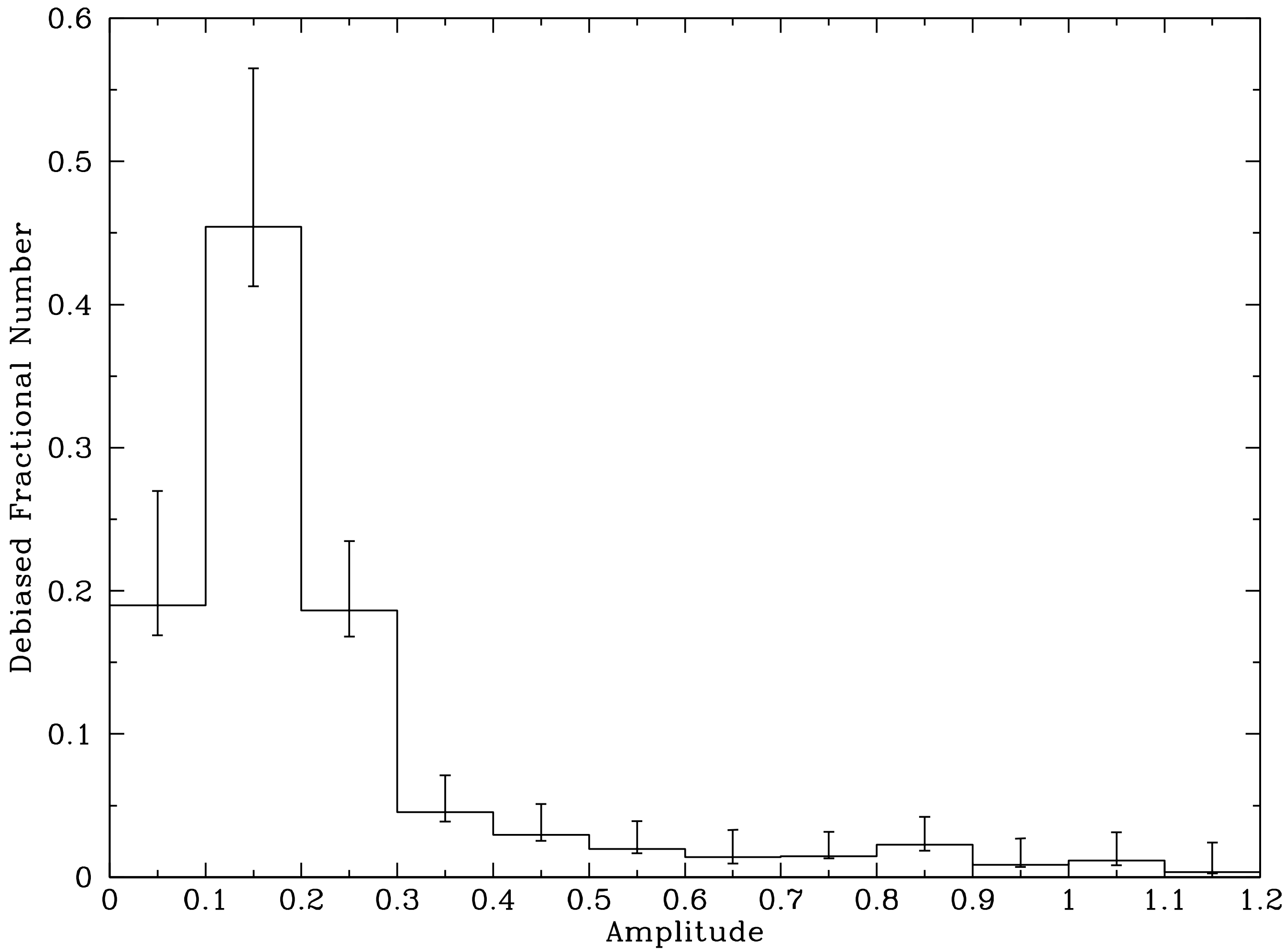

Fig. 10.— Debiased fractional differential distribution of light curve amplitudes for main belt asteroids.

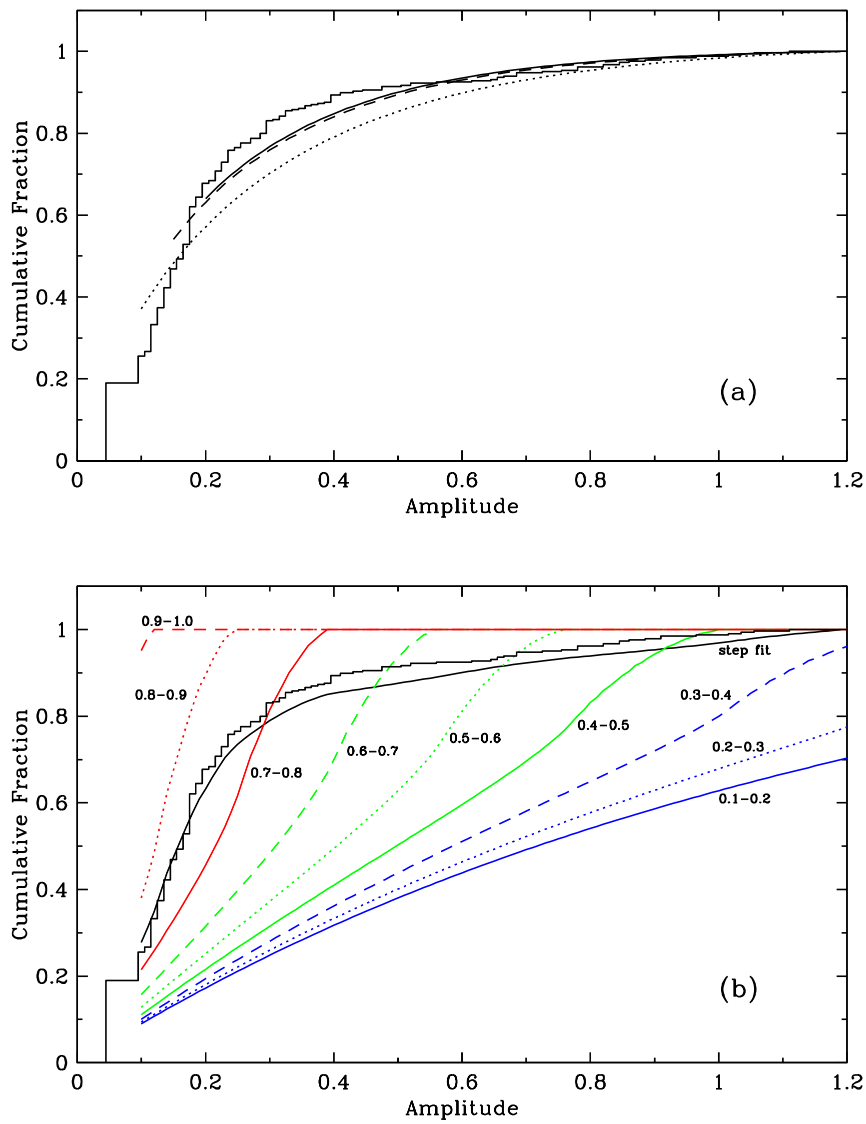

Fig. 11.— Debiased cumulative light curve amplitude distribution for TALCS objects. The amplitude<0.1 bin is an estimate of the total number of objects with amplitude below this level based on the number of objects in the survey with no apparent magnitude variation. a) The smooth curves provide the best fits to the amplitude distribution under the assumption that the b/a axis ratios for the underlying asteroid population is represented by a 2^{nd} order polynomial. The dotted/dashed/solid curves correspond to cutoff amplitudes (described in the text) of 0.1 *mag*, 0.15 *mag* and 0.2 *mag* respectively. b) The solid black line labeled 'step fit' is the best fit to the amplitude distribution when we represent the $0 < b/a \leq 1$ axis ratio distribution as a set of unconstrained 0.1 'steps' as explained in detail in the text. The other curves represent the shape of the cumulative amplitude distribution assuming that all the objects fall into a single 0.1 wide b/a ratio bin.

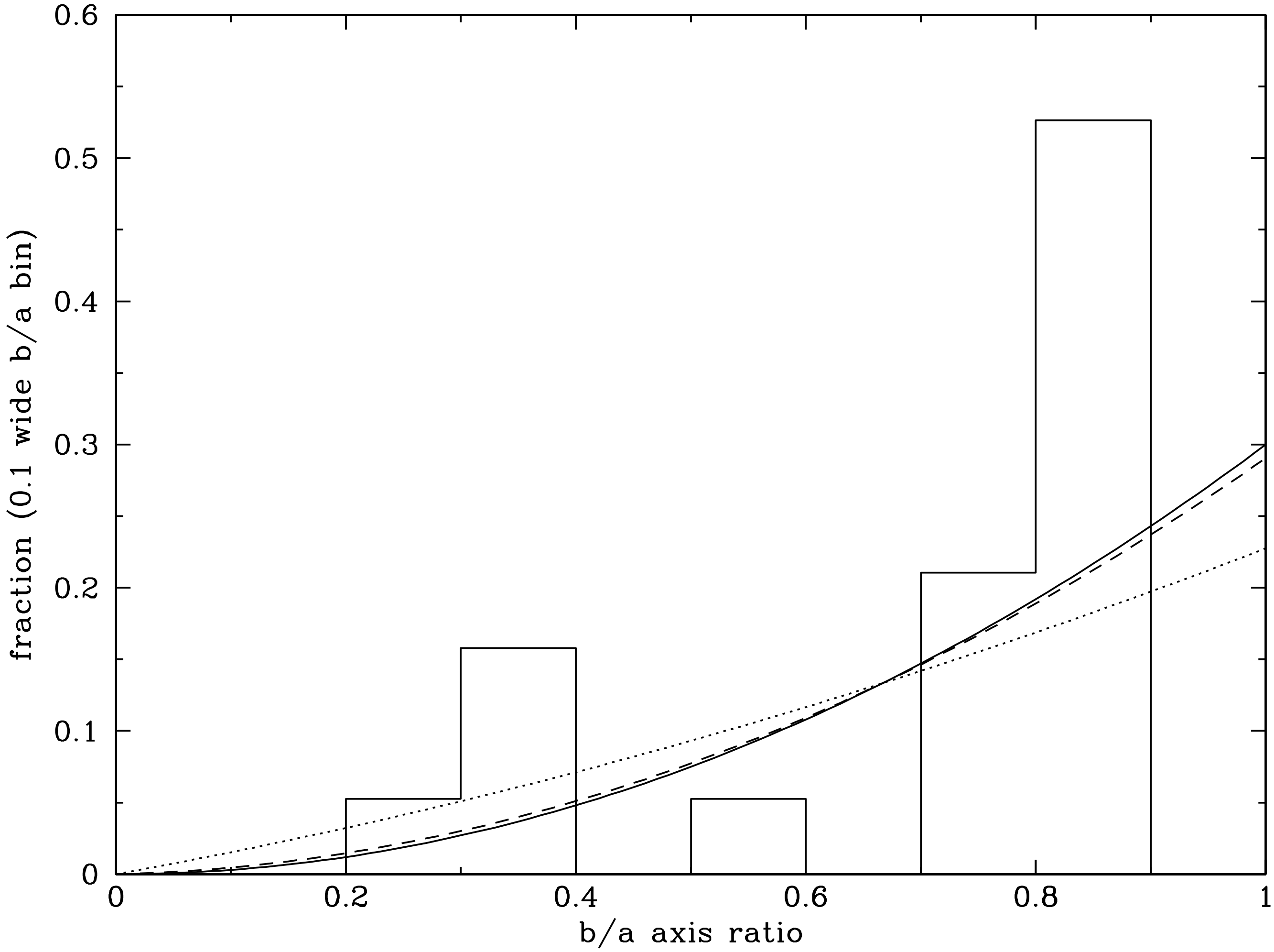

Fig. 12.— The fractional distribution of main belt asteroid b/a axis ratios from fits to the cumulative amplitude distribution of Fig. 11. The 3 smooth curves are 2^{nd} order polynomials with the same meaning as in Fig.11: cutoff amplitudes (described in the text) of 0.1 *mag*, 0.15 *mag* and 0.2 *mag* respectively. The histogram is the result of a fit to the cumulative amplitude distribution assuming that the b/a axis ratios of the asteroids can be represented 'step wise' in 0.1 wide bins as described in the text.